VISUALIZATION OF CELLULAR SIGNALING BY FLUORESCENCE RESONANCE ENERGY TRANSFER IN RESPONSE TO BIOCHEMICAL AND MECHANICAL MICROENVIRONMENTS

BY

TAE JIN KIM

DISSERTATION

Submitted in partial fulfillment of the requirements
for the degree of Doctor of Philosophy in Neuroscience
in the Graduate College of the
University of Illinois at Urbana-Champaign, 2013

Urbana, Illinois

Doctoral Committee:

Associate Professor Yingxiao Wang, Chair
Professor Deborah E Leckband
Professor Ning Wang
Assistant Professor Hyunjoon Kong

ABSTRACT

Biochemical and mechanical microenvironments have a great impact on a variety of cellular processes including cell adhesion and migration. While substantial progress has been made toward the understanding of the way in which these factors regulate many cellular functions, the molecular mechanism by which stem cells perceive such biochemical/mechanical cues to coordinate a signaling network to determine their behavior remains elusive. Hence, visualization of the intracellular signals is a challenge of major importance for an in-depth understanding of the relationship between biochemical/mechanical cues and various cellular responses. In this thesis, I have focused on Ca^{2+}, cAMP-dependent protein kinase A (PKA), and focal adhesion kinase (FAK) signaling in human mesenchymal stem cells utilizing the genetically-encoded biosensors that are based on fluorescence resonance energy transfer (FRET). FRET technology is a powerful tool to detect and visualize protein-protein interactions and enzymatic activities in living cells with high spatiotemporal resolution. In this thesis, I show that substrate rigidity regulates the spontaneous Ca^{2+} oscillations which are mediated by RhoA pathway. Using optical laser tweezers in combination with the FRET Ca^{2+} sensors targeting the cytoplasm and endoplasmic reticulum reveals how Ca^{2+} signaling at the plasma membrane and ER membrane channels can be differently regulated by mechanical stimulation, in particular, distinct roles between active actomyosin contractility and passive cytoskeleton supports. In addition to these Ca^{2+} signals, I show that agonist-induced PKA activation is regulated by the different magnitude of substrate rigidity, which further reveals to mediate endocytosis of β_2-adrenergic receptors in a microtubule-dependent manner. These findings appear to be very valuable due to cross-talk between Ca^{2+} and PKA during cell adhesion and migration. Moreover, this thesis shows that Ca^{2+} and FAK signals are differently activated in response to substrate

rigidity at plasma membrane microdomains in the adhesion process. These results suggest that biochemical/mechanical factors have a great influence on various cellular signals such as Ca^{2+}, PKA and FAK by means of various mechanisms.

In summary, the integration of live cell imaging and FRET based biosensors capable of targeting the different subcellular compartments can provide more accurate cellular information in living cells. This thesis will also advance our in-depth understanding as to how biochemical and mechanical microenvironments affect various cellular signals and their behavior.

Dedicated to my family and friends

ACKNOWLEDGEMENTS

As I look back on my graduate studies, I consider the time I have spent in Champaign-Urbana as a truly irreplaceable life experience. I have met so many precious people and dear friends. Needless to say, completing my Ph.D. would not have been possible without their continuous encouragement.

Foremost, I would like to express my sincere thanks to my advisor, Prof. Yingxiao Peter Wang. He indeed has given me outstanding guidance and strong support throughout this whole journey. Not only do I look up to him as a great scientist, but also as my mentor. His passion and profound insights about science have inspired me in many ways, and I am honored to have had him as my advisor here in Illinois.

My doctoral committee members, Prof. Deborah Leckband, Prof. Ning Wang, and Prof. Hyunjoon Kong, have also given me generous support, for which I am truly grateful. Whenever I discussed my project or other scientific issues with them, they readily shared their deep knowledge and gave me invaluable advice. I believe that they are the greatest scientists I have ever met.

I would like to give special thanks to Dr. Sam Beshers for his caring and attention throughout the years. He has always been supportive and generous to me, and to all graduate students in the Neuroscience Program. I warmly thank Dr. Phoebe Lenear in EBICS, and Julie McCartney in the Beckman Institute, for their excellent administrative support.

I am also grateful to both my former and current lab members, Dr. Shaoying Lu, Dr. Mingxing Ouyang, Dr. Jihye Seong, Dr. Jie Sun, Dr. Li-Jung Lin, Dr. Lei Lei, Dr. Wagner Shin

Nishitani, Dr. John Eichorst, Dr. Bo Liu, Dr. Chirlmin Joo, Dr. Shuai Zheng, Yue Zhuo, He Huang, Real Chen, Yijia Pan, and Pengzhi Wang, Yi Wang for their professional and personal contributions. Their true friendship will not be forgotten.

I express special gratitude to pastors Jongheon Ham, Sangwon Shin, and Taewon Kim in KC-CU, and to my mentor pastor, Yongseob Jang in Korea. They are great friends and their support had been a wonderful blessing. I want to thank my English teacher, Katie Martin, for her teaching and warm encouragement.

Completing my Ph.D. would also never have been possible without the support of my family. I appreciate my beautiful wife, Myungeun Suk, and my adorable daughter, Grace Eunhye Kim, more that words can express. Without them, my life would be meaningless. I also appreciate my parents, Jeongsik Kim and Jeongjin Lee and my older sister, Seyoung Kim and my brother-in-law, Soowung Cheong in South Korea for their unconditional love and unwavering support.

Finally, everything in my life would not be possible without the grace of God, my Lord, Jesus Christ. Thanks be to God.

TABLE OF CONTENTS

CHAPTER 1. INTRODUCTION……1
1.1. Calcium signaling……1
1.2. Protein kinase A signaling……3
1.3. Genetically encoded FRET based sensors……5
1.4. References……8

CHAPTER 2. SUBSTRATE RIGIDITY REGULATES CALCIUM OSCILLATION VIA RHOA PATHWAY……11
2.1. Introduction……12
2.2. Materials and Methods……13
2.3. Results……17
2.4. Discussion……21
2.5. References……25
2.6. Figures……33

CHAPTER 3. DISTINCT CALCIUM SIGNALING IN RESPONSE TO MECHANICAL STIMULATION……44
3.1. Introduction……45
3.2. Materials and Methods……47
3.3. Results……52
3.4. Discussion……57
3.5. References……60
3.6. Figures……69

CHAPTER 4. cAMP-DEPENDENT PROTEIN KINASE A AND ENDOCYTOSIS OF β2-ADRENERGIC RECEPTOR IN RESPONSE TO SUBSTRATE RIGIDITY……79
4.1. Introduction……80
4.2. Materials and Methods……82
4.3. Results……84
4.4. Discussion……87
4.5. References……90
4.6. Figures……99

CHAPTER 5. CALCIUM SIGNALING AT PLASMA MEMBRANE MICRODOMAINS IN RESPONSE TO SUBSTRATE RIGIDTY IN THE ADHESION PROCESS……110
5.1. Introduction……111
5.2. Materials and Methods……112
5.3. Results……115
5.4. Discussion……119
5.5. References……122
5.6. Figures……127

CHAPTER 6. SUMMARY AND POTENTIAL OUTCOME OF THE RESEARCH…..137

CHAPTER 1

INTRODUCTION

1.1 Calcium signaling

1.1.1 Fundamental mechanism of Ca^{2+} signaling

Most cells maintain their cytosolic Ca^{2+} concentration at a low level (approximately 100 nM) by major players such as the Na^{+}/ Ca^{2+} exchanger (NCX), the plasma-membrane Ca^{2+}-ATPase (PMCA), and the sarco(endo)plasmic reticulum Ca^{2+}-ATPase (SERCA) for Ca^{2+} homeostasis (Berridge, 1995; Berridge et al., 2003). When cells are stimulated, the intracellular Ca^{2+} concentration ($[Ca^{2+}]i$) rapidly increases and reaches the micromolar range, which subsequently impacts many different cellular processes. In general, Ca^{2+} entry from the extracellular pool is mediated by three main entry channels: (1) voltage-operated channels (VOCs), (2) receptor-operated channels (ROCs), and (3) store-operated channels (SOCs) (Jagannathan et al., 2002; Lewis, 2007; Li et al., 2002). Ca^{2+} release from internal stores is mediated by two families of Ca^{2+} channels—ryanodine receptors (RyRs) and 1,4,5- trisphophate receptors (IP3Rs)—each of which has three major isoforms identified. Restoration of Ca^{2+} homeostasis is achieved primarily by pumping across the plasma membrane by NCX and PMCA, and uptaking into ER/SR by SERCA (Oceandy et al., 2007; Sher et al., 2008).

1.1.2 Calcium entry mechanisms

Ca^{2+} entry is driven primarily by a large electrochemical gradient across the plasma membrane. Cells utilize the external Ca^{2+} by activating various Ca^{2+} entry channels that have very different kinetic properties. Voltage-operated Ca^{2+} channels (VOCCs) have been studied extensively in excitable cells in brain, skeletal, cardiac and smooth muscle endocrine glands, and other tissues. Fundamentally, VOCCs respond to changes in membrane potential through a voltage-sensor domain integral to the channel pore forming protein, which results in a conformation change that opens the channels to allow for the influx of extracellular Ca^{2+}. VOCCs can be activated very rapidly in response to depolarization and generate rapid Ca^{2+} increases in the cytoplasm to regulate fast cellular processes such as muscle contraction, excitability, and exocytosis. ROCs open in response to the binding of extracellular ligands. For instance, NMDA (N-methyl-D-aspartate) receptors (NMDARs) are NMDA-gated ion channels that are permeable to Ca^{2+}. When glutamate binds to the NMDARs, Ca^{2+} and Na^{+} enter the cell and K^{+} leaves through NMDA-gated channels (Berridge et al., 2003). Belonging to ATP receptors and Ach receptors, P2X7 and nicotinic acetylcholine (nACh) are also permeable to Ca^{2+} upon ligand binding (Fucile, 2004; North, 2002).

SOCs are regulated by filling or depleting internal stores through a mechanism known as capacitative Ca^{2+} entry, later called store-operated Ca^{2+} entry (SOCE) (Lewis, 2007; Putney Jr., 1986; 1990). When the internal Ca^{2+} stores are empty, Ca^{2+} channels are activated in the plasma membrane to aid in refilling the Ca^{2+} store. Most SOC channels appear to belong to the transient receptor protein (TRP) channels associated with mechanosensitive channels, such as thermosensors and stretch-activated channels. These channels have been largely classified into three groups—canonical TRPC, vanilloid TRPV, and melastatin TRPM—which are all involved in mechanical transduction. In particular, TRP channels have low conductance and play a crucial

role in controlling slow cellular processes such as smooth-muscle contractility and cell proliferation. To date, the detailed mechanism of SOCE remains unclear because the identity of the entry channels is not clear. However, the discovery of stromal interaction molecules (STIM) sheds new light on our understanding of the molecular mechanism of SOCE. This STIM1 is localized mainly in the ER membrane. STIM1 senses ER Ca^{2+} to activate Orai1, a pore-forming subunit of the Ca^{2+} release-activated Ca^{2+} channel (CRCA) in the plasma membrane for SOCE (Feske et al., 2006). Thus, STIM1 can activate SOCE and help refill the ER Ca^{2+} store.

1.1.3 Calcium release from internal stores

There are two main channels responsible for releasing Ca^{2+} from the internal stores: (1) IP3 receptors (IP3Rs) and (2) ryanodine receptors (RyRs). Activation of phospholipase C (PLCγ) by G protein coupled receptors (GPCRs) and PLCγ by receptor tyrosine kinases can induce cleavage of phosphatidylinositol 4, 5 bisphosphate (PIP2) into 1,4,5-inositol trisphosphate (IP3) and diacylglycerol (DAG). IP3 can bind to the IP3 receptors located in ER membrane to trigger Ca^{2+} from ER stores. RyRs are also intracellular Ca^{2+} channels located primarily in the ER/SR of various excitable cells, particularly muscle and neuronal cells. RyRs are similar to IP3Rs, which can be stimulated to transport Ca^{2+} into the cytosol by recognizing the low level of Ca^{2+} on its cytosolic side. Both channels are very sensitive to calcium. Therefore, it appears that the process of Ca^{2+}-induced Ca^{2+} release (CICR) contributes to the increase in intracellular Ca^{2+} concentration, and as such CICR contributes to the generation of Ca^{2+} spikes and Ca^{2+} waves.

1.2 Protein kinase A signaling

1.2.1 The structure of PKA and function

cAMP-dependent protein kinase (PKA) is ubiquitously expressed in cells to regulate cellular functions including gene expression, metabolism, growth and proliferation (Ni et al., 2011). PKA is a heterotetrameric enzyme comprising two regulatory and two catalytic subunits. Upon cAMP binding, the catalytic subunits are released and able to phosphorylate numerous substrate proteins in the cell. Four regulatory subunit isoforms are encoded by four separate genes (RIα, RIβ, RIIα, RIIβ) and three catalytic subunit isoforms (Cα, Cβ, Cγ) have distinct biological properties playing a role in achieving signaling specificity. A-kinase anchoring proteins (AKAPs) assemble signaling complexes including PKA and its substrates, and regulators at different subcellular compartments, thereby facilitating specific phosphorylation and regulation of PKA substrates. PKA is a major mediator of cAMP signaling pathway. It not only controls downstream signaling cascades at various subcellular locations, but also directly regulates cAMP dynamics through upstream components such as G-protein coupled receptors (GPCR), adenylyl cyclases (AC) and phosphodiesterases (PDE) (Depry and Zhang, 2011)

1.2.2 Regulation of PKA during adhesion and migration

The PKA pathway is importantly regulated by integrin-mediated adhesion to the ECM. PKA is robustly, but transiently activated by cellular detachment process. Inhibition of this process can delay inactivation of specific anchorage-dependent enzymes including ERK, FAK and paxillin. PKA signaling can be initiated by relaxation of cytoskeletal stress. PKA appears to be suppressed in endothelial cells plated on collagen type I, but not on laminin-1 suggesting that it is ECM-specific. It also appears to be correlated with adhesion-mediated suppression of Rho

and activation of Rac and Cdc42. In addition, PKA activation in migrating cells is blocked by depletion of extracellular Ca^{2+} and inhibition of stretch-activated Ca^{2+} channels, implying that PKA signaling is regulated by intracellular tension through a mechanism that involves stretch-activated Ca^{2+} channels. Even though, it becomes clear that cAMP/PKA are dynamically regulated by cell adhesion and migration, the underlying mechanism by which cAMP/PKA becomes activated during these processes remains still unclear (Depry et al., 2011).

1.3 Genetically encoded FRET based sensors

1.3.1 FRET based Calcium biosensors

Fluorescence resonance energy transfer (FRET)-based Ca^{2+} biosensors for single cell imaging have allowed researchers to quantitatively monitor Ca^{2+} dynamics and their signaling cascades in live cells with high spatiotemporal resolution. FRET is a phenomenon of quantum mechanics and describes an energy transfer mechanism between two chromophores. When one chromophore (donor) and the other one (acceptor) are in proximity and the emission spectrum of the donor overlaps the excitation spectrum of the acceptor, the excitation of the donor will cause a sufficient energy transfer to the acceptor and result in emission from the acceptor. This FRET efficiency depends on the relative orientations and the distance between these two chromophores (Tsien, 1998; Wang and Chien, 2007). Hence, the conformational change in orientation and distance between the two chromophores can alter the FRET efficiency and change the acceptor/donor emission ratio.

A wide range of FRET-based Ca^{2+} biosensors has been developed to visualize Ca^{2+} dynamics and activities (Palmer and Tsien, 2006). In general, there are three different categories,

classified according to properties such as binding moiety and strategy for Ca^{2+} sensing: 1. Calmodulin/FRET based Ca^{2+} biosensors 2. Troponin C/FRET based Ca^{2+} biosensors 3. Single fluorophore biosensors. These genetically encoded Ca^{2+} biosensors have been applied for targeting various organelles such as the nucleus, endoplasmic reticulum (ER), mitochondria, Golgi, and plasma membrane in living single cells in an effort to visualize dynamic Ca^{2+} signals (Filippin et al., 2003; Griesbeck et al., 2001; Heim and Griesbeck, 2004; Ishii et al., 2006; Mank et al., 2006; Miyawaki et al., 1997; Nagai et al., 2004; Palmer et al., 2004; Palmer and Tsien, 2006). Here I briefly describe the Calmodulin/FRET based Ca^{2+} biosensor, which is one of the most popular and commonly used biosensors among the various kinds of FRET-based Ca^{2+} indicators.

Calmodulin (CaM) is a Ca^{2+} binding protein and is ubiquitously expressed in all eukaryotic cells. As a monomer with an approximate molecular weight of 17,000, CaM is located primarily in the cytosol, but can be translocated to the nucleus where it regulates transcription and gene expression. CaM mediates numerous fundamental cellular processes, such as inflammation, apoptosis, cell cycle progression, cell metabolism, and Ca^{2+} transport. Structurally, CaM has four EF-hand motifs, each of which binds a Ca^{2+} ion and undergoes a conformational change. These CaMs can be applied to the development of Ca^{2+} sensors. In fact, a variant of CaM and a CaM-binding peptide connected by two FPs was developed as FRET-based Ca^{2+} biosensors by Tsien and co-workers; this was the first generation of genetically encoded Ca^{2+} sensors called “Cameleons” (Miyawaki et al., 1997). The sensor originally consisted of blue and green FPs (BFP as the donor and GFP as the acceptor), flanking *Xenopus* Calmodulin (XcaM) and peptide M13. Upon Ca^{2+} binding, Ca^{2+}/Calmodulin wraps around the neighboring M13 peptide, thus causing a conformational change and increasing the energy

transfer efficiency from BFP to GFP. To overcome the weak fluorescence brightness and relatively poor photobleaching property of BFP, this BFP-GFP FRET pair was switched to cyan FP (CFP) and yellow FP (YFP) in Yellow Cameleon 2.0 (YC 2.0), which provided better signal-to-noise ratios and more stable FRET signals in live cells. Further efforts for making better Cameleons were carried out afterward, resulting in the improvement of signal strength of the biosensors and a reduction in perturbation to endogenous cell signaling cascades. At present, various improved versions of Cameleons have been developed, ranging from YC2.0 to YC6.1 (Griesbeck et al., 2001; Miyawaki et al., 1997; 1999; Truong et al., 2001).

1.3.2 FRET based PKA biosensors

Genetically encoded FRET-based A-kinase Activity Reporters (AKARs) have been developed to visualize endogenous PKA activity dynamics with high spatiotemporal resolutions in a living cell (Zhang J et al., 2005). Structurally, AKARs consist of a molecular switch sandwiched between a FRET pair, ECFP and YFP, which undergoes a conformational change and AKARs can detect a change in FRET when phosphorylated by PKA. The molecular switch is comprised of a surrogate substrate for PKA and a phospho-amino acid-binding domain (PABBD) (e.g., forkhead associated domain, FHA). As the substrate is phosphorylated by PKA, the PAABD binds the phosphorylated substrate. Fundamentally, the FRET response produced by AKARs depends on the properties of the fluorescent proteins used. An excited donor fluorophore (e.g. CFP) can transfer energy to an acceptor fluorophore (YFP) in close molecular proximity (<10 nm). The donor emission spectrum must overlap with the acceptor excitation spectrum to occur FRET. CFP and YFP are commonly available as a FRET pair because the emission

wavelength of CFP significantly overlaps with the excitation wavelength of YFP. However, more recently, CFP and YFP variant YPet are being utilized for the better dynamic change in FRET. Based on this strategy, AKARs can detect PKA activity dynamics and these changes are typically induced by drugs or other perturbations to stimulate or inhibit PKA.

1.4 References

Berridge MJ. 1997. Elementary and global aspects of calcium signalling. *J. Exp. Biol.* 200:315–319.

Berridge MJ, Bootman MD, and Roderick HL. 2003. Calcium signalling: dynamics, homeostasis and remodelling. *Nat. Rev. Mol. Cell Biol.* 4:517–529.

Feske S, Gwack Y, Prakriya M, Srikanth S, Puppel SH, Tanasa B, Hogan PG, Lewis RS, Daly M, and Rao A. 2006. A mutation in Orai1 causes immune deficiency by abrogating CRAC channel function. *Nature* 441:179–185.

Filippin L, Magalhaes PJ, Di Benedetto G, Colella M, and Pozzan T. 2003. Stable interactions between mitochondria and endoplasmic reticulum allow rapid accumulation of calcium in a subpopulation of mitochondria. *J. Biol. Chem.* 278:39224–39234.

Fucile S. 2004. Ca2+ permeability of nicotinic acetylcholine receptors. *Cell Calcium* 35:1–8.

Griesbeck O, Baird GS, Campbell RE, Zacharias DA, and Tsien RY. 2001. Reducing the environmental sensitivity of yellow fluorescent protein. *Mechanism and applications. J. Biol. Chem. 276:29188–29194.*

Heim N, and Griesbeck O. 2004. Genetically encoded indicators of cellular calcium dynamics based on troponin C and green fluorescent protein. *J. Biol. Chem.* 279:14280–14286.

Ishii K, Hirose K, and Iino M. 2006. Ca2+ shuttling between endoplasmic reticulum and mitochondria underlying Ca2+ oscillations. *EMBO Rep.* 7:390–396.

Jagannathan S, Publicover SJ, and Barratt CL. 2002. Voltage-operated calcium channels in male germ cells. *Reproduction* 123:203–215.

Lewis RS. 2007. The molecular choreography of a store-operated calcium channel. *Nature* 446:284–287.

Li SW, Westwick J, and Poll CT. 2002. Receptor-operated Ca2+ influx channels in leukocytes: a therapeutic target? *Trends Pharmacol. Sci.* 23:63–70.

Mank M, Reiff DF, Heim N, Friedrich MW, Borst A, and Griesbeck O. 2006. A FRET-based calcium biosensor with fast signal kinetics and high fluorescence change. *Biophys. J.* 90:1790–1796.

Miyawaki A, Griesbeck O, Heim R, and Tsien RY. 1999. Dynamic and quantitative Ca2+ measurements using improved cameleons. *Proc. Natl Acad. Sci. USA* 96:2135–2140.

Miyawaki A, Llopis J, Heim R, McCaffery JM, Adams JA, Ikura M, and Tsien RY. 1997. Fluorescent indicators for Ca2+ based on green fluorescent proteins and calmodulin. *Nature* 388:882–887.

Nagai T, Yamada S, Tominaga T, Ichikawa M, and Miyawaki A (2004). Expanded dynamic range of fluorescent indicators for Ca(2+) by circularly permuted yellow fluorescent proteins. *Proc. Natl Acad. Sci. USA* 101:10554–10559.

Oceandy D, Stanley PJ, Cartwright EJ, and Neyses L. 2007. The regulatory function of plasma-membrane Ca(2+)-ATPase (PMCA) in the heart. *Biochem. Soc. Trans.* 35:927–930.

Palmer AE, Jin C, Reed JC, and Tsien RY. 2004. Bcl-2-mediated alterations in endoplasmic reticulum Ca2+ analyzed with an improved genetically encoded fluorescent sensor. *Proc. Natl Acad. Sci. USA* 101:17404–17409.

Palmer AE and Tsien RY. 2006. Measuring calcium signaling using genetically targetable fluorescent indicators. *Nat. Protoc.* 1:1057–1065.

Putney Jr. JW. 1986. A model for receptor-regulated calcium entry. *Cell Calcium* 7:1–12.

Putney Jr. JW. 1990. Capacitative calcium entry revisited. *Cell Calcium* 11:611–624.

Sher AA, Noble PJ, Hinch R, Gavaghan DJ, and Noble D. 2008. The role of the Na+/Ca2+ exchangers in Ca2+ dynamics in ventricular myocytes. *Prog. Biophys. Mol. Biol.* 96:377–398.

Tsien RY. 1998. The green fluorescent protein. *Annu. Rev. Biochem.* 67:509–544.

Wang Y and Chien S. 2007. Analysis of integrin signaling by fluorescence resonance energy transfer. *Meth. Enzymol.* 426:177–201.

Zhang J, Hupfeld CJ, Taylor SS, Olefsky JM, Tsien RY. 2005. Insulin disrupts beta-adrenergic signalling to protein kinase A in adipocytes. *Nature*. 437(7058):569-73.

Depry C and Zhang J. 2011. Using FRET-based reporters to visualize subcellular dynamics of protein kinase A activity. *Methods Mol Biol*. 756:285-94.

Depry C, Allen MD, and Zhang J. 2011. Visualization of PKA activity in plasma membrane microdomains. *Mol Biosyst*. 1:52-8.

CHAPTER 2

SUBSTRATE RIGIDITY REGULATES CALCIUM OSCILLATION VIA RHOA PATHWAY

Recent reports demonstrated that substrate rigidity plays crucial roles in cellular functions such as cell spreading, traction forces, and stem cell differentiation. However, it is not clear how substrate rigidity influences early cell signaling events such as calcium oscillation in living cells. In this chapter, I investigated the molecular mechanism by which substrate rigidity affects calcium signaling in human mesenchymal stem cells (HMSCs) using highly-sensitive Ca^{2+} biosensors based on fluorescence resonance energy transfer (FRET). Spontaneous Ca^{2+} oscillations were observed inside the cytoplasm and the endoplasmic reticulum (ER) using the FRET biosensors targeted at subcellular locations in cells plated on rigid dishes. Lowering the substrate stiffness to 1 kPa significantly inhibited both the magnitudes and frequencies of the cytoplasmic Ca^{2+} oscillation in comparison to those on stiffer or rigid substrate. This Ca^{2+} oscillation was shown to be dependent on ROCK, a downstream effector molecule of RhoA, but independent of actin filaments, microtubules, myosin light chain kinase, or myosin activity. Lysophosphatidic acid, which activates RhoA, inhibited the magnitude and frequency of the Ca^{2+} oscillation. Either a constitutive active mutant of RhoA (RhoA-V14) or a dominant negative mutant of RhoA (RhoA-N19) inhibited the Ca^{2+} oscillation. Further experiments revealed that HMSCs cultured on gels with low elastic moduli displayed low RhoA activities. Therefore, these results in this chapter demonstrate that RhoA and its downstream molecule ROCK may mediate

the substrate rigidity-regulated Ca^{2+} oscillation, which regulates physiological functions of HMSCs in turn.

2.1 Introduction

Calcium ion (Ca^{2+}) is one of the most important early biological signals (Berridge et al., 2000). Most cells mobilize their Ca^{2+} signals via the Ca^{2+} entry across the plasma membrane and/or the Ca^{2+} traffic between cytoplasm and intracellular stores such as endoplasmic reticulum (ER) or sarcoplasmic reticulum (SR) (Wehrens et al., 2005; Clapham, 2007). Ca^{2+} entry across the plasma membrane occurs via several distinct pathways, including voltage-operated Ca^{2+} channels (VOCCs), agonist-dependant and store-operated Ca^{2+} (SOC) channels (Albert and Large, 2003; Bolotina, 2004; Nilius, 2004). Ca^{2+} traffic between cytoplasm and intracellular stores, e.g. endoplasmic reticulum (ER), is controlled by two distinct channels, inositol 1,4,5-triphosphate receptor (InsP3R) and ryanodine receptor (RYR) (Berridge, 1993; Berridge et al., 2000; Foskett et al., 2007; Lewis, 2007), as well as the sarcoendoplasmic reticulum calcium transport ATPase (SERCA), serving as a pump that transports Ca^{2+} ions from cytoplasm into ER (Misquitta et al., 1999; Periasamy and Kalyanasundaram, 2007).

One of the most interesting discoveries in the field of calcium study is the oscillatory Ca^{2+} signals (Sun et al., 2007). While the role of oscillatory Ca^{2+} signals is not fully understood, it is clear that oscillatory Ca^{2+} signals are crucial for a variety of cellular functions (Torihashi et al., 2002; Morita et al., 2003; Sun et al., 2007). For example, spontaneous Ca^{2+} oscillations were observed in human bone marrow-derived mesenchymal stem cells (HMSCs) and found to affect differentiation (D'Souza et al., 2001; den Dekker et al., 2001). The regulation of Ca^{2+} oscillation

by electrical stimulation can also promote the differentiation of HMSCs into osteoblasts (Sun et al., 2007). It remains unclear whether and how mechanical microenvironment such as substrate rigidity can affect Ca^{2+} oscillations.

Fluorescence resonance energy transfer (FRET) is a powerful tool for the detection of protein-protein interaction and enzymatic activities (Zhang et al., 2002). Genetically-encoded biosensors based on FRET have the advantage to be easily targeted to subcellular compartments and have been widely applied to monitor signaling transductions in live cells with high spatiotemporal resolution. In fact, a variety of FRET biosensors using fluorescence Proteins (FPs) have been developed, including Ca^{2+}, proteases, cAMP, phosphor-lipids, membrane receptor integrins, small GTPases Ras and Rap1, RhoA, Rac1, Cdc42, and tyrosine/serine/threonine kinases (Ouyang et al., 2008a; Wang et al., 2008). I have also developed a Calcium biosensor pairing an enhanced cyan FP (ECFP) with a newly developed yellow FP, YPet (Nguyen and Daugherty, 2005). This new Ca^{2+} biosensor provides a high dynamic range in monitoring intracellular Ca^{2+} oscillations (Ouyang et al., 2008b).

In this chapter, I investigated whether the substrate rigidity can regulate intracellular Ca^{2+} signaling in HMSCs. Genetically encoded Ca^{2+} biosensors based on FRET were applied to monitor the Ca^{2+} signals inside either the cytoplasm or ER in live HMSCs. These results show that the spontaneous Ca^{2+} oscillations observed in HMSCs can be regulated by extracellular substrate rigidity via RhoA/ROCK signaling pathway.

2.2 Materials and Methods

2.2.1 Gene construction and DNA plasmids

The construct of FRET-based Ca^{2+} biosensor (ECFP-CaM-M13-EYFP) has been described (Miyawaki et al., 1997). We have replaced EYFP with a recently developed YFP variant YPet to enhance the dynamic range of the biosensor. Briefly, the fragment containing ECFP, CaM, and M13 was fused to YPet and subcloned into pcDNA3.1 for mammalian cell expression by using *Bam*HI/*Eco*RI sites. To generate an ER-targeted Calcium biosensor, the calreticulin signal sequence MLLPVLLLGLLGAAAD was fused to the N-terminal of ECFP, and an ER retention sequence, KDEL, was added to the end of the C-terminal of YPet (Palmer et al., 2004). The construct of FRET-based RhoA biosensor was a kind gift from Professor Michiyuki Matsuda at Kyoto University, Japan (Yoshizaki et al., 2003). In brief, the RhoA biosensor consists of truncated RhoA (aa 1–189) and the RhoA-binding domain (RBD) of effector, concatenated between a pair of GFP mutants, YFP and CFP. The intramolecular binding of active RhoA (GTP-binding) to the PBD domain is expected to bring CFP in closer proximity to YFP, resulting in an increase in FRET from CFP to YFP. Hence, the increased FRET signals can be monitored to assess the RhoA activity. Plasmids encoded RhoA-V14, a constitutive active mutant of RhoA and RhoA-N19, a negative mutant of RhoA were previously described (Li et al., 1999).

2.2.2 Cell culture and transfection

Bone marrow-derived HMSCs (from ATCC) were kindly provided by Dr. Shu Chien (University of California, San Diego). The cells were cultured in human mesenchymal stem cell growth medium (MSCGM, PT-3001, Lonza Walkersvile, Inc., MD, USA) containing 10% fetal bovine serum, 2 mM L-glutamine, 100 unit/ml penicillin and 100 μg/ml streptomycin in a

humidified incubator of 95% O_2 and 5% CO_2 at 37˚C. The DNA plasmids were transfected into the cells by using Lipofectamine 2000 (Invitrogen) reagent according to the product instructions.

2.2.3 Immunostaining

STRO-1 was used as HMSCs marker (Gronthos et al., 1999; Kassem and Abdallah, 2008; Rosada et al., 2003). After being washed in cold phosphate buffered saline (PBS), the samples were fixed by 4% paraformaldehyde in PBS at RT for 15 min. The cells were incubated with STRO-1 antibody (1:100; Chemicon, Temecula, CA) at 4˚C overnight. They were subsequently incubated with Fluorescein (FITC)-conjugated anti-mouse IgG (1:200, Jackson ImmunoResearch Lab. Inc.) at RT for 1 hr.

2.2.4 Solutions and chemicals

Imaging experiments were conducted with CO_2-independent medium (Invitrogen, CA, USA). For experiments that requires Ca^{2+}-free conditions, Hanks balanced salt solution (HBSS, Invitrogen) was used containing 20 mM HEPES, 1 mM D-glucose, 2 mM $MgCl_2$, 2 mM $MgSO_4$ (pH 7.4). The chemical reagents 2-Amino-ethoxydiphenyl borate (2-APB, 100 μM), nifedipine (10 μM), thapsigargin (TG, 10 μM), $LaCl_3$ (100 μM), $GdCl_3$ (5 μM), Nocodazole (1 μM), cytochalasin D (2 μM), blebbistatin (10 μM), lysophosphatidic acid (LPA, 1 μM), and ML-7 (5 μM) were purchased from Sigma-Aldrich (St. Louis, MO, USA). The ROCK inhibitor Y-27632 (10 μM) was obtained from Calbiochem (San Diego, CA, USA).

2.2.5 Polyacrylamide gel for cell culture

Polyacrylamide gel solutions were prepared from 40% w/v acrylamide stock solution (5%; Bio-Rad) and 2% w/v bis-acrylamide stock solution (0.03-0.3%; Bio-Rad). To polymerize the solutions, 10% w/v ammonium persulfate (Bio-Rad) and N,N,N9,N9-Tetramethylethylenediamine (TEMED; Bio-Rad) were mixed with distilled water. Sulfo-SANPAH [sulfosuccinimidyl6(4_-azide-2_-nitrophenyl-amino) hexanoate; Pierce] was used to crosslink extracellular matrix molecules onto the gel surface. A detailed protocol about polyacrylamide gels was described previously (Pelham and Wang, 1997).

2.2.6 Microscopy and Imaging

Cells expressing various exogenous proteins were starved with 0.5% FBS for 36-48 hr before imaging experiments. During imaging process, the cells were maintained in CO_2-independent medium without serum at 37°C. All images were obtained by using Zeiss Axiovert inverted microscope equipped with a charge-coupled device (CCD) camera (Cascade 512B, Photometircs) and a 440DF20 excitation filter, a 455DRLP dichroic mirror, and two emission filters controlled by a filter changer (480DF30 for CFP and 535DF25 for YFP). Time lapse fluorescence images were acquired at 10 sec interval by MetaFluor 6.2 software (Universal Imaging). The emission ratio images were computed and generated by the MetaFluor software to represent the FRET efficiency before they were subjected to quantification and analysis by Excel (Microsoft).

2.2.7 Statistical analysis

All data were expressed as the mean ± standard error of the mean (S.E.M). Statistical evaluation of the data was performed by the unpaired student's *t*-test to determine the statistical differences between the two mean values. A significant difference was determined by the p-value (< 0.05).

2.3 Results

2.3.1 Genetically encoded FRET Ca^{2+} biosensors based on ECFP and YPet

Novel FRET Ca^{2+} biosensors based on ECFP and YPet were developed to visualize and monitor Ca^{2+} signaling with high sensitivity and spatiotemporal resolution (Fig. 2-1A). HMSCs were immunostained with anti-STRO-1 antibody, a HMSCs marker, to confirm their undifferentiated state (Fig. 2-1B). I found that the transfection efficiency of the Ca^{2+} biosensors was approximately 11.95% (27 of 226 cells) using lipofectamine method in HMSCs. As shown in Fig. 2-1C, a clear oscillation of cytoplasmic Ca^{2+} concentration can be observed by the transfected Ca^{2+} biosensor, which was initiated at a triggering corner and propagated to the whole cell body later. The oscillations of ER Ca^{2+} concentration can also be detected by a Ca^{2+} biosensor specifically targeted inside ER (Fig. 2-1D). These results suggest that our FRET-based biosensor can successfully monitor the spontaneous Ca^{2+} oscillation at subcellular locations inside HMSCs. This spontaneous Ca^{2+} oscillation was observed in fifty-nine percentages (26 of 44 cells) of HMSCs.

2.3.2 Ca^{2+} traffic across both the plasma membrane and ER membrane is important for the spontaneous cytoplasmic Ca^{2+} oscillation in HMSCs

The cytoplasmic Ca^{2+} concentration is regulated via the Ca^{2+} flux across the plasma membrane and/or the exchange with internal Ca^{2+} stores such as ER. In fact, spontaneous oscillations of Ca^{2+} can be observed in both cytoplasm and ER (Fig. 2-1C-D). When the extracellular Ca^{2+} was eliminated by incubating the cells in the Ca^{2+}-free HBSS, the spontaneous Ca^{2+} oscillation disappeared (Fig. 2-2A and Supplementary Fig. S2-1). The inhibition of Ca^{2+} channels at the plasma membrane by a selective L-type calcium channel blocker, nifedipine (10 μM), or by inhibitors for SOC, either $LaCl_3$ (100 μM) or $GdCl_3$ (5 μM), blocked the spontaneous cytoplasmic Ca^{2+} oscillation (Fig. 2-2B-D). These results suggest that extracellular Ca^{2+} pool and Ca^{2+} flux across the plasma membrane are essential for the spontaneous Ca^{2+} oscillation in HMSCs. I then examined how intracellular Ca^{2+} store ER contributes to the cytoplasmic Ca^{2+} oscillation by blocking InsP3R and Ca^{2+}-ATPase (SERCA) pump on ER membrane using 2-APB and thapsigargin (TG), respectively. Both 2-APB (100 μM) and TG (10 μM) blocked the spontaneous Ca^{2+} oscillation (Fig. 2-2E-F). TG treatment also caused a transient increase of cytoplasmic Ca^{2+} concentration, which returned to the basal level after TG treatment for more than 1 hr without the resumption of the Ca^{2+} oscillation (Supplementary Fig. S2-2). Hence, the internal calcium stores play an important role for the spontaneous calcium oscillation. Taken together, these results suggest that the Ca^{2+} traffic at both the plasma membrane and ER membrane regulate the cytoplasmic Ca^{2+} oscillation.

2.3.3 Regulation of the Ca^{2+} oscillations by substrate rigidity of extracellular environment

Since mechanical environment and Ca^{2+} signaling have been shown to regulate the stem cell commitment for differentiation (D'Souza et al., 2001; den Dekker et al., 2001; Engler et al., 2006), I then examined whether the mechanical environments can affect this cytoplasmic Ca^{2+} oscillation in HMSCs. Polyacrylamide gels were applied to control the substrate rigidity of extracellular environment with defined elastic moduli. As shown in Fig. 2-3A, gels with lower elasticity reduced the Ca^{2+} oscillation activities in HMSCs. This was further confirmed by statistical analysis results (Fig. 2-3B-C). Interestingly, 1 kPa gel inhibited both frequency and magnitude of Ca^{2+} oscillation whereas 8.5 and 5 kPa gels only affected the frequency (Fig. 2-3B-C). Therefore, the substrate rigidity of extracellular environment can affect Ca^{2+} oscillation in HMSCs. These results also suggest that the frequency of Ca^{2+} oscillation may be more sensitive to mechanical environment than the magnitude.

2.3.4 The roles of the cytoskeleton and RhoA signaling pathway on the spontaneous cytoplasmic Ca^{2+} oscillation

I hypothesized that the cytoskeleton and intracellular mechanical tension may mediate the oscillatory Ca^{2+} signals in sensing the substrate rigidity. In fact, substrate rigidity of extracellular environment was shown to affect cell morphology, cytoskeletal structure and cell adhesion (Yeung et al., 2005). To investigate the roles of cytoskeleton, cytochalasin D (Cyto D) and nocodazole (Noc) were applied to disrupt actin filaments and microtubules, respectively. As shown in Fig. 2-4A, neither Cyto D nor Noc had significant effects on the spontaneous Ca^{2+} oscillation in HMSCs, although Cyto D and Noc sufficiently disrupted actin filaments and microtubules, respectively (Supplementary Fig. S2-3). The spontaneous Ca^{2+} oscillation was also

immune to Jasplakinolide (1 μM), which stabilizes and induces the polymerization of actin filaments (Supplementary Fig. S2-4). Surprisingly, the Ca^{2+} oscillation was not affected by ML-7, an inhibitor of myosin light chain kinase (MLCK) (Soderling and Stull, 2001), nor by blebbistatin, a myosin II inhibitor which has been shown to mediate the effect of mechanical force on stem cell commitment (Engler et al., 2006) (Fig. 2-4A-C), . These results suggest that the spontaneous Ca^{2+} oscillation in HMSCs is independent of cytoskeleton and MLCK/myosin. Interestingly, Y-27632, an inhibitor of Rho-associated kinase (ROCK), and lysophosphatidic acid (LPA), a stimulator of RhoA, significantly inhibited the frequency, but not the magnitude of Ca^{2+} oscillation (Fig. 2-4A-C). These results suggest that RhoA and its downstream molecule ROCK may be involved in the regulation of Ca^{2+} oscillation in HMSCs.

2.3.5 Substrate rigidity alters the endogenous RhoA activity, which mediates the Ca^{2+} oscillation in HMSCs

I then examined whether substrate rigidity can regulate the endogenous RhoA activity using a FRET-based RhoA biosensor. The functionality of this RhoA biosensor was first confirmed in HMSCs in response to LPA, an activator of RhoA. As shown in supplementary Fig. S2-5, LPA significantly increased FRET signals of the RhoA biosensor, representing an elevated RhoA activity (Yoshizaki et al., 2003). Hence, the RhoA biosensor can report RhoA activity in our system. The application of this RhoA biosensor revealed that 1 kPa gels ($n= 6$, $*p<0.05$), but not 5 or 8.5 kPa, led to a significantly reduced RhoA activity (Fig. 2-5A). These data indicate that the substrate rigidity can directly affect the RhoA activity of HMSCs. To directly examine whether the spontaneous Ca^{2+} oscillation can be regulated by RhoA, I transfected the FRET Ca^{2+}

biosensor with an empty vector, a constitutively active (RhoA-V14) or a dominant-negative (RhoA-N19) mutant of RhoA into HMSCs. Both RhoA-V14 and RhoA-N19 significantly reduced the percentile of HMSCs with oscillating Ca^{2+} signals (Fig. 2-5B), with 15.38% (4 of 26 cells) for RhoA-V14 and 4.76% (1 of 21 cells) for RhoA-N19 comparing to the control group (59.09%, 26 of 44 cells). These results suggest that RhoA and possibly its optimized/balanced activity are important for the Ca^{2+} oscillation in HMSCs.

2.3.6 RhoA is not sufficient to restore the Ca^{2+} oscillation modulated by substrate rigidity

I then examined whether the restore of RhoA activity is sufficient to rescue the Ca^{2+} oscillation in HMSCs cultured on soft substrate. The inhibition of the Ca^{2+} oscillation in HMSCs cultured on the 1kPa gel could not be alleviated when RhoA is activated by incubating the cells with LPA, co-transfection of RhoA-V14, or the combination of LPA and RhoA-V14 (Fig. 2-6). These results suggest that other factors, independent of RhoA, may also participate in regulating the Ca^{2+} oscillation in response to substrate rigidity.

2.4 Discussion

In this chapter, I have applied highly-sensitive Ca^{2+} biosensors containing ECFP and YPet as the FRET pair to monitor subcellular Ca^{2+} concentration in HMSCs. The results indicate that there is a spontaneous cytoplasmic Ca^{2+} oscillation in HMSCs, which is controlled by the Ca^{2+} traffic at the plasma membrane and ER membrane. The substrate rigidity can affect the Ca^{2+} oscillation, which is mediated by RhoA signaling pathway, but not by cytoskeleton and myosin.

However, RhoA alone is not sufficient in negating the substrate rigidity effects on the Ca^{2+} oscillation. Hence, our results suggest that RhoA is essential, but not sufficient in mediating the effect of substrate rigidity on Ca^{2+} oscillation in HMSCs. These results can also shed new lights on the molecular mechanism by which mechanical environment determines the destiny of stem cell commitment and differentiation.

Ca^{2+} oscillations encode diverse cellular processes such as cell division, differentiation, migration, fertilization and apoptosis (Berridge et al., 2003; Berridge et al., 2000). Both non-excitable and excitable cells display oscillatory Ca^{2+} signals (Berridge, 1993; Jacob, 1990; Tsien and Tsien, 1990). Spontaneous Ca^{2+} oscillations have been observed in several cell types, including pancreatic acinar cells, cardiac myocytes, oocytes and fibroblasts (Fewtrell, 1993; Kiselyov et al., 1999; Osipchuk et al., 1990). In this chapter, I have observed the spontaneous Ca^{2+} oscillation in 59 % HMSCs, consistent with a previous study (Kawano et al., 2002). The molecular mechanism and biological role of spontaneous Ca^{2+} oscillation, in particular in HMSCs, are poorly understood. It was shown that Ca^{2+} release from ER and Ca^{2+} influx via plasma membrane in HMSCs are regulated by InsP3Rs and SOCs, respectively, but not by L-type Ca^{2+} channels (Kawano et al., 2002). The contribution of Ca^{2+} release from ER to the cytoplasmic Ca^{2+} oscillation was also supported by the observation of Ca^{2+} oscillation in both cytoplasm and ER using FRET biosensors targeted at cytoplasm and ER (Fig. 2-1C-D). Consistently, our results indicate that the inhibition of Ca^{2+} flux at ER membrane abolished the oscillatory Ca^{2+} signals in cytoplasm (Fig. 2-2). However, I found that both SOCs and L-type Ca^{2+} channels at the plasma membrane are necessary for the spontaneous Ca^{2+} oscillation (Fig. 2-2B-D). While the discrepancy of our results and Kawano's on L-type Ca^{2+} is not clear, I reasoned that different developmental stages of HMSCs may play a role here. In fact, the

functional L-type Ca^{2+} channels can be detected after day 7 of murine embryoid bodies and is dependent on the differentiated state of cells (Gollasch et al., 1998; Kolossov et al., 1998).

Ca^{2+} oscillations play an important role in regulating cell differentiation (D'Souza et al., 2001; den Dekker et al., 2001). For example, the modulation of Ca^{2+} oscillation by electrical stimulation can promote osteo-differentiation of HMSCs (Sun et al., 2007). The substrate rigidity can also determine the differentiation fate of HMSCs (Engler et al., 2006). In the process of myofibrillogenesis, differentiation is regulated by substrate compliance and adhesive tension (Engler et al., 2004). In fact, Soft gels with well-controlled mechanical properties have been developed for stem cell culture (Dang et al., 2006; Li et al., 2006). These results showed that Ca^{2+} oscillations are significantly affected by the rigidity of the substrate gels where HMSCs are seeded (Fig. 2-3). Hence, the substrate rigidity may determine the commitment and differentiation of HMSCs via the regulation of Ca^{2+} oscillation. It, however, remains unclear as to the detailed molecular mechanism by which the substrate rigidity affects Ca^{2+} oscillation. It was postulated that substrates with different rigidity may regulate cellular functions by differentially altering signaling molecules and cytoskeletal structures involved in cell adhesion and force-sensing (Engler et al., 2007). It has also been shown that a remarkable change in cytoskeleton occurs when HMSCs differentiate into osteogenic cell types (Rodriguez et al., 2004) and that the Ca^{2+} oscillation in HMSCs was not observed in differentiated osteoblasts (Sun et al., 2007). It appears plausible that cytoskeleton may mediate the effects of substrate rigidity on the Ca^{2+} oscillation in HMSCs, as it is the case for differentiated cells, e.g. human umbilical vein endothelial cells (HUVECs) (Hayakawa et al., 2008). To our surprise, the disruption of neither actin filaments nor microtubules caused significant effect on the Ca^{2+} oscillation (Fig. 2-4).

These results suggest that the Ca^{2+} oscillation in HMSCs is independent of cytoskeletal actin filaments and microtubules.

It appears that the substrate rigidity may regulate Ca^{2+} oscillation via RhoA/ROCK signaling pathway. In fact, a specific ROCK inhibitor, Y-27632, decreased the frequency of the spontaneous Ca^{2+} oscillation (Fig. 2-4). LPA, an agonist for G protein coupled receptors (GPCR) and a known stimulator of RhoA/ROCK signaling pathway (Emmert et al., 2004; McBeath et al., 2004; Sun et al., 2007), inhibited the Ca^{2+} oscillation (Fig. 2-4). Consistently, the introduction of either active RhoA-V14 or negative RhoA-N19 into HMSCs inhibited the Ca^{2+} oscillation. These results suggest that a balanced RhoA/ROCK activity is essential for an optimized Ca^{2+} oscillation in HMSCs. Either the elevation or reduction of endogenous RhoA/ROCK activity may cause significant inhibitory effects on the Ca^{2+} oscillation. However, the inhibition of myosin light chain kinase (MLCK), a Ca^{2+}/calmodulin dependent kinase downstream to ROCK (Ducibella and Fissore, 2008; Soderling and Stull, 2001), did not have significant effect on the Ca^{2+} oscillation (Fig. 2-4). The difference between the effects of ROCK and MLCK on Ca^{2+} oscillation may be attributed to their different subcellular localization (Totsukawa et al., 2000; Wozniak et al., 2003). In addition, the ROCK may regulate myosin by the direct phosphorylation of MLC as well as the inhibition of MLC phosphatase (Amano et al., 1996; Kimura et al., 1996; Kureishi et al., 1997), bypassing the regulatory effect of MLCK on myosin phosphorylation (Wozniak et al., 2003). Surprisingly, blebbistatin, an inhibitor of myosin II, did not have significant effect on Ca^{2+} oscillation (Fig. 2-4). While the exact mechanism is unclear at the current stage, it is possible that molecules other than myosin may function downstream to RhoA and ROCK in regulating Ca^{2+} oscillation. This central role of RhoA/ROCK in mediating the effects of substrate rigidity on Ca^{2+} oscillation is consistent with previous reports that the

substrate rigidity can affect not only adhesions, but also RhoA/ROCK signaling pathway (Bhadriraju et al., 2007). Indeed, the RhoA/ROCK pathway was also documented to play important roles in Ca^{2+} sensitization for the contraction of smooth muscle and prostatic tissues (Kimura et al., 1996; Takahashi et al., 2007). It appears that mechanical environment has more profound impact on the Ca^{2+} oscillation than simply regulating RhoA/ROCK. In fact, the loss of Ca^{2+} oscillation on soft gels cannot be restored by increasing the intracellular tension via the introduction of RhoA-V14 or the incubation of LPA (Fig. 2-6). Therefore, some unknown molecules/mechanisms independent of RhoA/ROCK may also participate in the regulation of Ca^{2+} oscillation in response mechanical environment. Further studies are warranted to elucidate the underlying mechanism for this Ca^{2+} regulation by the substrate rigidity.

2.5 References

Albert AP, Large WA. 2003. Store-operated Ca2+-permeable non-selective cation channels in smooth muscle cells. Cell Calcium 33(5-6):345-356.

Amano M, Ito M, Kimura K, Fukata Y, Chihara K, Nakano T, Matsuura Y, Kaibuchi K. 1996. Phosphorylation and activation of myosin by Rho-associated kinase (Rho-kinase). J Biol Chem 271(34):20246-20249.

Berridge MJ. 1993. Inositol trisphosphate and calcium signalling. Nature 361(6410):315-325.

Berridge MJ, Bootman MD, Roderick HL. 2003. Calcium signalling: dynamics, homeostasis and remodelling. Nat Rev Mol Cell Biol 4(7):517-529.

Berridge MJ, Lipp P, Bootman MD. 2000. The versatility and universality of calcium signalling. Nat Rev Mol Cell Biol 1(1):11-21.

Bhadriraju K, Yang M, Alom Ruiz S, Pirone D, Tan J, Chen CS. 2007. Activation of ROCK by RhoA is regulated by cell adhesion, shape, and cytoskeletal tension. Exp Cell Res 313(16):3616-3623.

Bolotina VM. 2004. Store-operated channels: diversity and activation mechanisms. Sci STKE 2004(243):pe34.

Chiu WT, Tang MJ, Jao HC, Shen MR. 2008. Soft Substrate Up-regulates the Interaction of STIM1 with Store-operated Ca2+ Channels That Lead to Normal Epithelial Cell Apoptosis. Mol Biol Cell 19(5):2220-2230.

Clapham DE. 2007. Calcium signaling. Cell 131(6):1047-1058.

D'Souza SJ, Pajak A, Balazsi K, Dagnino L. 2001. Ca2+ and BMP-6 signaling regulate E2F during epidermal keratinocyte differentiation. J Biol Chem 276(26):23531-23538.

Dang JM, Sun DD, Shin-Ya Y, Sieber AN, Kostuik JP, Leong KW. 2006. Temperature-responsive hydroxybutyl chitosan for the culture of mesenchymal stem cells and intervertebral disk cells. Biomaterials 27(3):406-418.

den Dekker E, Molin DG, Breikers G, van Oerle R, Akkerman JW, van Eys GJ, Heemskerk JW. 2001. Expression of transient receptor potential mRNA isoforms and Ca(2+) influx in differentiating human stem cells and platelets. Biochim Biophys Acta 1539(3):243-255.

Discher DE, Janmey P, Wang YL. 2005. Tissue cells feel and respond to the stiffness of their substrate. Science 310(5751):1139-1143.

Ducibella T, Fissore R. 2008. The roles of Ca2+, downstream protein kinases, and oscillatory signaling in regulating fertilization and the activation of development. Dev Biol 315(2):257-279.

Emmert DA, Fee JA, Goeckeler ZM, Grojean JM, Wakatsuki T, Elson EL, Herring BP, Gallagher PJ, Wysolmerski RB. 2004. Rho-kinase-mediated Ca2+-independent contraction in rat embryo fibroblasts. Am J Physiol Cell Physiol 286(1):C8-21.

Engler AJ, Griffin MA, Sen S, Bonnemann CG, Sweeney HL, Discher DE. 2004. Myotubes differentiate optimally on substrates with tissue-like stiffness: pathological implications for soft or stiff microenvironments. J Cell Biol 166(6):877-887.

Engler AJ, Sen S, Sweeney HL, Discher DE. 2006. Matrix elasticity directs stem cell lineage specification. Cell 126(4):677-689.

Engler AJ, Sweeney HL, Discher DE, Schwarzbauer JE. 2007. Extracellular matrix elasticity directs stem cell differentiation. J Musculoskelet Neuronal Interact 7(4):335.

Fewtrell C. 1993. Ca2+ oscillations in non-excitable cells. Annu Rev Physiol 55:427-454.

Foskett JK, White C, Cheung KH, Mak DO. 2007. Inositol trisphosphate receptor Ca2+ release channels. Physiol Rev 87(2):593-658.

Gollasch M, Haase H, Ried C, Lindschau C, Morano I, Luft FC, Haller H. 1998. L-type calcium channel expression depends on the differentiated state of vascular smooth muscle cells. Faseb J 12(7):593-601.

Gronthos S, Zannettino AC, Graves SE, Ohta S, Hay SJ, Simmons PJ. 1999. Differential cell surface expression of the STRO-1 and alkaline phosphatase antigens on discrete developmental stages in primary cultures of human bone cells. J Bone Miner Res 14(1):47-56.

Hayakawa K, Tatsumi H, Sokabe M. 2008. Actin stress fibers transmit and focus force to activate mechanosensitive channels. J Cell Sci 121(Pt 4):496-503.

Jacob R. 1990. Calcium oscillations in electrically non-excitable cells. Biochim Biophys Acta 1052(3):427-438.

Kassab GS. 2006. Biomechanics of the cardiovascular system: the aorta as an illustratory example. J R Soc Interface 3(11):719-740.

Kassem M, Abdallah BM. 2008. Human bone-marrow-derived mesenchymal stem cells: biological characteristics and potential role in therapy of degenerative diseases. Cell Tissue Res 331(1):157-163.

Kawano S, Shoji S, Ichinose S, Yamagata K, Tagami M, Hiraoka M. 2002. Characterization of Ca(2+) signaling pathways in human mesenchymal stem cells. Cell Calcium 32(4):165-174.

Kimura K, Ito M, Amano M, Chihara K, Fukata Y, Nakafuku M, Yamamori B, Feng J, Nakano T, Okawa K, Iwamatsu A, Kaibuchi K. 1996. Regulation of myosin phosphatase by Rho and Rho-associated kinase (Rho-kinase). Science 273(5272):245-248.

Kiselyov KI, Semyonova SB, Mamin AG, Mozhayeva GN. 1999. Miniature Ca2+ channels in excised plasma-membrane patches: activation by IP3. Pflugers Arch 437(2):305-314.

Kolossov E, Fleischmann BK, Liu Q, Bloch W, Viatchenko-Karpinski S, Manzke O, Ji GJ, Bohlen H, Addicks K, Hescheler J. 1998. Functional characteristics of ES cell-derived cardiac precursor cells identified by tissue-specific expression of the green fluorescent protein. J Cell Biol 143(7):2045-2056.

Kureishi Y, Kobayashi S, Amano M, Kimura K, Kanaide H, Nakano T, Kaibuchi K, Ito M. 1997. Rho-associated kinase directly induces smooth muscle contraction through myosin light chain phosphorylation. J Biol Chem 272(19):12257-12260.

Laurent VM, Canadas P, Fodil R, Planus E, Asnacios A, Wendling S, Isabey D. 2002. Tensegrity behaviour of cortical and cytosolic cytoskeletal components in twisted living adherent cells. Acta Biotheor 50(4):331-356.

Lewis RS. 2007. The molecular choreography of a store-operated calcium channel. Nature 446(7133):284-287.

Li Q, Wang J, Shahani S, Sun DD, Sharma B, Elisseeff JH, Leong KW. 2006. Biodegradable and photocrosslinkable polyphosphoester hydrogel. Biomaterials 27(7):1027-1034.

Li S, Chen BP, Azuma N, Hu YL, Wu SZ, Sumpio BE, Shyy JY, Chien S. 1999. Distinct roles for the small GTPases Cdc42 and Rho in endothelial responses to shear stress. J Clin Invest 103(8):1141-1150.

McBeath R, Pirone DM, Nelson CM, Bhadriraju K, Chen CS. 2004. Cell shape, cytoskeletal tension, and RhoA regulate stem cell lineage commitment. Dev Cell 6(4):483-495.

Misquitta CM, Mack DP, Grover AK. 1999. Sarco/endoplasmic reticulum Ca2+ (SERCA)-pumps: link to heart beats and calcium waves. Cell Calcium 25(4):277-290.

Miyawaki A, Llopis J, Heim R, McCaffery JM, Adams JA, Ikura M, Tsien RY. 1997. Fluorescent indicators for Ca2+ based on green fluorescent proteins and calmodulin. Nature 388(6645):882-887.

Morita M, Higuchi C, Moto T, Kozuka N, Susuki J, Itofusa R, Yamashita J, Kudo Y. 2003. Dual regulation of calcium oscillation in astrocytes by growth factors and pro-inflammatory cytokines via the mitogen-activated protein kinase cascade. J Neurosci 23(34):10944-10952.

Nguyen AW, Daugherty PS. 2005. Evolutionary optimization of fluorescent proteins for intracellular FRET. Nat Biotechnol 23(3):355-360.

Nilius B. 2004. Store-operated Ca2+ entry channels: still elusive! Sci STKE 2004(243):pe36.

Osipchuk YV, Wakui M, Yule DI, Gallacher DV, Petersen OH. 1990. Cytoplasmic Ca2+ oscillations evoked by receptor stimulation, G-protein activation, internal application of inositol trisphosphate or Ca2+: simultaneous microfluorimetry and Ca2+ dependent Cl- current recording in single pancreatic acinar cells. Embo J 9(3):697-704.

Ouyang M, Sun J, Chien S, Wang Y. 2008 Determination of hierarchical relationship of Src and Rac at subcellular locations with FRET biosensors. *Proc Natl Acad Sci USA.*In Press

Palmer AE, Jin C, Reed JC, Tsien RY. 2004. Bcl-2-mediated alterations in endoplasmic reticulum Ca2+ analyzed with an improved genetically encoded fluorescent sensor. Proc Natl Acad Sci U S A 101(50):17404-17409.

Pelham RJ, Jr., Wang Y. 1997. Cell locomotion and focal adhesions are regulated by substrate flexibility. Proc Natl Acad Sci U S A 94(25):13661-13665.

Periasamy M, Kalyanasundaram A. 2007. SERCA pump isoforms: their role in calcium transport and disease. Muscle Nerve 35(4):430-442.

Rodriguez JP, Gonzalez M, Rios S, Cambiazo V. 2004. Cytoskeletal organization of human mesenchymal stem cells (MSC) changes during their osteogenic differentiation. J Cell Biochem 93(4):721-731.

Rosada C, Justesen J, Melsvik D, Ebbesen P, Kassem M. 2003. The human umbilical cord blood: a potential source for osteoblast progenitor cells. Calcif Tissue Int 72(2):135-142.

Soderling TR, Stull JT. 2001. Structure and regulation of calcium/calmodulin-dependent protein kinases. Chem Rev 101(8):2341-2352.

Solon J, Levental I, Sengupta K, Georges PC, Janmey PA. 2007. Fibroblast adaptation and stiffness matching to soft elastic substrates. Biophys J 93(12):4453-4461.

Sun S, Liu Y, Lipsky S, Cho M. 2007. Physical manipulation of calcium oscillations facilitates osteodifferentiation of human mesenchymal stem cells. Faseb J 21(7):1472-1480.

Takahashi R, Nishimura J, Seki N, Yunoki T, Tomoda T, Kanaide H, Naito S. 2007. RhoA/Rho kinase-mediated Ca2+ sensitization in the contraction of human prostate. Neurourol Urodyn 26(4):547-551.

Torihashi S, Fujimoto T, Trost C, Nakayama S. 2002. Calcium oscillation linked to pacemaking of interstitial cells of Cajal: requirement of calcium influx and localization of TRP4 in caveolae. J Biol Chem 277(21):19191-19197.

Totsukawa G, Yamakita Y, Yamashiro S, Hartshorne DJ, Sasaki Y, Matsumura F. 2000. Distinct roles of ROCK (Rho-kinase) and MLCK in spatial regulation of MLC phosphorylation for assembly of stress fibers and focal adhesions in 3T3 fibroblasts. J Cell Biol 150(4):797-806.

Tsien RW, Tsien RY. 1990. Calcium channels, stores, and oscillations. Annu Rev Cell Biol 6:715-760.

Wang Y, Shyy JY-J, Chien S. 2008. Fluorescence Proteins, Live Cell Imaging, and Mechanobiology: Seeing is Believing. Annu Rev Biomed Eng 10:In Press.

Wehrens XH, Lehnart SE, Marks AR. 2005. Intracellular calcium release and cardiac disease. Annu Rev Physiol 67:69-98.

Wozniak MA, Desai R, Solski PA, Der CJ, Keely PJ. 2003. ROCK-generated contractility regulates breast epithelial cell differentiation in response to the physical properties of a three-dimensional collagen matrix. J Cell Biol 163(3):583-595.

Yeung T, Georges PC, Flanagan LA, Marg B, Ortiz M, Funaki M, Zahir N, Ming W, Weaver V, Janmey PA. 2005. Effects of substrate stiffness on cell morphology, cytoskeletal structure, and adhesion. Cell Motil Cytoskeleton 60(1):24-34.

Yoshizaki H, Ohba Y, Kurokawa K, Itoh RE, Nakamura T, Mochizuki N, Nagashima K, Matsuda M. 2003. Activity of Rho-family GTPases during cell division as visualized with FRET-based probes. J Cell Biol 162(2):223-232.

Zhang J, Campbell RE, Ting AY, Tsien RY. 2002. Creating new fluorescent probes for cell biology. Nat Rev Mol Cell Biol 3(12):906-918.

2.6 Figures

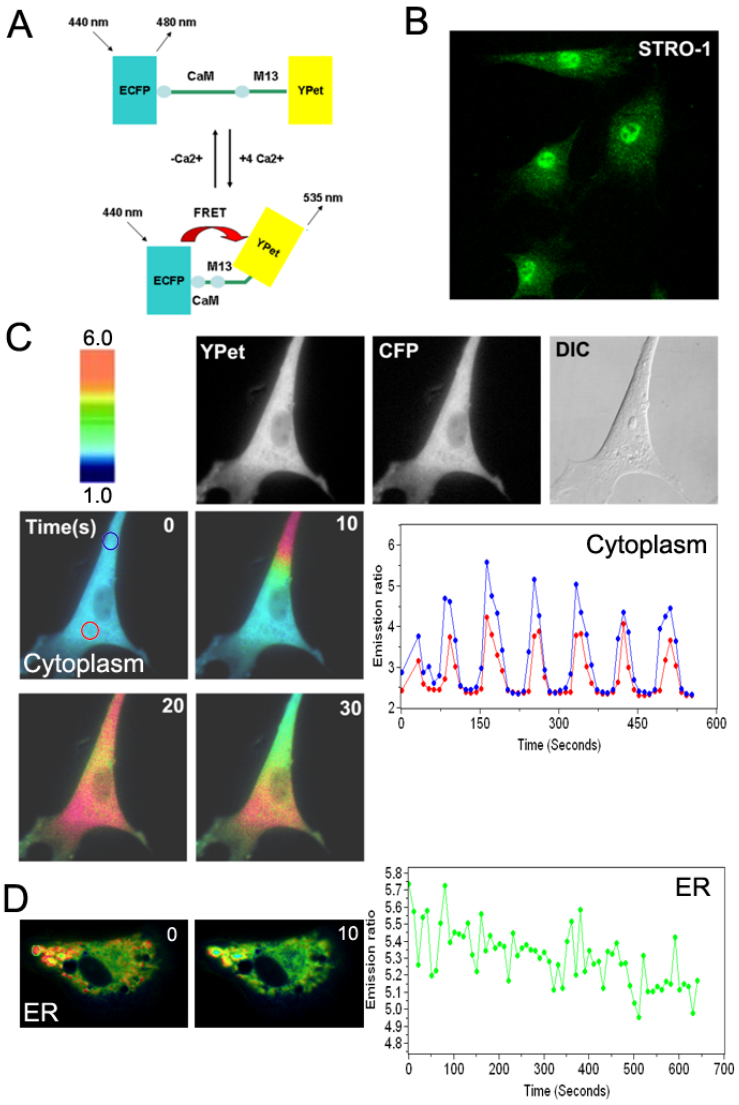

Figure 2-1. The application of FRET-based Ca^{2+} biosensors in human mesenchymal stem cells (HMSCs). (**A**): A schematic drawing of the activation mechanism of the Ca^{2+} FRET biosensor. (**B**): HMSCs were immunostained by monoclonal antibody against STRO-1, a MSCs marker. (**C**) The FRET change of the Ca^{2+} biosensor targeted at cytoplasm. HMSCs were transfected with the cytoplasmic Ca^{2+} biosensor, which visualized a spontaneous Ca^{2+} oscillation. Color images represent the YPet/ECFP emission ratio of the cytoplasmic Ca^{2+} biosensor. The color scale bar represents the YPet/CFP emission ratio, with cold and hot colors indicating low and high levels of Ca^{2+} concentration, respectively. The time course curves represent the YPet/CFP emission ratio averaged over regions on (blue) and distal (red) to the triggering corner. (**D**) The color images and time course curves represent the oscillatory FRET changes of the Ca^{2+} biosensor targeted inside ER.

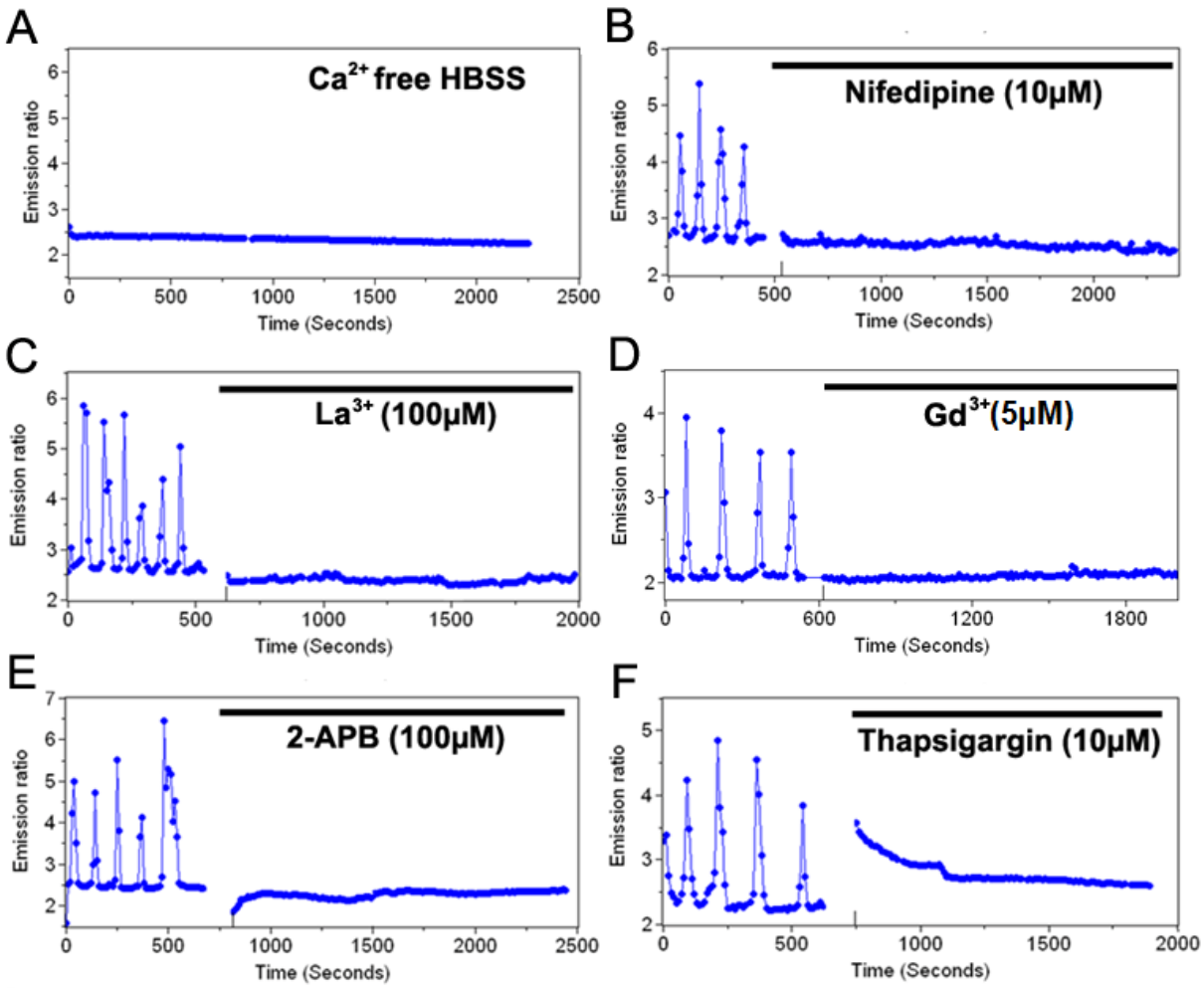

Figure 2-2. The spontaneous Ca^{2+} oscillations in HMSCs are regulated by Ca^{2+} traffic across the plasma membrane and ER membrane. (**A**): The time course represents the cytoplasmic Ca^{2+} concentration in Ca^{2+} free buffer solution. (**B**-**D**): The time course represents the cytoplasmic Ca^{2+} concentration in cells pre-treated with (**B**) 10μM nifedipine, a L-type Ca^{2+} channel blocker, or (**C**) 100μM $LaCl_3$ or (**D**) 5μM $GdCl_3$, SOC blockers. (**E**) and (**F**): The time course represents the cytoplasmic Ca^{2+} concentration in cells pre-treated with (**E**) 100μM 2-APB, an InsP3R blocker, or (**F**) 10μM thapsigargin, a SERCA pump blocker.

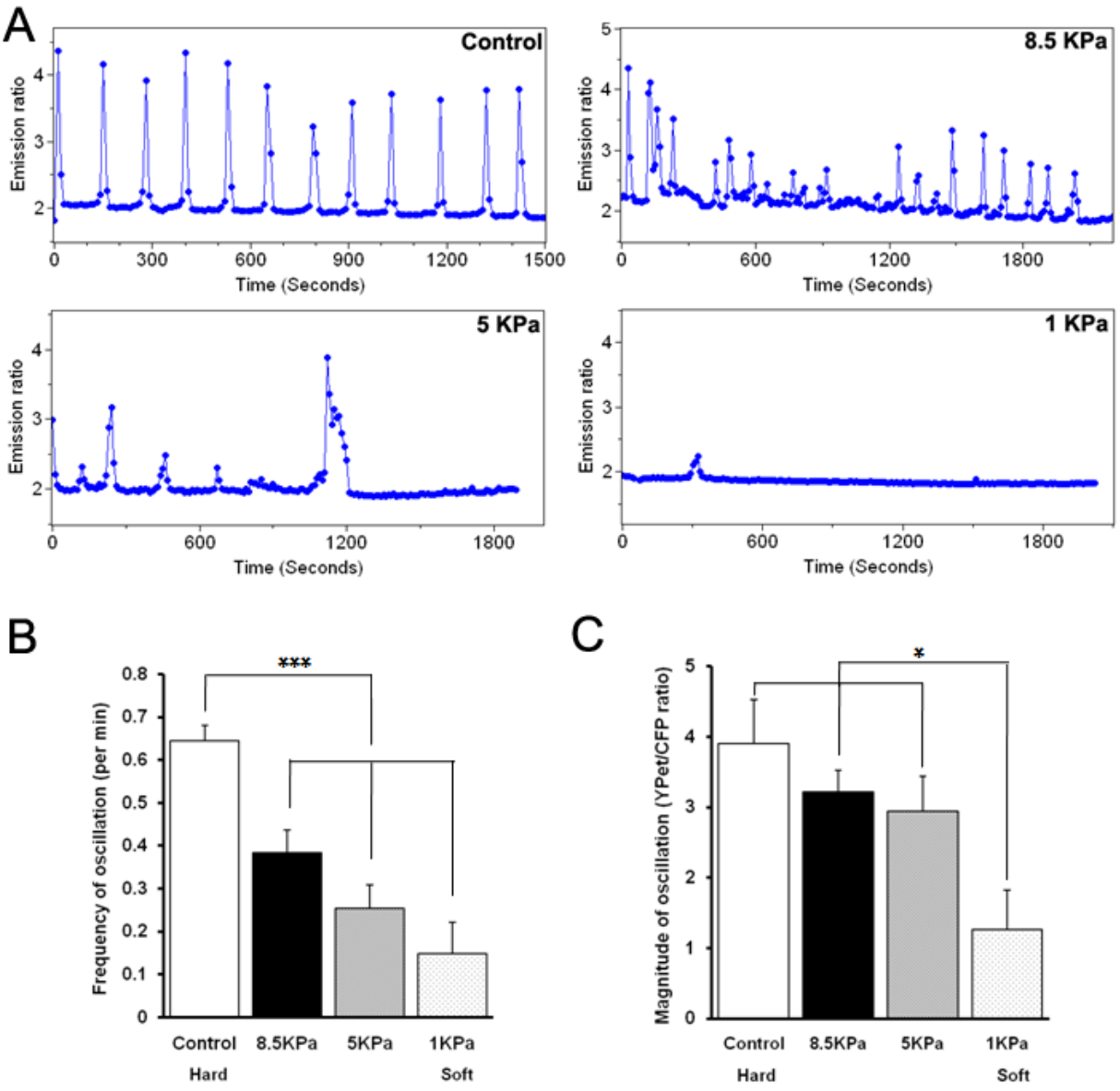

Figure 2-3. The effect of substrate stiffness on the spontaneous Ca^{2+} oscillation. (**A**): The time courses represent the cytoplasmic Ca^{2+} concentrations in cells cultured on gels with different rigidity, as indicated. (**B**) and (**C**): Bar graphs (mean ± S.E.M.) represent the (**B**) frequency and (**C**) magnitude of spontaneous Ca^{2+} oscillations in cells cultured on gels with different rigidity, as indicated. Error bars indicate standard errors of mean; *p<0.05; ***P<0.001, n=6

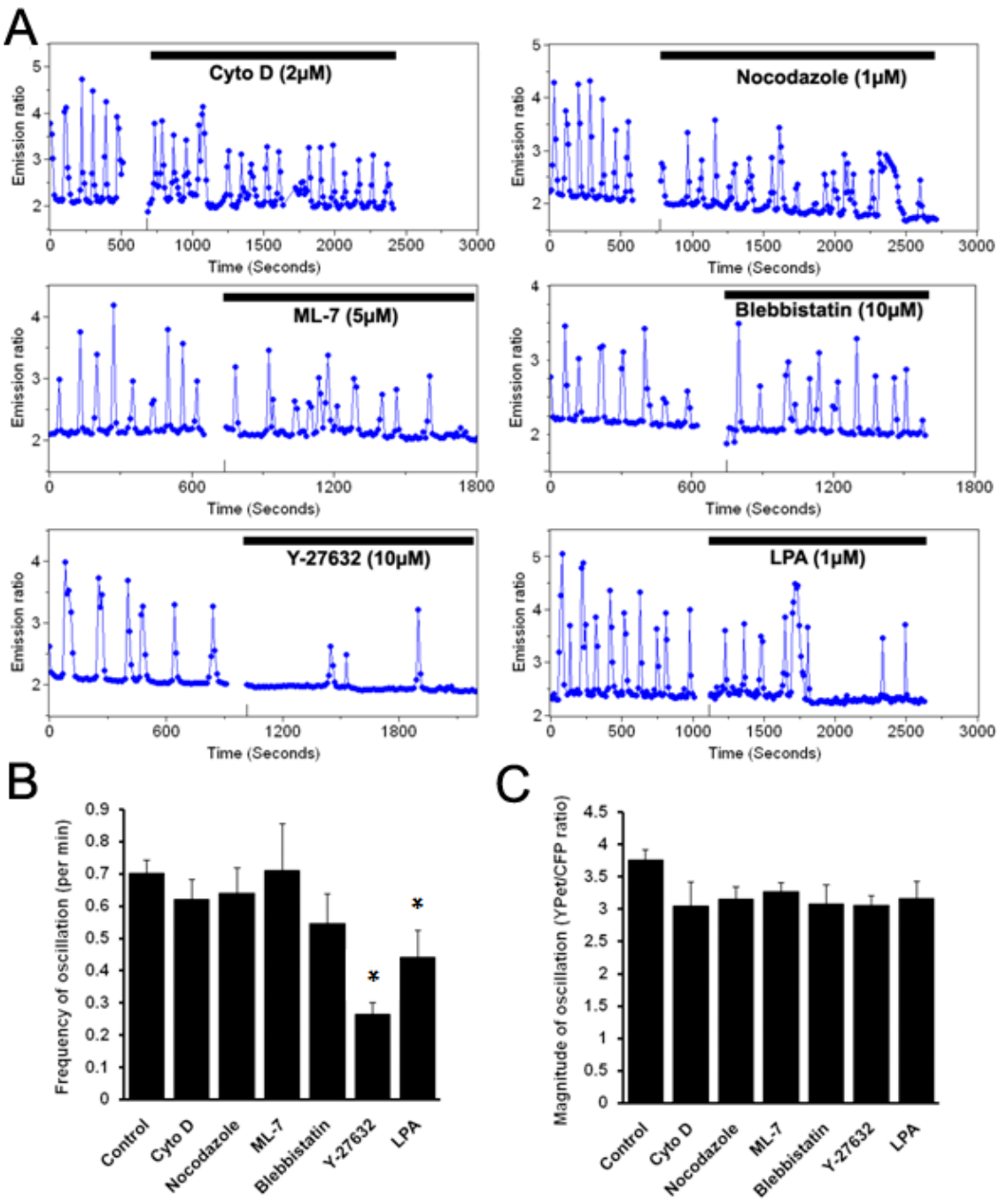

Figure 2-4. The roles of the cytoskeleton and RhoA signaling pathway on the spontaneous cytoplasmic Ca^{2+} oscillation. (**A**): Representative time courses of the cytoplasmic Ca^{2+} concentration in cells pre-treated with Cyto D (2μM, n=3), Noc (1μM, n=3), ML-7 (5μM, n=5), blebbistatin (10μM, n=5), Y-27632 (10μM, n=5), and LPA (1μM, n=10). (**B**) and (**C**): Bar graphs (mean ± S.E.M.) represent the (**B**) frequency and (**C**) magnitude of spontaneous Ca^{2+} oscillations in cells pretreated with different reagents, as indicated. Error bars indicate standard errors of mean; *$p<0.05$.

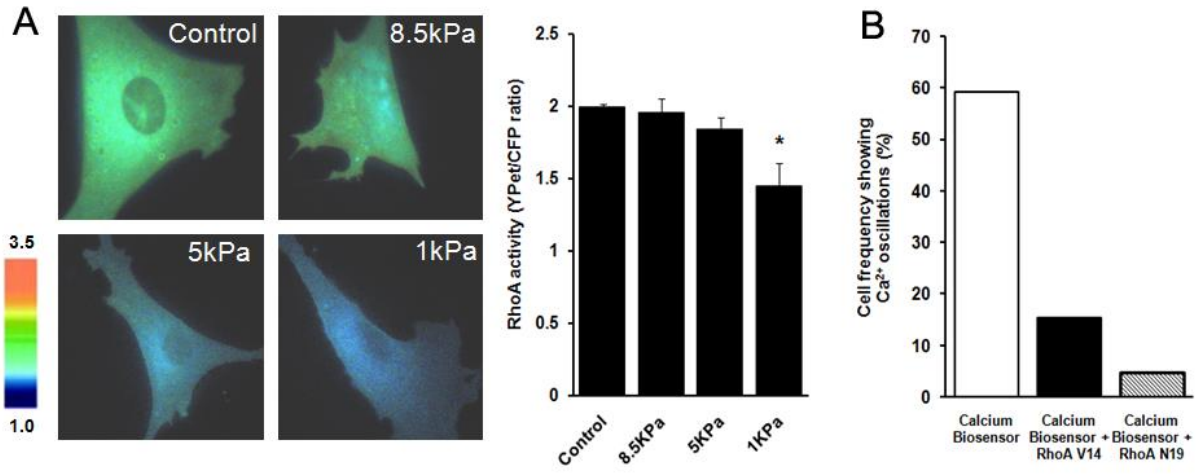

Figure 2-5. The substrate rigidity affects the endogenous RhoA activity, which mediates the Ca^{2+} oscillation in HMSCs. (**A**): Left: the YFP/CFP emission ratio images of cells transfected with the RhoA biosensor on different substrate gels; Right: bar graphs represent the endogenous RhoA activity (mean ± S.E.M.) measured by the RhoA FRET biosensor. (**B**): Bar graphs represent the percentile of HMSCs showing Ca^{2+} oscillations in cells transfected with the control vector, an active RhoA-V14, or a negative RhoA-N19. Error bars indicate standard errors of mean; *$p<0.05$., n=6

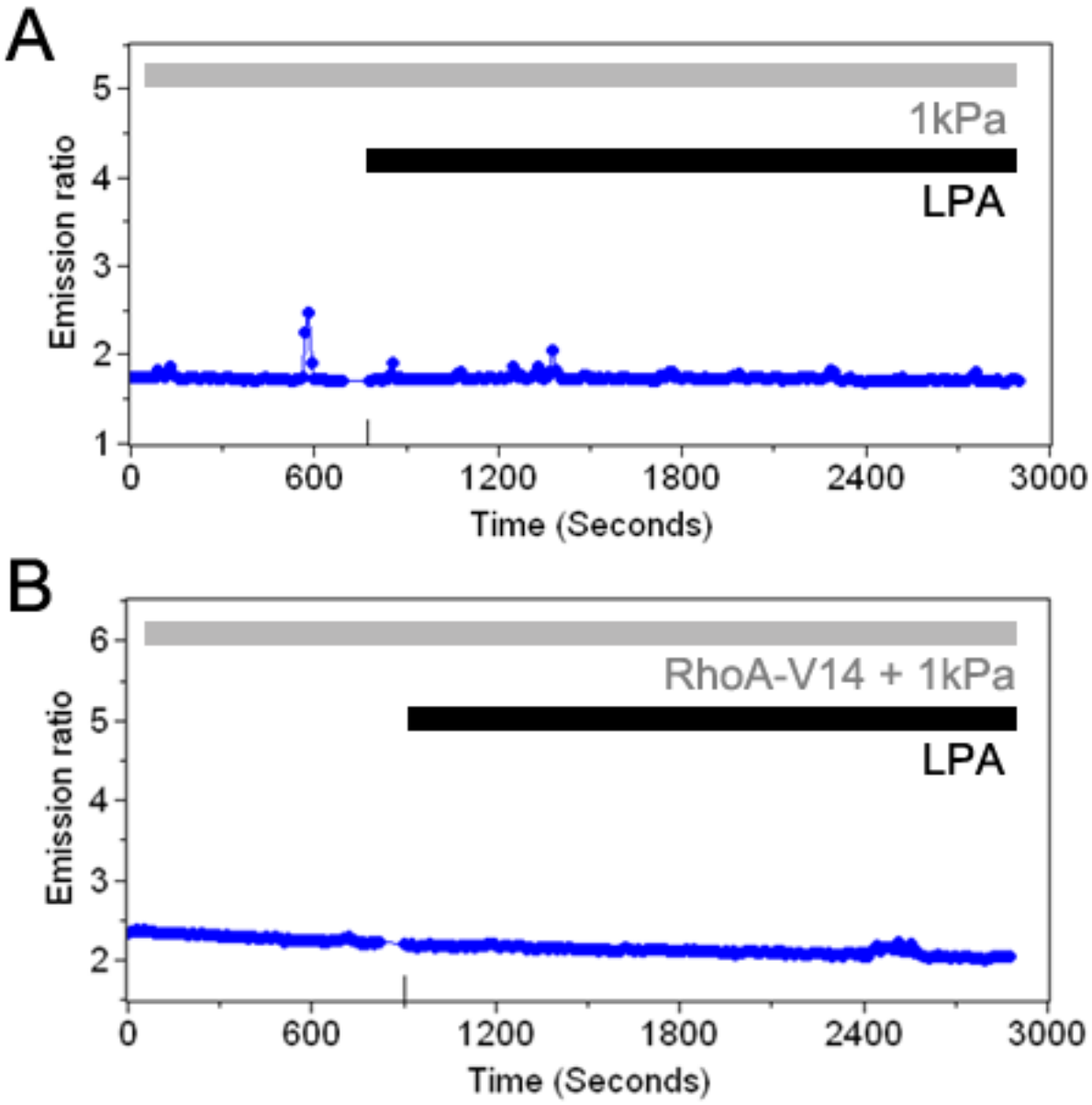

Figure 2-6. Ca^{2+} oscillations in HMSCs on soft gels were not restored by the activation of RhoA. Time courses represent the cytoplasmic Ca^{2+} oscillations before and after LPA stimulation in HMSCs cultured on 1 kPa gels and transfected (**A**) with or (**B**) without active RhoA-V14.

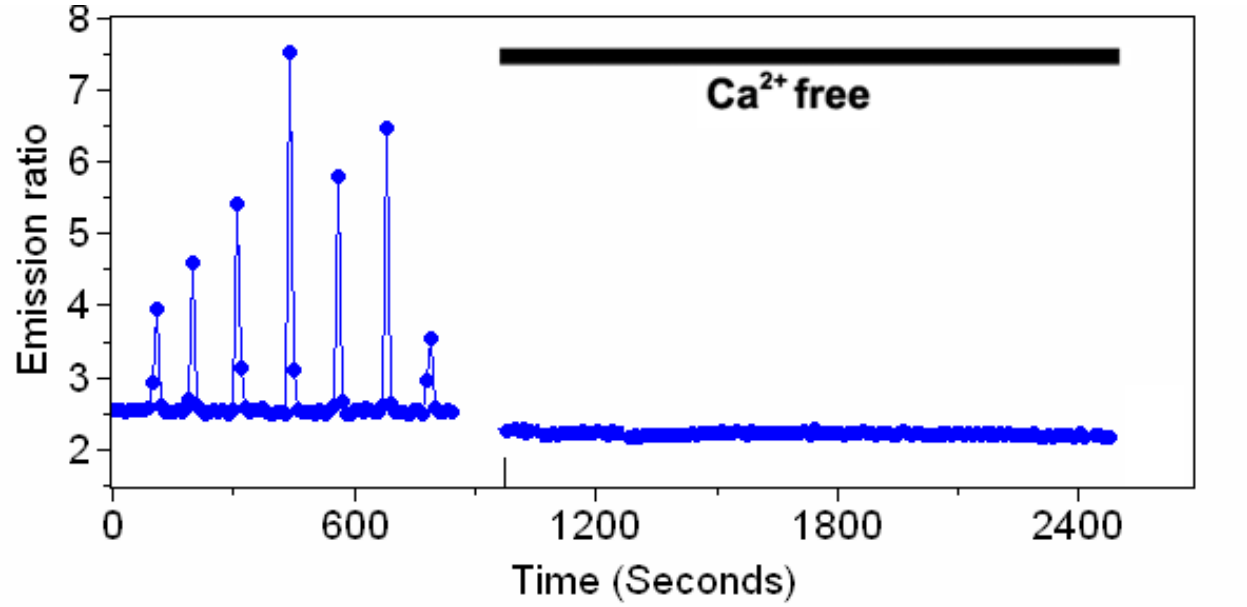

Supplementary Figure S2-1. The effect of removal of extracellular Ca^{2+}. After replacing Ca^{2+} free buffer solution, Ca^{2+} oscillations were immediately disappeared

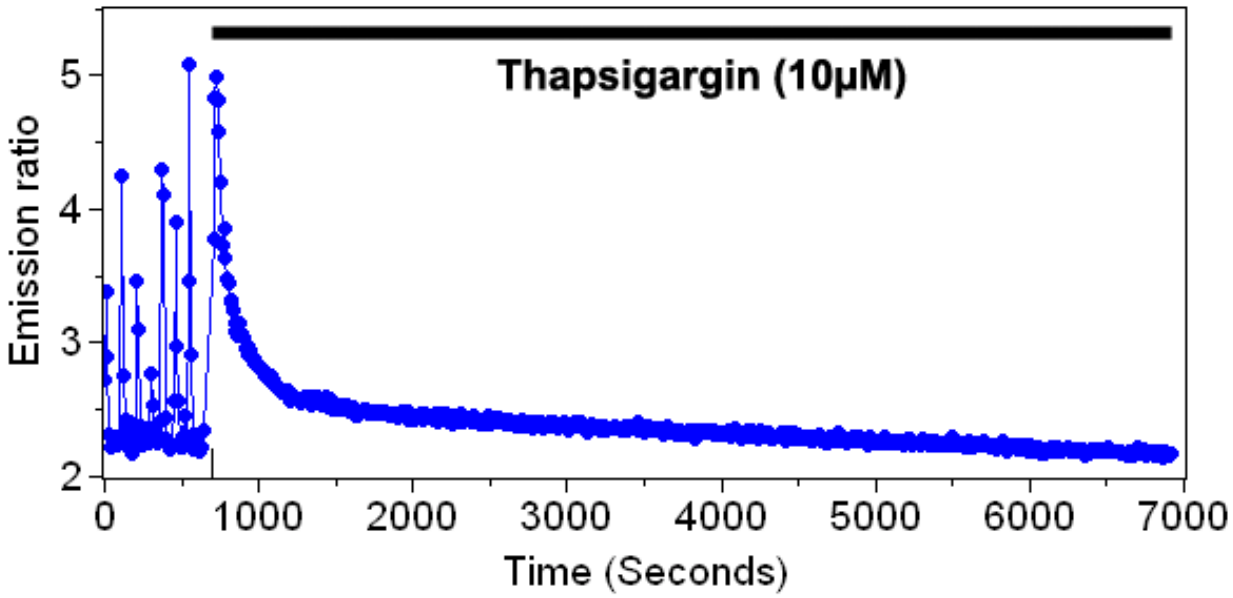

Supplementary Figure S2-2. TG-mediated Ca^{2+} signals in HMSCs. After TG treatment, although the elevated Ca^{2+} levels have returned to basal level, any Ca^{2+} oscillation was not restored.

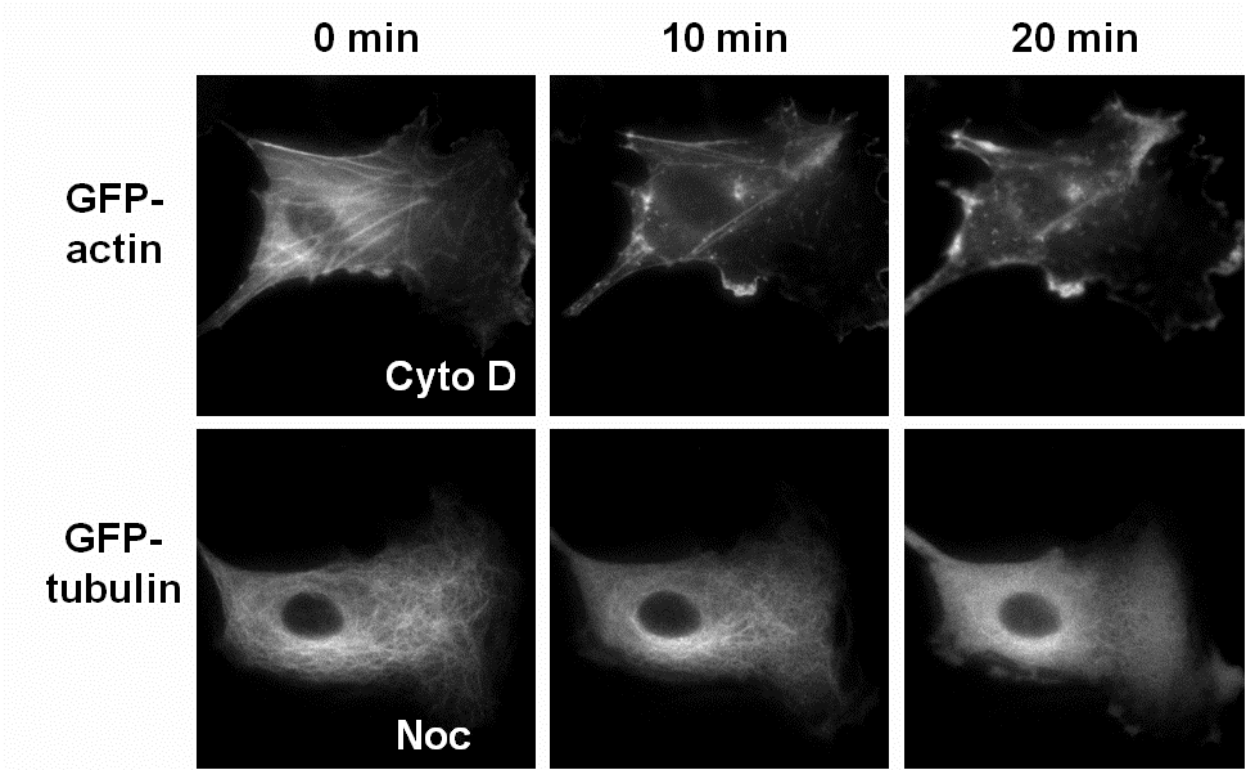

Supplementary Figure S2-3. The effect of cyto D and nocodazole in HMSCs expressing GFP-actin and GFP-tubulin. Cyto D (2μM) and nocodazole (1μM) destroyed the actin filaments and microtubules effectively within 20 min.

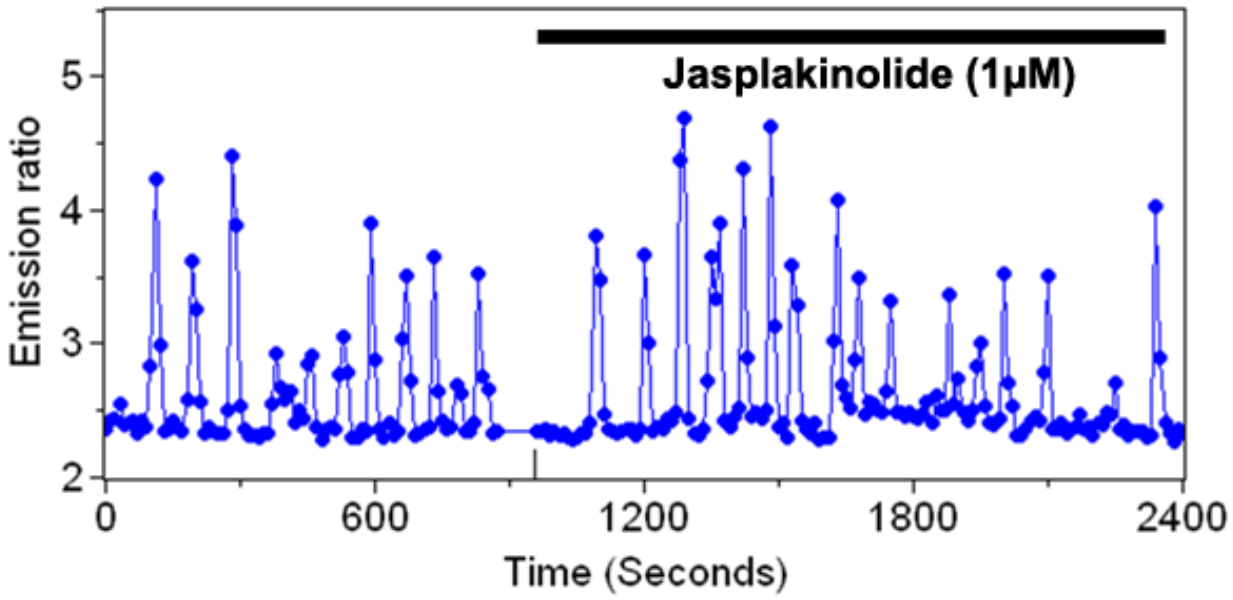

Supplementary. Figure S2-4. The effect of polymerization of actin filaments on HMSCs. Jasplakinolide (1μM) stabilizing and inducing polymerization of the actin filaments does not affect spontaneous Ca2+ oscillations in HMSCs.

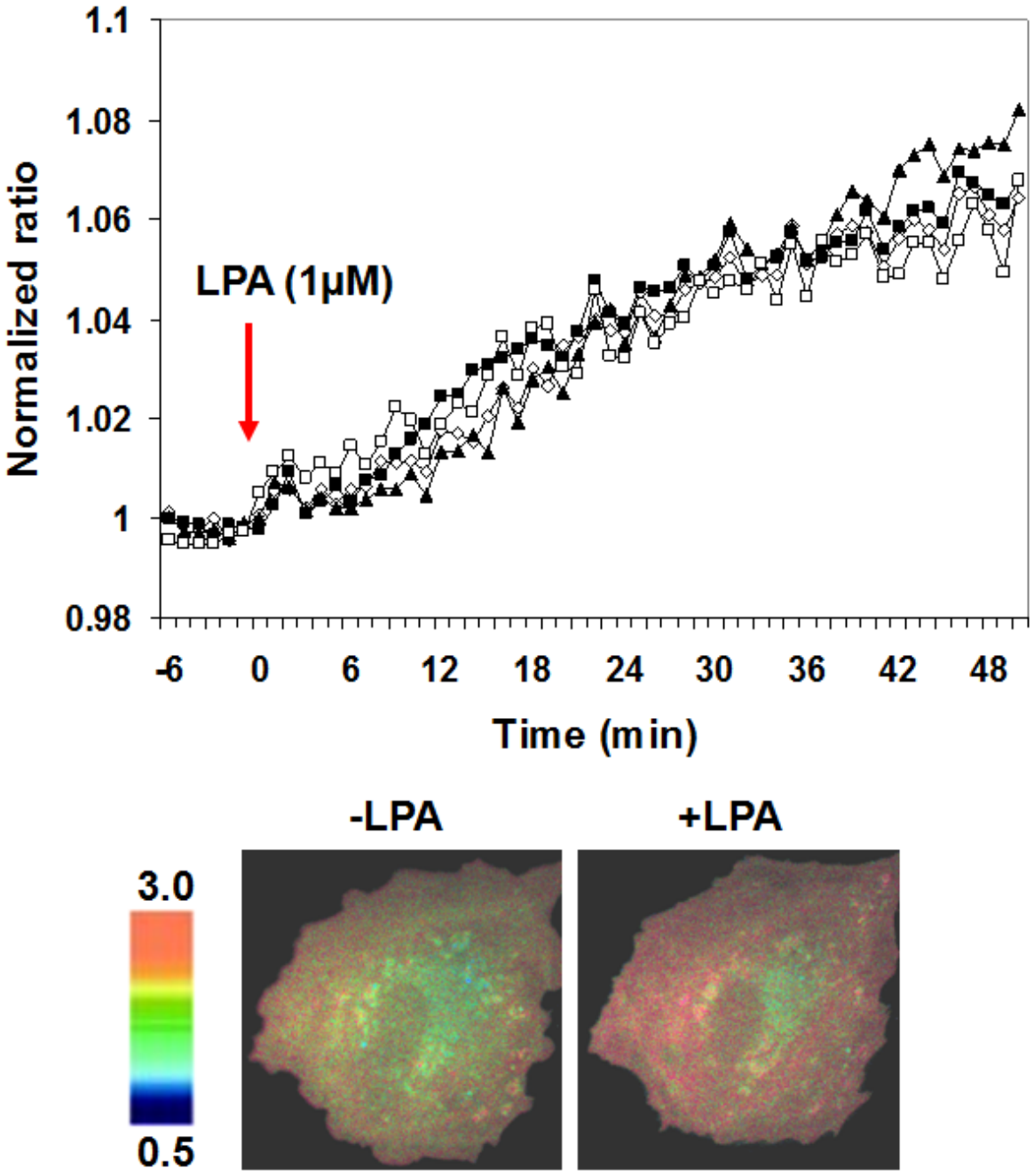

Supplementary Figure S2-5. Treatment of LPA in HMSCs transfected with RhoA biosensor. LPA increased RhoA FRET ratio, representing an elevated RhoA activity. Color images denote the YFP/CFP emission ratio of the RhoA biosensor. The color scale bar represents the YFP/CFP emission ratio, with cold and hot colors indicating low and high levels of Ca^{2+} concentration, respectively.

CHAPTER 3

DISTINCT CALCIUM SIGNALING IN RESPONSE TO MECHANICAL STIMULATION

Mechanical environment plays pivotal roles in regulating stem cell commitment and functions. However, it remains unclear on how mechanical stimuli are transmitted into biochemical signals in stem cells. In this chapter, I investigated the molecular and biophysical mechanisms by which mechanical forces regulate Ca^{2+} signaling in human mesenchymal stem cells (HMSCs), integrating genetically encoded Ca^{2+} biosensor based on fluorescence resonance energy transfer (FRET) and optical laser tweezers. Laser-tweezer-traction of the cell membrane induces intracellular Ca^{2+} oscillations caused by Ca^{2+} release from endoplasmic reticulum (ER) in the absence of extracellular Ca^{2+}. These force-induced Ca^{2+} oscillations produced by ER Ca^{2+} release are mediated not only by the mechanical support of cytoskeleton and actomyosin contractility, but also by mechanosensitive Ca^{2+} channels on the plasma membrane, specifically TRPM7. When the ER Ca^{2+} release is inhibited and the extracellular Ca^{2+} level is restored, laser-tweezer-traction of the cell can induce the intracellular Ca^{2+} increase, which is mediated by the cytoskeletal structure but not actomyosin contractility. Taken together, these results indicate that active actomyosin contractility regulated by MLCK and myosin II is essential for the force transmission into the deep intracellular organelles but dispensable for the mechanical regulation of plasma membrane channels.

3.1 Introduction

Mechanical forces transferred to cells have been regarded as one of the crucial factors influencing cellular signal transduction, referred as mechanotransduction. However, it remains unclear on how these mechanical forces can be converted into biochemical responses in individual cells. Cell surface receptors such as integrins and cadherins physically couple the cytoskeleton to extracellular matrix (ECM) or to neighboring cells (Ingber, 1997; Wang et al., 2000). Mechanical forces can hence be perceived at the cell membrane and possibly transmitted by these receptor into intracellular signals to trigger downstream molecular events that consequently lead to mechanical force-dependent changes in gene expressions and cellular processes (Chien, 2007; Orr et al., 2006; Vogel and Sheetz, 2006).

Calcium ion (Ca^{2+}) is involved in a wide range of cellular processes, including muscle contraction, embryogenesis, cell differentiation, proliferation, gene expression, secretion, learning and memory, and apoptosis (Berridge et al., 2000; Clapham, 2007; Landsberg and Yuan, 2004; Maeda et al., 2007; Mckinsey et al., 2002; Rong and Distelhorst, 2008; West et al., 2001). Ca^{2+} signals can function in waves or sparks to mediate the cell-to-cell communication and various other signal transductions (Guan et al., 2007). Recently, it has been discovered that mechanical stimuli can affect intracellular Ca^{2+} signaling and subsequently regulate cellular functions. For example, Ca^{2+} is necessary for the activation of development in Drosophila oocytes, which can be triggered by mechanical stimuli such as osmotic and hydrostatic pressure (Horner and Wolfner, 2008). Shear fluid flow was shown to induce the accumulation and release of Ca^{2+} in mitochondria of cardiac myocytes (Belmonte and Morad, 2008). Such shear forces can also induce the translocation of TRPM7 channel, a stretch-activated Ca^{2+} channel, to the plasma membrane in vascular smooth muscle cells (Oancea et al., 2006). In addition, it has been

reported that mechanical forces generated by pulling attached beads on the cell membrane of vascular smooth muscle cells can trigger Ca^{2+} sparks, followed by global Ca^{2+} mobilization (Balasubramanian et al., 2007). This kind of mechanical stimulation upon laser tweezers traction can also activate mechanosensitive Ca^{2+} channel and subsequently cause a local intracellular Ca^{2+} increase near focal adhesions in human umbilical vein endothelial cells (Hayakawa et al., 2008). In addition, mechanical forces applied to beta 1 integrins induce ultra-rapid activation of intracellular Ca^{2+} increase which can be mediated by TRPV4 channels (Matthews et al., 2010).

Mechanical forces also play crucial roles in regulating the development and function of stem cells. In fact, mechanical forces such as shear stress can affect embryogenesis, vascular cell fate and osteogenic differentiation (Stolberg and McCloskey, 2009). It can activate mechanosensitive ion channels, membrane receptors, and structural elements to regulate the expression of a variety of genes (Barakat et al., 2006; Chen et al., 2000). Mechanical environment has also been reported to play important roles in regulating the differentiation and commitment of HMSCs (Engler et al., 2006; Park et al., 2004). Although stem cells have differential Ca^{2+} signals when they are seeded under mechanical environment with different stiffness (Kim et al., 2009), it remains unclear on whether and how mechanical loading can affect Ca^{2+} signaling in HMSCs.

Optical laser tweezers can provide a precise and powerful tool to apply mechanical stimulation at subcellular levels. When a bead is mechanically coupled to a cell surface through the ligation of membrane adhesion receptors, the forces generated in the bead by laser tweezers can be transmitted into the cell at subcellular locations to trigger signal transduction and regulate cellular functions (Berns, 2007; Botvinick and Wang, 2007). With biosensors based on fluorescence resonance energy transfer (FRET) to detect protein-protein interaction and

enzymatic activities (Zhang et al., 2002), the dynamic molecular signals in response to these mechanical stimuli can be visualized at subcellular levels. In fact, this FRET technology has been applied in combination with optical laser tweezers to visualize the Src activation at the plasma membrane (Wang et al., 2005). In this chapter, I investigated whether and how mechanical forces can physically regulate Ca^{2+} signals in HMSCs, utilizing FRET based Ca^{2+} biosensors (Miyawaki et al., 1997; Ouyang et al., 2008) and optical laser tweezers. Mechanical forces were shown to induce Ca^{2+} release from the endoplasmic reticulum (ER) and intracellular Ca^{2+} oscillations in the absence of extracellular Ca^{2+}. This transmission of force is dependent on the passive cytoskeletal support as well as active actomyosin contractility. In contrast, the Ca^{2+} influx in the absence of ER Ca^{2+} release induced by mechanical force is dependent only on the passive cytoskeletal support, but not on the active actomyosin contractility. Our results hence suggest differential regulation mechanisms for the ER Ca^{2+} release and the Ca^{2+} influx across the plasma membrane under mechanical stimulation.

3.2 Materials and Methods

3.2.1 Gene Construction and DNA Plasmid

The construct of FRET-based Ca^{2+} biosensor has been described well in our previous articles (Kim et al., 2009; Ouyang et al., 2008). In brief, the fragment containing enhanced cyan fluorescent protein (ECFP), calmodulins (CaMs), and M13 was fused to YPet and subcloned into pcDNA3.1 (Invitrogen) for mammalian cell expression by using BamHI and EcoRI sites. The ECFP/YPet pair has allowed a higher sensitivity of FRET biosensors than those based on ECFP/Citrine pair. To generate an improved ER-targeting Ca^{2+} biosensor, the mutant peptide and

CaMs regions were replaced with those regions of D3cpv and cloned between a truncated ECFP and YPet. For the ER targeting motifs, the calreticulin signal sequence MLLPVLLLGLLGAAAD was added 5' to ECFP, and an ER retention sequence KDEL to the 3' end of YPet. The construct of a FRET-based IP3 biosensor, LIBRAIIs was kindly provided by Professor Akihiko Tanimura at University of Hokkaido, Japan (Tanimura et al., 2009).

3.2.2 Cell culture and transfection

Human mesenchymal stem cells (HMSCs) and bovine aortic endothelial cells (BAECs) were obtained from the American Type Culture Collection (ATCC, Rockville, MD). HMSCs and BAECs were cultured in human mesenchymal stem cell growth medium (MSCGM, PT-3001, Lonza Walkersvile, Inc., Walkersvile, MD) and in Dulbecco's modified Eagle's medium (DMEM), respectively, supplemented with 10% fetal bovine serum (FBS), 2mM L-glutamine, 100 U/ml penicillin and 100 µg/ml streptomycin. The cells were cultured in a humidified incubator of 95% O_2 and 5% CO_2 at 37°C. The DNA plasmids were transfected into the cells by using Lipofectamine 2000 (Invitrogen, Carlsbad, CA) according to the product instructions.

3.2.3 RNA Interference assays

Double-stranded small interfering RNA (siRNA) sequences targeting human TRPM7 (ON-TARGETplus SMARTpool siRNA) and non-targeting control sequences were designed by Dharmacon RNAi Technology (Dharmacon Inc., CO). HMSCs were transfected with 1-2 µg

siRNA specific for TRPM7 or a non-silencing control sequence according to the product instructions.

3.2.4 Western blotting

The cells transfected with TRPM7 or non-targeting siRNA were washed twice with cold phosphate buffered saline (PBS) and then lysed in lysis buffer containing 50mM Tris, pH 7.4, 150 mM NaCl, 1 mM EDTA, 1% Triton X-100 and a mix of serine and cysteine protease inhibitors. Lysates were centrifuged at 10,000xg at 4°C for 10 min. Cell lysates were then applied to 15% SDS-polyacrylamide gel electrophoresis, transferred to nitrocellulose, blocked with 5% non-fat milk, and detected by Western blotting using polyclonal goat anti-TRPM7 antibody (1:100; Abcam Inc., Cambridge, MA).

3.2.5 Immunostaining

A polyclonal antibody against TRPM7 was used in both normal HMSCs and TRPM7-knockdown HMSCs. After being washed in cold phosphate buffered saline (PBS), the samples were fixed by 4% paraformaldehyde in PBS at room temperature for 15 min. The samples were incubated with a goat polyclonal antibody against TRPM7 (1:100; Abcam Inc., Cambridge, MA) at room temperature for 2 hr, followed by the incubation with TRITC-conjugated anti-goat IgG (1:100, Jackson ImmunoResearch Lab., Inc., West Grove, PA) at room temperature for 1 hr before the mounting of anti-photobleaching reagent (Vector Lab., Inc., Burlingame, CA).

3.2.6 Solutions and chemicals

Imaging experiments were conducted with Ca^{2+} free Hanks balanced salt solution (HBSS, Invitrogen) containing 20mM HEPES, 1mM D-glucose, 0.5mM EGTA, 1mM $MgCl_2$ and 1mM $MgSO_4$ (pH 7.4). During imaging experiments, the solution was kept in streptomycin free condition to prevent a possible effect on mechanosensitive ion channels. The chemical reagents 2-Amino-ethoxydiphenyl borate (2APB), nifedipine, thapsigargin (TG), $LaCl_3$, $GdCl_3$, streptomycin, nocodazole, cytochalasin D, blebbistatin, and ML-7 were purchased from Sigma-Aldrich (Sigma, St. Louis, MO). PP1 and LY294002 were commercially obtained from Calbiochem (San Diego, CA). PF228 was obtained from Tocris Bioscience (Ellisville, MO). The amount of drug administration was determined by the scientifically proven research articles or the product instruction (Kim et al., 2009; Lu et al., 2011; Seong et al., 2011).

3.2.7 Preparation of beads and optical laser tweezers

A fiber-coupled IR (infra-red) laser (1064nm, 5W, 5mm diameter, YLD-5-1064-LP, IPG Photonics) was used for the experiment. I used a piezo-electirc system for a steering mirror and the piezo-mirror system was designed with a closed loop, and an automated shutter (LS6ZM2, Uniblitz) with a shutter controller (VCM-D1, Uniblitz). Mirrors (designed for IR), lenses (BK7, plano-convex) and other basic optics were purchased from Thorlabs. A hot mirror (FM01, wide band, Thorlabs) was installed inside a microscope to block the IR scattering. Thepiezo-mirror (S-334.2, (PI) Physik instrumente) was installed together with the computer interface module of (E-516.I3, PI). The interface module set up with the other drivers (E-503.00 and E509.S3, PI) makes it possible to control the piezo-mirror system by a computer. The laser beam passes through a

laser-beam expander, a steering mirror, and a dichroic long-pass beamsplitter to enter the microscope side port. Beads coated with fibronectin (Fn; 50 μg/ml) or BSA as the control were prepared as previously reported (Wang et al., 2006). The size of a bead is 10 μm and the beads were incubated for 10-20 min to allow them to adhere to cell membrane surface. Single-beam gradient optical laser tweezers with controlled 300 pN of mechanical force were applied to pull the adhered beads. A similar optical trapping system has been described in our previous report (Botvinick and Wang, 2007).

3.2.8 Microscopy, Imaging acquisition, and Analysis

Cells expressing various exogenous proteins were starved with 0.5% FBS for 36-48 hr before imaging experiments. All images were obtained by using Zeiss Axiovert inverted microscope equipped with a charge-coupled device (CCD) camera (Cascade 512B, Photometrics) and a 420DF20 excitation filter, a 450DRLP dichroic mirror, and two emission filters controlled by a filter changer (480DF30 for ECFP and 535DF25 for YPet). Time lapse fluorescence images were acquired at 10 sec interval by MetaFluor 6.2 software (Universal Imaging, West Chester, PA). The emission ratio of YPet/ECFP were directly computed and generated by the MetaFluor software to represent the FRET efficiency before they were subjected to quantification and analysis by Excel (Microsoft, Redmond, WA).

3.2.9 Statistical analysis

The results were expressed as the mean standard error of the mean (S.E.M). Statistical analysis of the data was performed by the unpaired student's t-test to determine the statistical differences between the two mean values. The statistically significant level was determined by $P<0.05$.

3.3 Results

3.3.1 Mechanical pulling force can induce intracellular Ca^{2+} oscillations via ER in the absence of extracellular Ca^{2+} in HMSCs

It has been reported that spontaneous intracellular Ca^{2+} oscillations can occur in HMSCs (Kawano et al., 2002; Sun et al., 2007), which can be abolished in the absence of extracellular Ca^{2+} (Kim et al., 2009; Kawano et al., 2002). Interestingly, when fibronectin (Fn)-coated beads were seeded onto HMSCs in the absence of extracellular Ca^{2+} and 300 pN of mechanical force was applied to mechanically stimulate these cells by pulling the beads with optical laser tweezers as described previously (Wang et al., 2005), intracellular Ca^{2+} oscillatory signals can be observed in these HMSCs. In contrast, laser-tweezer-traction of BSA-coated beads did not cause any Ca^{2+} oscillations in the absence of extracellular Ca^{2+} (Fig. 3-1). Unlike HMSCs, the force-induced Ca^{2+} oscillations did not occur in BAECs without extracellular Ca^{2+} (Supplementary Fig. S3-1). This result indicates that this mechano-response of Ca^{2+} signal may be a specific character of HMSCs, suggesting that HMSCs may be more sensitive in perceiving the mechanical stimuli and transducing them into intracellular Ca^{2+} signals.

3.3.2 The role of ER and the plasma membrane channels in mediating the mechanical force-induced intracellular Ca^{2+} oscillations in the absence of extracellular Ca^{2+}

In the absence of extracellular Ca^{2+}, these mechanical-force-induced intracellular Ca^{2+} signals may be originated from the internal Ca^{2+} stores such as ER in HMSCs (Kim et al., 2009; Kawano et al., 2002). Indeed, thapsigargin (TG, 10 μM) or 2-Amino-ethoxydiphenylborate (2APB, 100 μM), which block Ca^{2+}- ATPase (SERCA) pump or inositol 1,4,5-triphosphate receptors (IP_3Rs) to deplete the ER Ca^{2+} storage or inhibit the Ca^{2+} release from ER, entirely abolished these mechanical-force-induced intracellular Ca^{2+} oscillations (Fig. 3-2A and 2B). These results confirmed that the ER Ca^{2+} store is the main source for the mechanical force-induced Ca^{2+} oscillations in HMSCs when the extracellular Ca^{2+} is not available. I have then examined the effects of stretch-activated Ca^{2+} channels and store-operated Ca^{2+} channels at the plasma membrane upon the force-induced Ca^{2+} oscillations using their inhibitors, Gd^{3+} (5 μM) and La^{3+} (100 μM), respectively. As shown in Figure 3-2C and 2D, the mechanical force-induced Ca^{2+} oscillations were surprisingly blocked by either Gd^{3+} or La^{3+}. Streptomycin (200 μM), a more specific inhibitor against stretch-activated Ca^{2+} channels, also blocked the force-induced transient Ca^{2+} oscillations (Fig. 3-2E). On the other hand, the inhibition of L-type Ca^{2+} channels, one of the voltage operated Ca^{2+} channels by nifedipine (10 μM), did not affect the transient Ca^{2+} oscillations in response to mechanical force (Fig. 3-2F). These results suggest that the Ca^{2+} traffic at ER is responsible for the mechanical-force-induced Ca^{2+} signals in the absence of extracellular Ca^{2+} in HMSCs, which is also surprisingly regulated by stretch-activated and store-operated Ca^{2+} channels on the plasma membrane.

3.3.3 TRPM7 mediates the force-induced intracellular Ca^{2+} oscillations in the absence of extracellular Ca^{2+}

TRPM7 has been shown as one of the major Ca^{2+} permeable mechanosensitive channels on the plasma membrane (Wei et al., 2009). To examine whether TRPM7 is specifically involved in regulation of the mechanical force-induced Ca^{2+} signals, I utilized siRNA method to knockdown endogenous TRPM7 in HMSCs. Immunostaining and western blot analysis have shown that the expression level of TRPM7 in its knockdown cells was apparently decreased compared to control group (Fig. 3-3A). Statistical results further confirmed that TRPM7 knockdown group remarkably reduced the percentile of HMSCs with oscillating Ca^{2+} signals (4.76 %, 1 of 21 cells) in comparison to the non-targeting siRNA transfected cells (45%, 9 of 20 cells) (Fig. 3-3B). The knockdown of TRPM7 resulted in a substantial abrogation of the force-induced Ca^{2+} oscillations, suggesting that TRPM7 seems specifically associated with the force-induced Ca^{2+} oscillations (Fig. 3-3C).

3.3.4 The mechanical-force-induced intracellular Ca^{2+} oscillations in the absence of extracellular Ca^{2+} are abolished by the disruption of cytoskeleton and actomyosin contractility

Since Ca^{2+} channels on the plasma membrane and ER Ca^{2+} traffic have been reported to associate with cytoskeleton (Berridge et al., 2000; Beliveau and Guillemette, 2009), I investigated the role of cytoskeleton and its associated signals in mediating the force-induced transient Ca^{2+} oscillations in the absence of extracellular Ca^{2+}. As shown in Figure 3-4A and 4B, the disruption of cytoskeletal actin filaments by cytochalasin D (Cyto D, 2 μM, n=8) and microtubules by nocodazole (Noc, 1 μM, n=8) completely eliminated the mechanical-force-

induced intracellular Ca^{2+} oscillations in the absence of extracellular Ca^{2+}. Interestingly, the modulation of actomyosin contractility by the inhibition of myosin light chain kinase (MLCK) with ML-7 (5 μM, n=8) or of myosin II with blebbistatin (5 μM, n=8) also inhibited this force-induced Ca^{2+} oscillation (Fig. 4-4C and 4D). Thus, the force-induced Ca^{2+} oscillation of HMSCs in the absence of extracellular Ca^{2+} is dependent on cytoskeletal support and actomyosin contractility. It may be consistent with the previous report that long-distance force propagation to the deep cytoplasm depends on cytoskeleton tension (Hu et al., 2003).

3.3.5 The monitoring of ER Ca^{2+} release in HMSCs in the absence of extracellular Ca^{2+} upon mechanical stimulation

I have further confirmed that mechanical force can directly induce the ER Ca^{2+} release in the absence of extracellular Ca^{2+}, by having monitored the decrease of ER Ca^{2+} concentration upon mechanical stimulation utilizing a FRET-based ER Ca^{2+} biosensor (Fig. 3-5A). Other experiments also revealed that the ER Ca^{2+} release upon the external mechanical force application is mediated not only by passive cytoskeletal support of actin filaments and microtubules, but also by active actomyosin contractility regulated by MLCK and myosin II (Fig. 3-5B). TRPM7 siRNA also inhibited this ER Ca^{2+} release induced by the application of force, suggesting TRPM7 may be one of key mediators in mechanical force-induced ER Ca^{2+} release (Fig. 3-5B). These results suggest that stretchable membrane channels and cytoskeletal support are important for the mechanical-force-induced ER Ca^{2+} release and hence intracellular Ca^{2+} oscillation in the absence of extracellular Ca^{2+}.

3.3.6 Actin filaments and microtubules regulate the membrane channel-mediated Ca^{2+} influx in response to mechanical stimulation

To examine how the plasma membrane channels are involved in response to mechanical stimulation, 2APB (100 μM), which can specifically inhibit IP_3Rs and Ca^{2+} release from ER, was applied to block the ER Ca^{2+} release in HSMCs cultured with 2 mM extracellular Ca^{2+}. Ca^{2+} influx across the plasma membrane was then monitored to examine the function of membrane channels. As shown in Figure 3-6, the blockade of L-type Ca^{2+} channel by nifedipine did not have any effect on the mechanical force-induced Ca^{2+} influx. In contrast, Gd^{3+} (5 μM), La^{3+} (100 μM), streptomycin (200 μM), and TRPM7 suppression by siRNA significantly inhibited this force-induced Ca^{2+} influx in 2APB-treated cells (Fig. 3-6), confirming the involvement of mechanosensitive channels in response to mechanical stimulation. The disruption of actin filaments and microtubules by Cyto D (2 μM) and nocodazole (1 μM) inhibited this mechanical force induced Ca^{2+} influx (Fig. 3-7), suggesting that cytoskeletal integrity is essential for the membrane channels to respond to mechanical force. This is consistent with that membrane channel activities can be modulated by cytoskeleton (Hayakawa et al., 2008). Interestingly, ML-7 and blebbistatin did not affect this mechanical-force-induced Ca^{2+} influx, suggesting that active actomyosin contractility mediated by MLCK and myosin II may not be involved (Fig. 3-7).

Src and the focal adhesion kinase (FAK) appear to play a central role in integrin-cytoskeleton mediated signaling pathway. Since mechanical stimulation such as stretch affects integrin adhesion and integrin-associated signaling, including Src and FAK (Orr et al., 2006; Wang et al., 2005), I reasoned that Src and FAK may mediate the mechanical force-induced Ca^{2+} signals. Our results indicate that neither PP1, an inhibitor of Src family tyrosine kinases, nor PF228, an inhibitor of FAK, had a significant effect on the force-induced Ca^{2+} influx or

intracellular Ca^{2+} oscillations. Inhibition of phosphoinositide 3-kinases (PI3Ks) with LY294002 did not affect the force-induced Ca^{2+} signals in HMSCs either (Supplementary Fig. S3-2). Taken together, these results indicate that the activation of mechanosensitive Ca^{2+} channels in response to mechanical stimulation is mediated by the cytoskeletal structures, but neither by active actomyosin contractile machinery nor related signaling molecules including Src, FAK or PI3K.

3.4 Discussion

Changes in intracellular Ca^{2+} are crucial in regulating a wide variety of cellular processes, including cell growth, motility, contraction, and stem cell differentiation and proliferation (Clapham, 2007; Maeda et al., 2007; Rong and Distelhorst. 2008; West et al., 2001; Guan et al., 2007). Such changes in intracellular Ca^{2+} can be caused by Ca^{2+} influx across the plasma membrane from the extracellular environment, Ca^{2+} mobilization from internal stores, and Ca^{2+} efflux into the extracellular space and internal stores. In this study, I have found that mechanical force evoked intracellular Ca^{2+} oscillations in HMSCs when extracellular Ca^{2+} was eliminated. Such Ca^{2+} responses are likely due to Ca^{2+} release through ER. Indeed, previous studies have shown that mechanical stimulation can elevate intracellular Ca^{2+} concentration by inducing Ca^{2+} release from internal stores (Boitano et al., 1994; Charles et al., 1991; Demer et al., 1993; Oike et al., 1994). However, whether mechanical force can directly induce Ca^{2+} release from internal stores without the involvement of extracellular Ca^{2+} remains unclear. There are two possible mechanisms regulating Ca^{2+} release from internal stores upon external mechanical laser-tweezer-traction: (1) external mechanical force can be transmitted deep inside the cell and mechanically alter the channels on the internal stores to cause Ca^{2+} release (Himmel et al., 1993; Missiaen et

al., 1996; Rath et al., 2010). (2) External mechanical force can trigger biochemical signaling cascades including a mechanosensitive phospholipase C or a phospholipase A2 to produce IP_3 at the proximity of plasma membrane and diffuse inside to activate IP_3-sensitive Ca^{2+} release channel (Lehtonen and Kinnunen, 1995). In our system, ATP can clearly induce IP_3 production monitored by a FRET based IP_3 biosensor, LIBRAIIs. However, there was no change in IP_3 upon laser-tweezer-traction in HMSCs (Supplementary Fig. S3-3). These results suggest that laser-tweezer-traction may be transmitted deep inside the cells to mechanically open ER channels and cause Ca^{2+} release in HMSCs.

The importance of cytoskeleton for transmitting mechanical forces and conducting mechanotransduction has been well documented previously (Orr et al., 2006; Hamill and Martinac, 2001; Schwartz and DeSimone, 2008). It is clear that the deep penetration and transmission of mechanical force inside the cell is dependent on not only the passive cytoskeletal support of actin filaments and microtubules, but also the active actomyosin contractility controlled by myosin light chain kinase (MLCK) and myosin (Herring et al., 2006). Indeed, the mechanical force-induced Ca^{2+} release from ER was inhibited by the treatment of ML-7, a MLCK inhibitor, and blebbistatin, a myosin II inhibitor. This is consistent with the pivotal role of MLCK and myosin II in regulating actomyosin-based cytoskeletal functions as well as force development (Fajmut and Brumen, 2008; He et al., 2008; Olsson et al., 2004). Interestingly, neither MLCK nor myosin II is needed for the plasma membrane channels and Ca^{2+} influx across the plasma membrane from extracellular space, while the cytoskeletal support is crucial. These results indicate that the active actomyosin contractility is crucial for the deep penetration and transmission of external mechanical force inside the cells, but dispensable for the regulation of plasma membrane channels upon mechanical stimulation. In contrast, actin filaments and

microtubules are essential for the regulation of both plasma membrane and ER channels in response to mechanical perturbation.

It is also intriguing that the inhibition of plasma membrane channels can block the mechanical transmission via cytoskeleton into ER. It is possible that these mechanosensitive channels on the plasma membrane need to be activated before they can be coupled to the cytoskeleton for the deep mechanical transmission. TRP channels belong to these mechanosensitive Ca^{2+} permeable channels. In particular, TRPM7 channel is directly activatable by a membrane stretch in HeLa cell and human epithelial cells to allow Ca^{2+} influx across the plasma membrane (Numata et al., 2007a; Numata et al., 2007b). TRPM7 can also evoke and mediate Ca^{2+} flickers in response to shear stress in fibroblasts (Wei et al., 2009). Recently, TRPM7 was shown to serve as a novel regulator for actomyosin contractility and cell adhesion by controlling the Ca^{2+} dependent protease m-calpain (Clark et al., 2006; Su et al., 2006). These results clearly show that TRPM7 knockdown using small interfering RNA (siRNA) abolished the mechanical force induced Ca^{2+} release from ER as well as Ca^{2+} influx across the plasma membrane. These results suggest that TRPM7 is the key molecule responsible for transducing the mechanical signals into HMSCs, possibly facilitating the coupling of membrane receptor structures to cytoskeleton.

Src and FAK can regulate integrin-cytoskeleton interaction and facilitate the force-dependent reinforcement of integrin-cytoskeleton linkage (Felsenfeld et al., 1999; Giannone and Sheetz, 2006). However, we showed that Src and FAK had no effect on the mechanical force induced Ca^{2+} signaling. Although integrin-medicated Src phosphorylation and activation can regulate L-type Ca^{2+} channel functions (Gui et al., 2010), the force-induced Ca^{2+} oscillations seem independent of L-type Ca^{2+} channels in HMSCs (Fig. 3-2F). Mechanical stretch also

induces the phosphorylation of FAK and nitric oxide (NO) formation in myocardiocytes (Khan et al., 2003; Pinsky et al., 1997), which can modulate ryanodine receptor 2 (RYR2) and Ca^{2+} release at the sarcoplasmic reticulum (Vila Petroff and Mattiazzi, 2001). However, there appears a minimal expression of RYRs in HMSCs. Together with the PI3K inhibition result, these biochemical activities associated with the integrin-cytoskeleton coupling appear not involved in the force-induced Ca^{2+} signals.

3.5 References

Balasubramanian, L., Ahmed, A., Lo, C.M., Sham, J.S., and Yip, K.P. (2007). Integrin-mediated mechanotransduction in renal vascular smooth muscle cells: activation of calcium sparks. Am J Physiol Regul Integr Comp Physiol 293, R1586-1594.

Barakat, A.I., Lieu, D.K., and Gojova, A. (2006). Secrets of the code: do vascular endothelial cells use ion channels to decipher complex flow signals? Biomaterials 27, 671-678.

Beliveau, E., and Guillemette, G. (2009). Microfilament and microtubule assembly is required for the propagation of inositol trisphosphate receptor-induced Ca2+ waves in bovine aortic endothelial cells. J Cell Biochem 106, 344-352.

Belmonte, S., and Morad, M. (2008). Shear fluid-induced Ca2+ release and the role of mitochondria in rat cardiac myocytes. Ann N Y Acad Sci 1123, 58-63.

Berns, M.W. (2007). Optical tweezers: tethers, wavelengths, and heat. Methods Cell Biol 82, 457-466.

Berridge, M.J., Lipp, P., and Bootman, M.D. (2000). The versatility and universality of calcium signalling. Nat Rev Mol Cell Biol 1, 11-21.

Boitano, S., Sanderson, M.J., and Dirksen, E.R. (1994). A role for Ca(2+)-conducting ion channels in mechanically-induced signal transduction of airway epithelial cells. J Cell Sci 107 (Pt 11), 3037-3044.

Bootman, M.D., Collins, T.J., Mackenzie, L., Roderick, H.L., Berridge, M.J., and Peppiatt, C.M. (2002). 2-aminoethoxydiphenyl borate (2-APB) is a reliable blocker of store-operated Ca2+ entry but an inconsistent inhibitor of InsP3-induced Ca2+ release. Faseb J 16, 1145-1150.

Botvinick, E.L., and Wang, Y. (2007). Laser tweezers in the study of mechanobiology in live cells. Methods Cell Biol 82, 497-523.

Caldwell, R.A., Clemo, H.F., and Baumgarten, C.M. (1998). Using gadolinium to identify stretch-activated channels: technical considerations. Am J Physiol 275, C619-621.

Charles, A.C., Merrill, J.E., Dirksen, E.R., and Sanderson, M.J. (1991). Intercellular signaling in glial cells: calcium waves and oscillations in response to mechanical stimulation and glutamate. Neuron 6, 983-992.

Chen, N.X., Ryder, K.D., Pavalko, F.M., Turner, C.H., Burr, D.B., Qiu, J., and Duncan, R.L. (2000). Ca(2+) regulates fluid shear-induced cytoskeletal reorganization and gene expression in osteoblasts. Am J Physiol Cell Physiol 278, C989-997.

Chien, S. (2007). Mechanotransduction and endothelial cell homeostasis: the wisdom of the cell. Am J Physiol Heart Circ Physiol 292, H1209-1224.

Clapham, D.E. (2007). Calcium signaling. Cell 131, 1047-1058.

Clark, K., Langeslag, M., van Leeuwen, B., Ran, L., Ryazanov, A.G., Figdor, C.G., Moolenaar, W.H., Jalink, K., and van Leeuwen, F.N. (2006). TRPM7, a novel regulator of actomyosin contractility and cell adhesion. Embo J 25, 290-301.

Demer, L.L., Wortham, C.M., Dirksen, E.R., and Sanderson, M.J. (1993). Mechanical stimulation induces intercellular calcium signaling in bovine aortic endothelial cells. Am J Physiol 264, H2094-2102.

Engler, A.J., Sen, S., Sweeney, H.L., and Discher, D.E. (2006). Matrix elasticity directs stem cell lineage specification. Cell 126, 677-689.

Fajmut, A., and Brumen, M. (2008). MLC-kinase/phosphatase control of Ca2+ signal transduction in airway smooth muscles. J Theor Biol 252, 474-481.

Felsenfeld, D.P., Schwartzberg, P.L., Venegas, A., Tse, R., and Sheetz, M.P. (1999). Selective regulation of integrin--cytoskeleton interactions by the tyrosine kinase Src. Nat Cell Biol 1, 200-206.

Giannone, G., and Sheetz, M.P. (2006). Substrate rigidity and force define form through tyrosine phosphatase and kinase pathways. Trends Cell Biol 16, 213-223.

Guan, C.B., Xu, H.T., Jin, M., Yuan, X.B., and Poo, M.M. (2007). Long-range Ca2+ signaling from growth cone to soma mediates reversal of neuronal migration induced by slit-2. Cell 129, 385-395.

Gui, P., Chao, J.T., Wu, X., Yang, Y., Davis, G.E., and Davis, M.J. Coordinated regulation of vascular Ca2+ and K+ channels by integrin signaling. Adv Exp Med Biol 674, 69-79.

Hamill, O.P., and Martinac, B. (2001). Molecular basis of mechanotransduction in living cells. Physiol Rev 81, 685-740.

Hayakawa, K., Tatsumi, H., and Sokabe, M. (2008). Actin stress fibers transmit and focus force to activate mechanosensitive channels. J Cell Sci 121, 496-503.

He, W.Q., Peng, Y.J., Zhang, W.C., Lv, N., Tang, J., Chen, C., Zhang, C.H., Gao, S., Chen, H.Q., Zhi, G., et al. (2008). Myosin light chain kinase is central to smooth muscle contraction and required for gastrointestinal motility in mice. Gastroenterology 135, 610-620.

Herring, B.P., El-Mounayri, O., Gallagher, P.J., Yin, F., and Zhou, J. (2006). Regulation of myosin light chain kinase and telokin expression in smooth muscle tissues. Am J Physiol Cell Physiol 291, C817-827.

Himmel, H.M., Whorton, A.R., and Strauss, H.C. (1993). Intracellular calcium, currents, and stimulus-response coupling in endothelial cells. Hypertension 21, 112-127.

Ho, T.C., Horn, N.A., Huynh, T., Kelava, L., and Lansman, J.B. (2012). Evidence TRPV4 contributes to mechanosensitive ion channels in mouse skeletal muscle fibers. Channels (Austin) 6, 246-254.

Horner, V.L., and Wolfner, M.F. (2008). Mechanical stimulation by osmotic and hydrostatic pressure activates Drosophila oocytes in vitro in a calcium-dependent manner. Dev Biol 316, 100-109.

Hu, S., Chen, J., Fabry, B., Numaguchi, Y., Gouldstone, A., Ingber, D.E., Fredberg, J.J., Butler, J.P., and Wang, N. (2003). Intracellular stress tomography reveals stress focusing and structural anisotropy in cytoskeleton of living cells. Am J Physiol Cell Physiol 285, C1082-1090.

Ingber, D.E. (1997). Tensegrity: the architectural basis of cellular mechanotransduction. Annu Rev Physiol 59, 575-599.

Kawano, S., Shoji, S., Ichinose, S., Yamagata, K., Tagami, M., and Hiraoka, M. (2002). Characterization of Ca(2+) signaling pathways in human mesenchymal stem cells. Cell Calcium 32, 165-174.

Khan, S.A., Skaf, M.W., Harrison, R.W., Lee, K., Minhas, K.M., Kumar, A., Fradley, M., Shoukas, A.A., Berkowitz, D.E., and Hare, J.M. (2003). Nitric oxide regulation of myocardial contractility and calcium cycling: independent impact of neuronal and endothelial nitric oxide synthases. Circ Res 92, 1322-1329.

Kim, T.J., Seong, J., Ouyang, M., Sun, J., Lu, S., Hong, J.P., Wang, N., and Wang, Y. (2009). Substrate rigidity regulates Ca2+ oscillation via RhoA pathway in stem cells. J Cell Physiol 218, 285-293.

Landsberg, J.W., and Yuan, J.X. (2004). Calcium and TRP channels in pulmonary vascular smooth muscle cell proliferation. News Physiol Sci 19, 44-50.

Lehtonen, J.Y., and Kinnunen, P.K. (1995). Phospholipase A2 as a mechanosensor. Biophys J 68, 1888-1894.

Lu, S., Kim, T.J., Chen, C.E., Ouyang, M., Seong, J., Liao, X., and Wang, Y. Computational analysis of the spatiotemporal coordination of polarized PI3K and Rac1 activities in micro-patterned live cells. PLoS One 6, e21293.

Maeda, Y., Nitanai, Y., and Oda, T. (2007). From the crystal structure of troponin to the mechanism of calcium regulation of muscle contraction. Adv Exp Med Biol 592, 37-46.

Matsumoto, H., Baron, C.B., and Coburn, R.F. (1995). Smooth muscle stretch-activated phospholipase C activity. Am J Physiol 268, C458-465.

Matthews, B.D., Thodeti, C.K., Tytell, J.D., Mammoto, A., Overby, D.R., and Ingber, D.E. Ultra-rapid activation of TRPV4 ion channels by mechanical forces applied to cell surface beta1 integrins. Integr Biol (Camb) 2, 435-442.

McKinsey, T.A., Zhang, C.L., and Olson, E.N. (2002). MEF2: a calcium-dependent regulator of cell division, differentiation and death. Trends Biochem Sci 27, 40-47.

Missiaen, L., De Smedt, H., Parys, J.B., Sienaert, I., Vanlingen, S., Droogmans, G., Nilius, B., and Casteels, R. (1996). Hypotonically induced calcium release from intracellular calcium stores. J Biol Chem 271, 4601-4604.

Miyawaki, A., Llopis, J., Heim, R., McCaffery, J.M., Adams, J.A., Ikura, M., and Tsien, R.Y. (1997). Fluorescent indicators for Ca2+ based on green fluorescent proteins and calmodulin. Nature 388, 882-887.

Numata, T., Shimizu, T., and Okada, Y. (2007a). Direct mechano-stress sensitivity of TRPM7 channel. Cell Physiol Biochem 19, 1-8.

Numata, T., Shimizu, T., and Okada, Y. (2007b). TRPM7 is a stretch- and swelling-activated cation channel involved in volume regulation in human epithelial cells. Am J Physiol Cell Physiol 292, C460-467.

Oancea, E., Wolfe, J.T., and Clapham, D.E. (2006). Functional TRPM7 channels accumulate at the plasma membrane in response to fluid flow. Circ Res 98, 245-253.

Oike, M., Gericke, M., Droogmans, G., and Nilius, B. (1994). Calcium entry activated by store depletion in human umbilical vein endothelial cells. Cell Calcium 16, 367-376.

Olsson, M.C., Patel, J.R., Fitzsimons, D.P., Walker, J.W., and Moss, R.L. (2004). Basal myosin light chain phosphorylation is a determinant of Ca2+ sensitivity of force and activation dependence of the kinetics of myocardial force development. Am J Physiol Heart Circ Physiol 287, H2712-2718.

Orr, A.W., Helmke, B.P., Blackman, B.R., and Schwartz, M.A. (2006). Mechanisms of mechanotransduction. Dev Cell 10, 11-20.

Ouyang, M., Sun, J., Chien, S., and Wang, Y. (2008). Determination of hierarchical relationship of Src and Rac at subcellular locations with FRET biosensors. Proc Natl Acad Sci U S A 105, 14353-14358.

Park, J.S., Chu, J.S., Cheng, C., Chen, F., Chen, D., and Li, S. (2004). Differential effects of equiaxial and uniaxial strain on mesenchymal stem cells. Biotechnol Bioeng 88, 359-368.

Pinsky, D.J., Patton, S., Mesaros, S., Brovkovych, V., Kubaszewski, E., Grunfeld, S., and Malinski, T. (1997). Mechanical transduction of nitric oxide synthesis in the beating heart. Circ Res 81, 372-379.

Rath, A.L., Bonewald, L.F., Ling, J., Jiang, J.X., Van Dyke, M.E., and Nicolella, D.P. Correlation of cell strain in single osteocytes with intracellular calcium, but not intracellular nitric oxide, in response to fluid flow. J Biomech 43, 1560-1564.

Rong, Y., and Distelhorst, C.W. (2008). Bcl-2 protein family members: versatile regulators of calcium signaling in cell survival and apoptosis. Annu Rev Physiol 70, 73-91.

Schwartz, M.A., and DeSimone, D.W. (2008). Cell adhesion receptors in mechanotransduction. Curr Opin Cell Biol 20, 551-556.

Seong, J., Ouyang, M., Kim, T., Sun, J., Wen, P.C., Lu, S., Zhuo, Y., Llewellyn, N.M., Schlaepfer, D.D., Guan, J.L., et al. Detection of focal adhesion kinase activation at membrane microdomains by fluorescence resonance energy transfer. Nat Commun 2, 406.

Stolberg, S., and McCloskey, K.E. (2009). Can shear stress direct stem cell fate? Biotechnol Prog 25, 10-19.

Su, L.T., Agapito, M.A., Li, M., Simonson, W.T., Huttenlocher, A., Habas, R., Yue, L., and Runnels, L.W. (2006). TRPM7 regulates cell adhesion by controlling the calcium-dependent protease calpain. J Biol Chem 281, 11260-11270.

Sun, S., Liu, Y., Lipsky, S., and Cho, M. (2007). Physical manipulation of calcium oscillations facilitates osteodifferentiation of human mesenchymal stem cells. Faseb J 21, 1472-1480.

Tanimura, A., Morita, T., Nezu, A., Shitara, A., Hashimoto, N., and Tojyo, Y. (2009). Use of Fluorescence Resonance Energy Transfer-based Biosensors for the Quantitative Analysis of Inositol 1,4,5-Trisphosphate Dynamics in Calcium Oscillations. J Biol Chem 284, 8910-8917.

Vila Petroff, M.G., and Mattiazzi, A.R. (2001). Angiotensin II and cardiac excitation-contraction coupling: questions and controversies. Heart Lung Circ 10, 90-98.

Vogel, V., and Sheetz, M. (2006). Local force and geometry sensing regulate cell functions. Nat Rev Mol Cell Biol 7, 265-275.

Wang, N., Tytell, J.D., and Ingber, D.E. (2009). Mechanotransduction at a distance: mechanically coupling the extracellular matrix with the nucleus. Nat Rev Mol Cell Biol 10, 75-82.

Wang, Y., Botvinick, E.L., Zhao, Y., Berns, M.W., Usami, S., Tsien, R.Y., and Chien, S. (2005). Visualizing the mechanical activation of Src. Nature 434, 1040-1045.

Wang, Y., Jin, G., Miao, H., Li, J.Y., Usami, S., and Chien, S. (2006). Integrins regulate VE-cadherin and catenins: dependence of this regulation on Src, but not on Ras. Proc Natl Acad Sci U S A 103, 1774-1779.

Wei, C., Wang, X., Chen, M., Ouyang, K., Song, L.S., and Cheng, H. (2009). Calcium flickers steer cell migration. Nature 457, 901-905.

West, A.E., Chen, W.G., Dalva, M.B., Dolmetsch, R.E., Kornhauser, J.M., Shaywitz, A.J., Takasu, M.A., Tao, X., and Greenberg, M.E. (2001). Calcium regulation of neuronal gene expression. Proc Natl Acad Sci U S A 98, 11024-11031.

Zhang, J., Campbell, R.E., Ting, A.Y., and Tsien, R.Y. (2002). Creating new fluorescent probes for cell biology. Nat Rev Mol Cell Biol 3, 906-918.

3.6 Figures

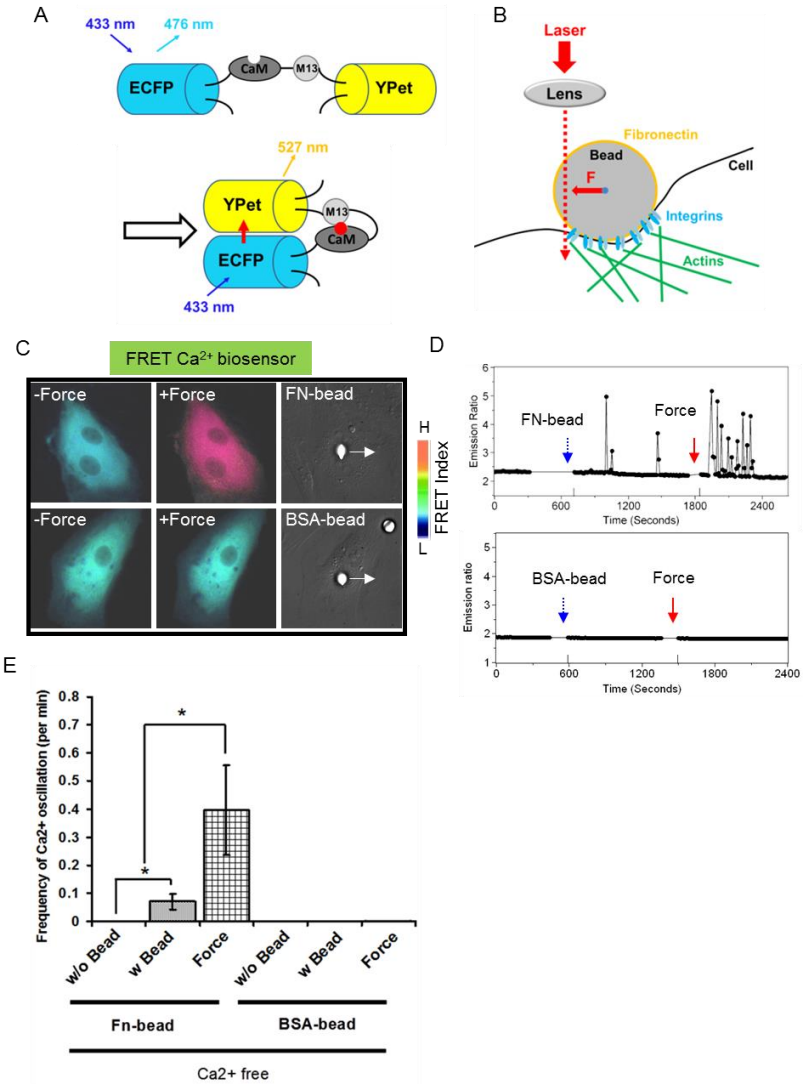

Figure 3-1. Intracellular Ca^{2+} oscillations in response to mechanical force in HMSCs under Ca^{2+}-free medium. (A) A schematic drawing of the activation mechanism of the Ca^{2+} FRET biosensor. (B) Beads coated with Fn or BSA were seeded onto the cell and mechanical force was applied by pulling a Fn-coated bead using optical laser tweezers. (C) Color images represent the YPet/ECFP emission ratio of the cytoplasmic Ca^{2+} biosensor. The color scale bars represents the range of emission ratio, with cold and hot colors indicating low and high levels of Ca^{2+} concentration, respectively. (D) The time courses represent the YPet/ECFP emission ratio averaged over the cell body outside of nucleus. (E) Bar graphs represent the frequency of the intracellular Ca^{2+} oscillations evoked by mechanical force. Error bars indicate standard error of mean; *$p<0.05$, $n=14$

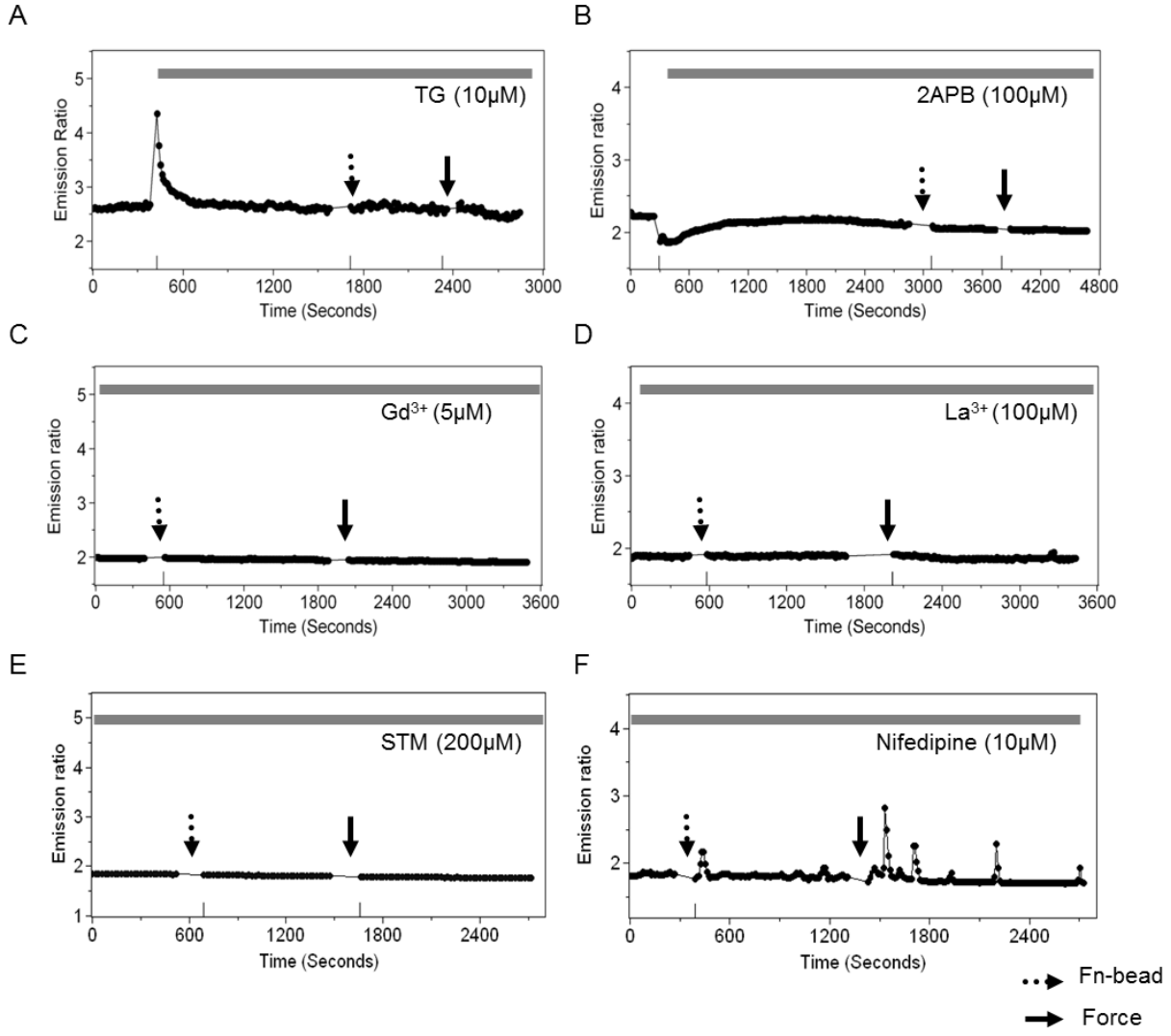

Figure 3-2. **The mechanical force-induced Ca^{2+} oscillations are regulated by Ca^{2+} traffic across ER membrane and mechanosensitive channels on the plasma membrane, but not by L-type Ca^{2+} channels.** The time courses represent the YPet/ECFP emission ratio of cytoplasmic Ca^{2+} in HMSCs pre-treated with (**A**) thapsigargin (TG, 10 μM), a SERCA pump blocker, (**B**) 2APB (100 μM), an IP_3R blocker, (**C**) $GdCl_3$ (5 μM), a stretch-activated Ca^{2+} channel inhibitor, (**D**) $LaCl_3$ (100 μM), a non-selective Ca^{2+} channel blocker, (**E**) streptomycin (200 μM), a mechanosensitive channel inhibitor, or (**F**) nifedipine (10 μM), an L-type Ca^{2+} channel inhibitor, all in the absence of extracellular Ca^{2+} (n=6).

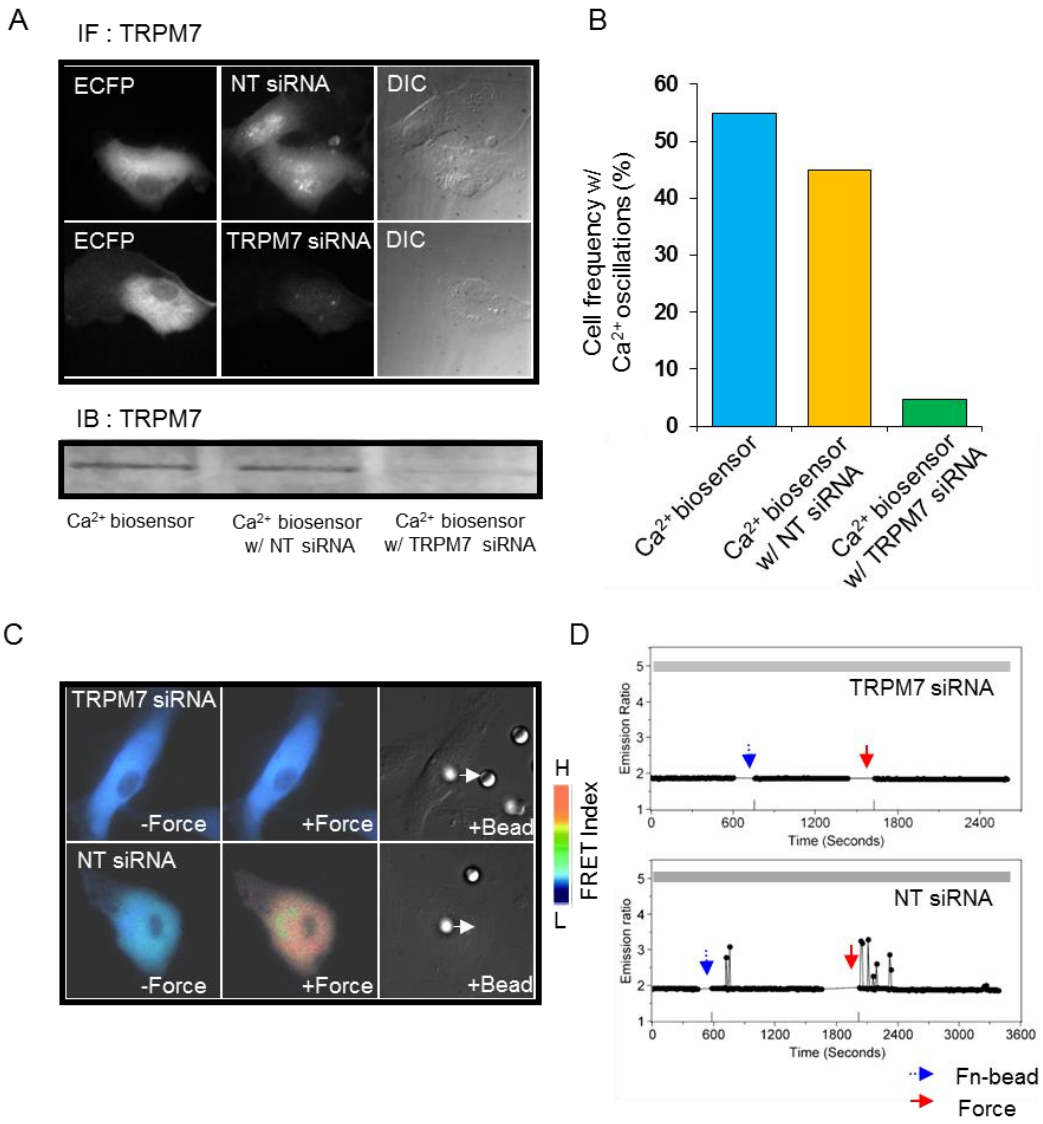

Figure 3-3. TRPM7 channels mediate the force-induced intracellular Ca^{2+} oscillations. (**A**) HMSCs expressing Ca^{2+} biosensor and transfected with non-targeting (NT) or TRPM7 siRNA were immunostained (upper images) or immunoblotted (lower panels) with polyclonal TRPM7 antibody to assess the TRPM7 amount. (**B**) Bar graphs represent the percentile of HMSCs showing intracellular Ca^{2+} oscillations. Three kinds of cell groups (1: Ca^{2+} biosensor only, 2: biosensor and non-targeting (NT) siRNA, and 3: biosensor and TRPM7 siRNA) were measured and compared. The number of cells displaying Ca^{2+} oscillations in both control group (55%, 11 of 20 cells) and NT-siRNA group (45%, 9 of 20 cells) was approximately 9 to 11 fold higher than that of TRPM7 siRNA group (4.76%, 1 of 21 cells). (**C**) Color images on the left represent the YPet/ECFP emission ratio of the cytoplasmic Ca^{2+} biosensor in HMSCs transfected with NT or TRPM7 siRNA. The color scale bars represents the range of emission ratio, with cold and hot colors indicating low and high levels of Ca^{2+} concentration, respectively. The time courses on the right represent the YPet/ECFP emission ratio averaged over the cell bodies outside of nucleus (n=6).

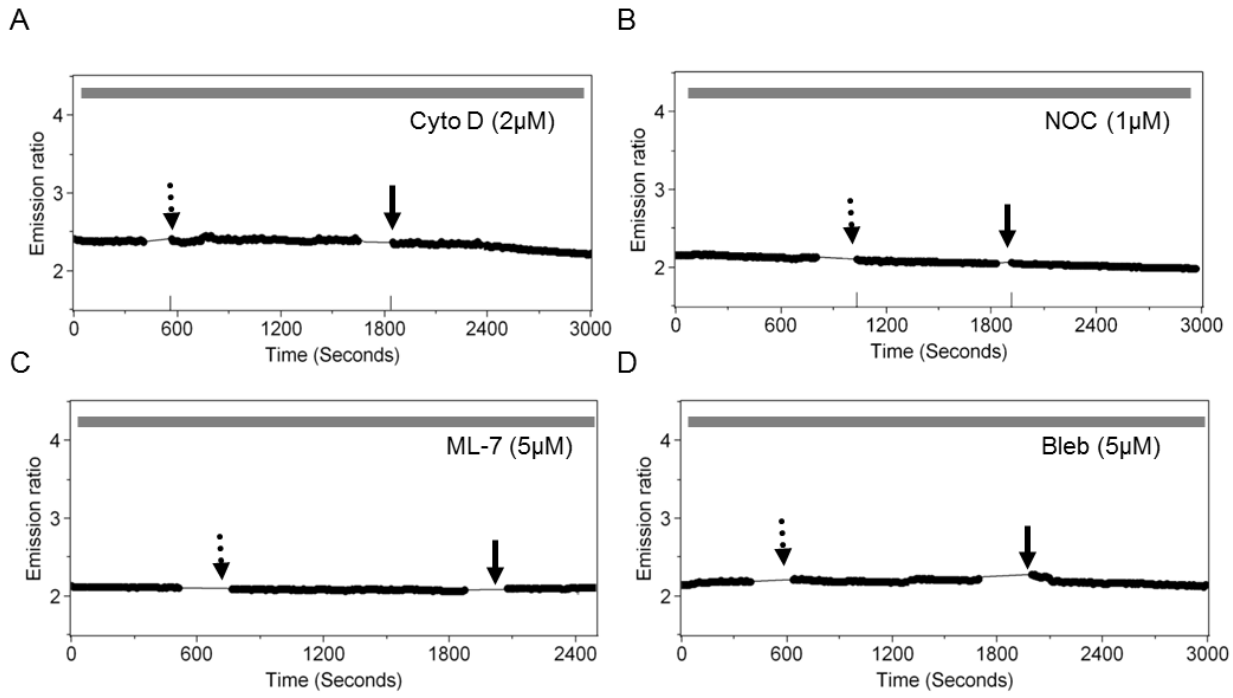

Figure 3-4. **The roles of cytoskeletal support and actomyosin contractility in regulating the mechanical force-induced Ca^{2+} oscillations.** The time courses represent the YPet/ECFP emission ratio of cytoplasmic Ca^{2+} in HMSCs in the absence of extracellular Ca^{2+} when these cells were pretreated with (**A**) 2 μM Cyto D (n=8), (**B**) 1 μM Noc (n=8), (**C**) 5 μM ML-7 (n=8), and (**D**) Bleb (n=8).

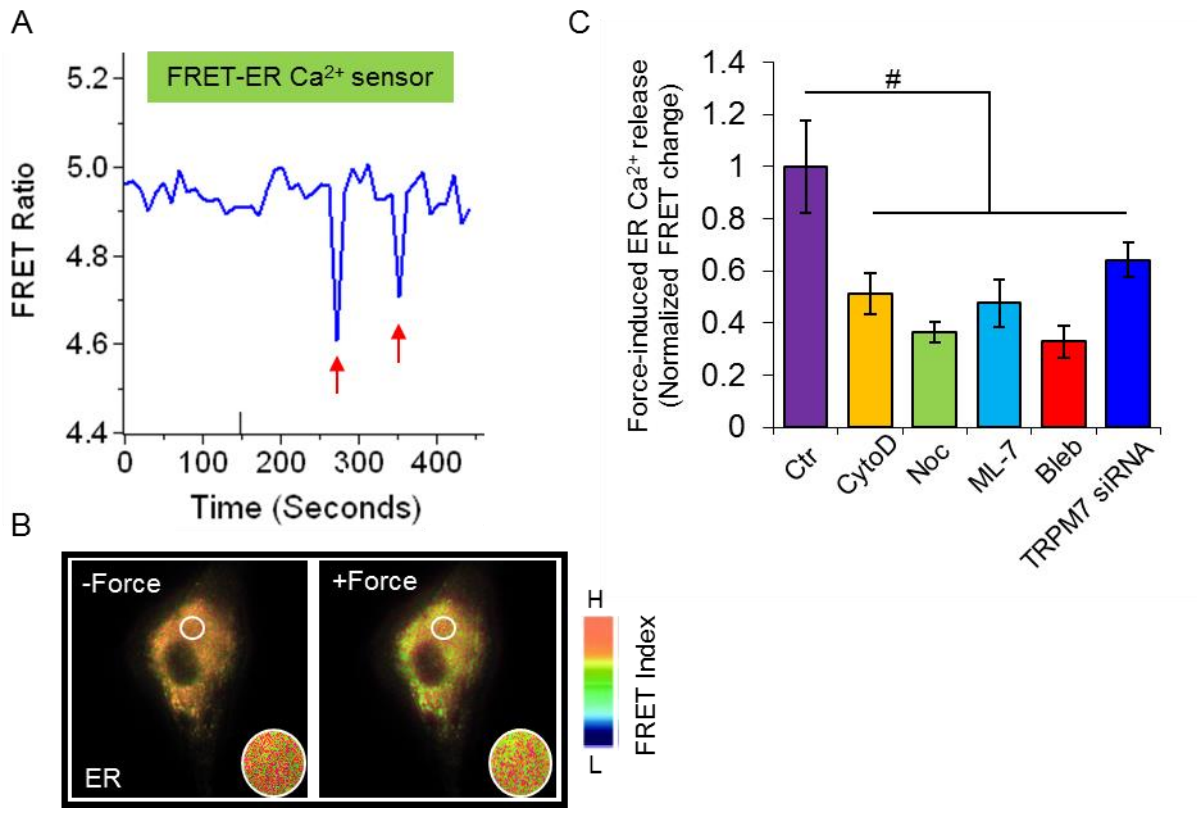

Figure 3-5. **The visualization of force-induced ER Ca^{2+} concentration using a FRET-based ER Ca^{2+} biosensor (D3ER)**. (**A**) The time course (upper panel) and the color images (lower panels) of YPet/ECFP emission ratio in HMSCs expressing the D3ER before and after force application. (**B**) The bar graphs represent the percentile changes of YPet/ECFP emission ratio of the D3ER in HMSCs upon force application in the absence of extracellular Ca^{2+} when the cells were untreated as the control group (n=3) or pretreated with CytoD (n=5), Noc (n=5), ML-7 (n=6), Bleb (n=5), or TRPM7 siRNA (n=9) as indicated. * represents $P<0.05$

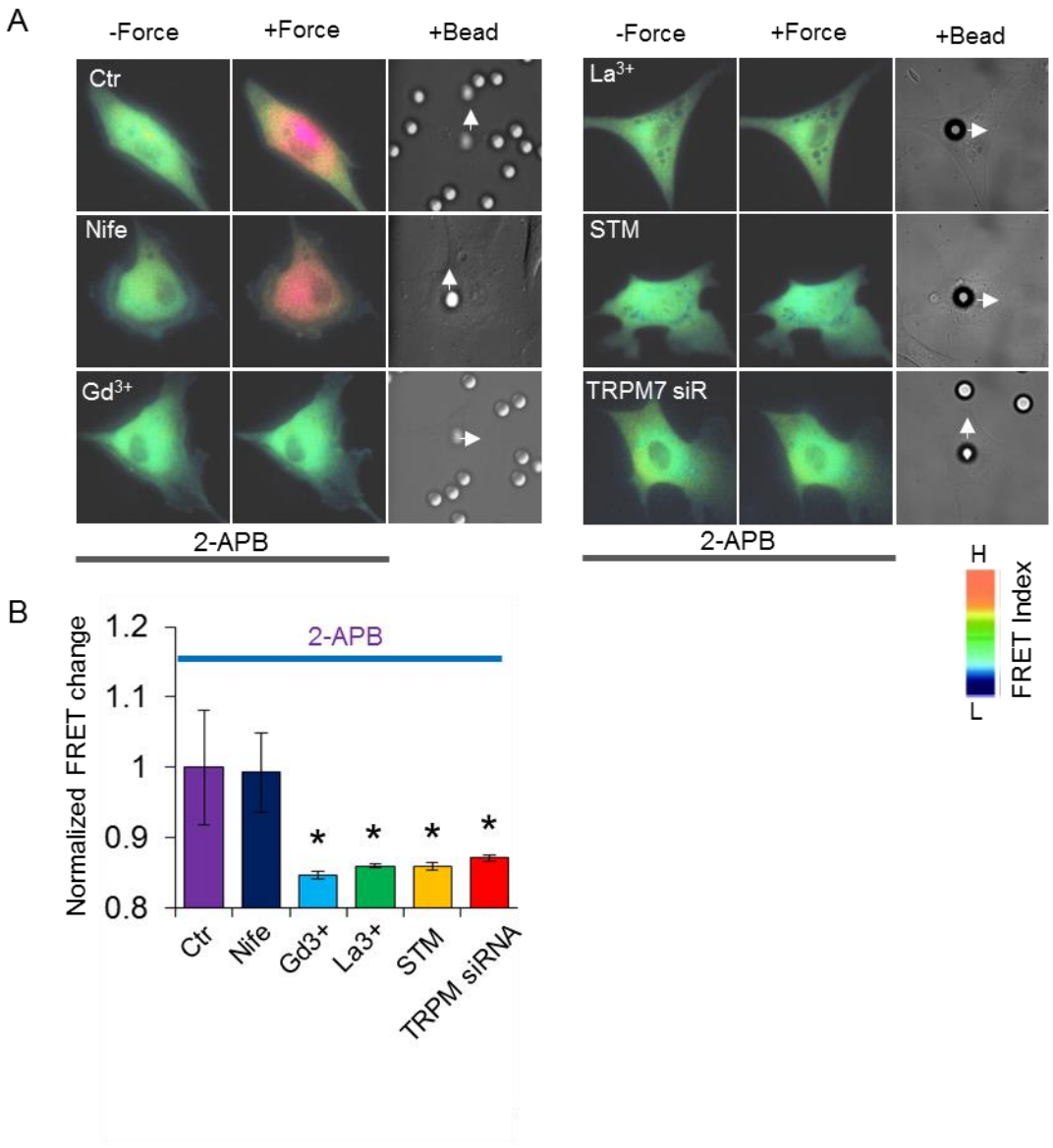

Figure 3-6. Ca^{2+} influx via mechanosensitive channels in response to mechanical force in Ca^{2+}-medium (2 mM Ca^{2+}). Ca^{2+} release from ER in all the HMSCs was blocked by pre-treatment with 2APB. (**A**) Color images represent the YPet/ECFP emission ratio of the cytoplasmic Ca^{2+} biosensor in control cells treated by 2APB only (n=5) or those co-treated by nifedipine (n=5), Gd^{3+} (n=3), La^{3+} (n=6), STM (n=8), or TRPM7 siRNA (n=9). Arrows in DIC images point to the direction of applied force. (**B**) Bar graphs represent the normalized change of YPet/ECFP emission ratio of the cytoplasmic Ca^{2+} biosensor under different conditions as indicated in (**A**). Error bars indicate standard errors of mean; * represents $P<0.05$.

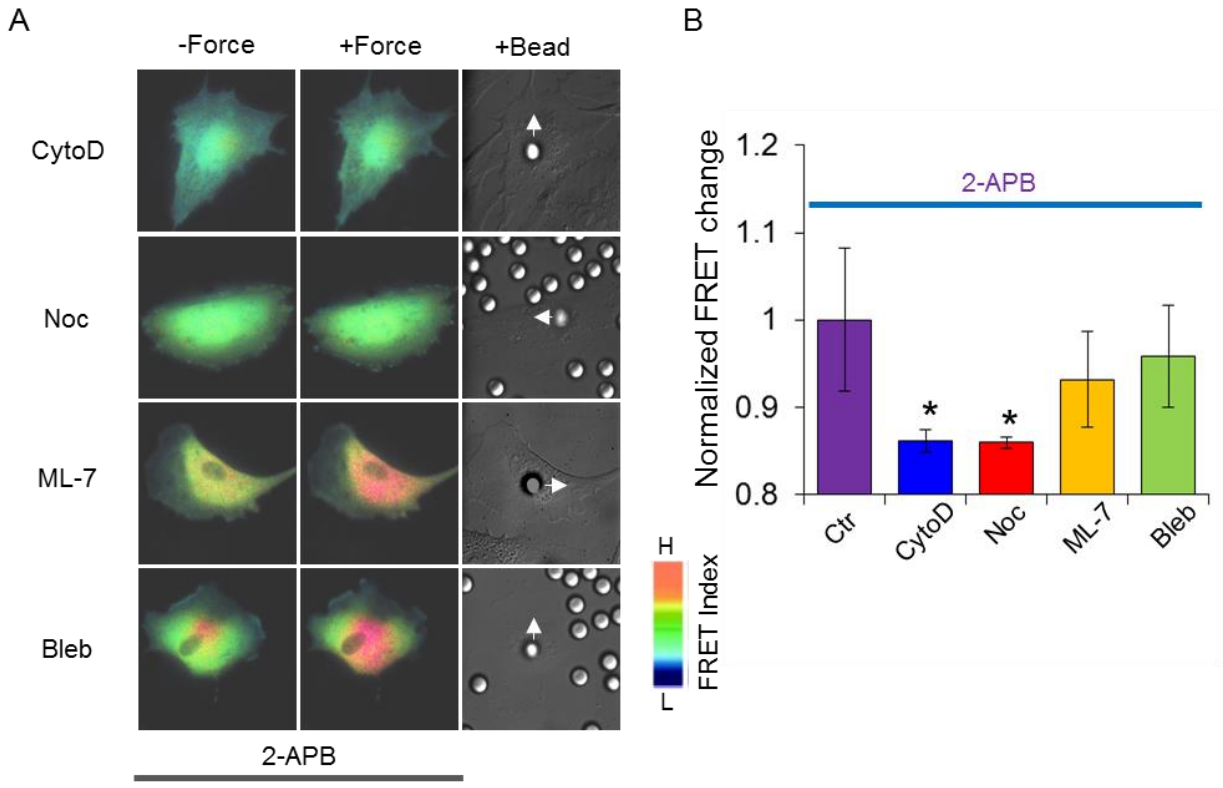

Figure 3-7. Ca^{2+} influx via the mechanosensitive channels in response to mechanical force is mediated by cytoskeletal support, but not by actomyosin contractility. Ca^{2+} release from ER in all the HMSCs was blocked by pre-treatment with 2APB. (**A**) Color images represent the YPet/ECFP emission ratio of the cytoplasmic Ca^{2+} biosensor in cells pretreated by 2APB together with CytoD (n=8), Nocodazole (n=4), ML-7 (n=9) or Blebbistatin (n=6). Arrows in DIC images point to the direction of applied force. (**B**) Bar graphs represent the normalized change of YPet/ECFP emission ratio of the cytoplasmic Ca^{2+} biosensor under different conditions as indicated in (**A**). Error bars indicate standard errors of mean; * represents $P<0.05$.

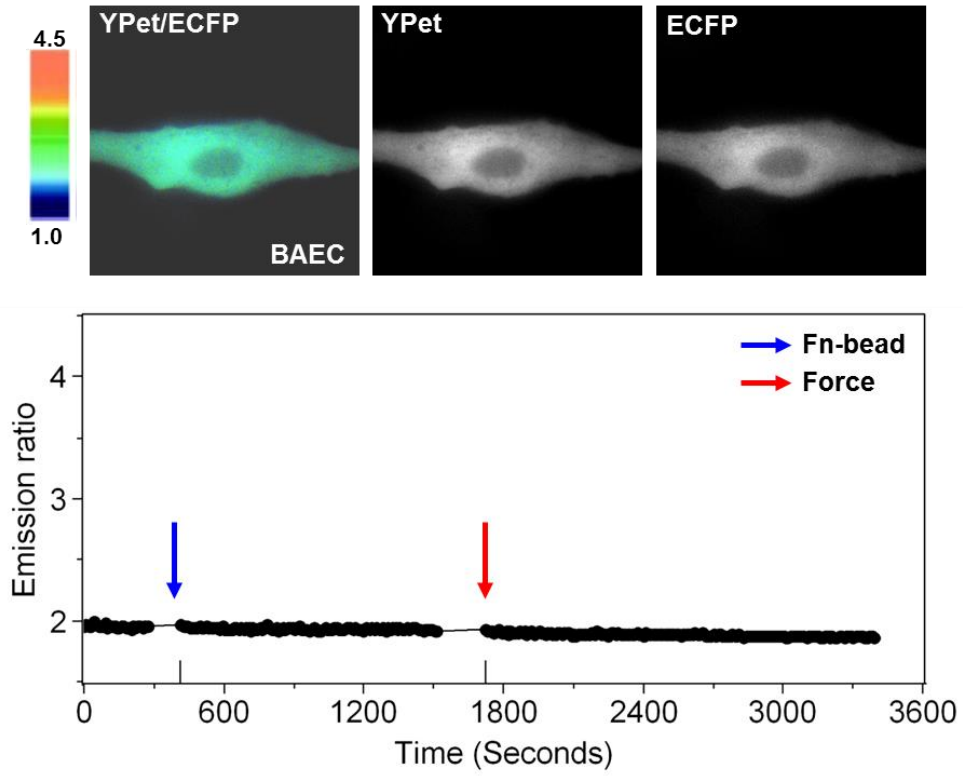

Supplementary Figure S3-1. Laser-tweezer pulling of a Fn-bead on a BAEC under Ca^{2+}-free medium. Color images (upper panels) represent the YPet/ECFP emission ratio of the cytoplasmic Ca^{2+} biosensor. The color scale bars represents the range of emission ratio, with cold and hot colors indicating low and high levels of Ca^{2+} concentration, respectively. The time courses of the YPet/ECFP emission ratio averaged over the cell body outside of nucleus is shown in the lower graph (n=6).

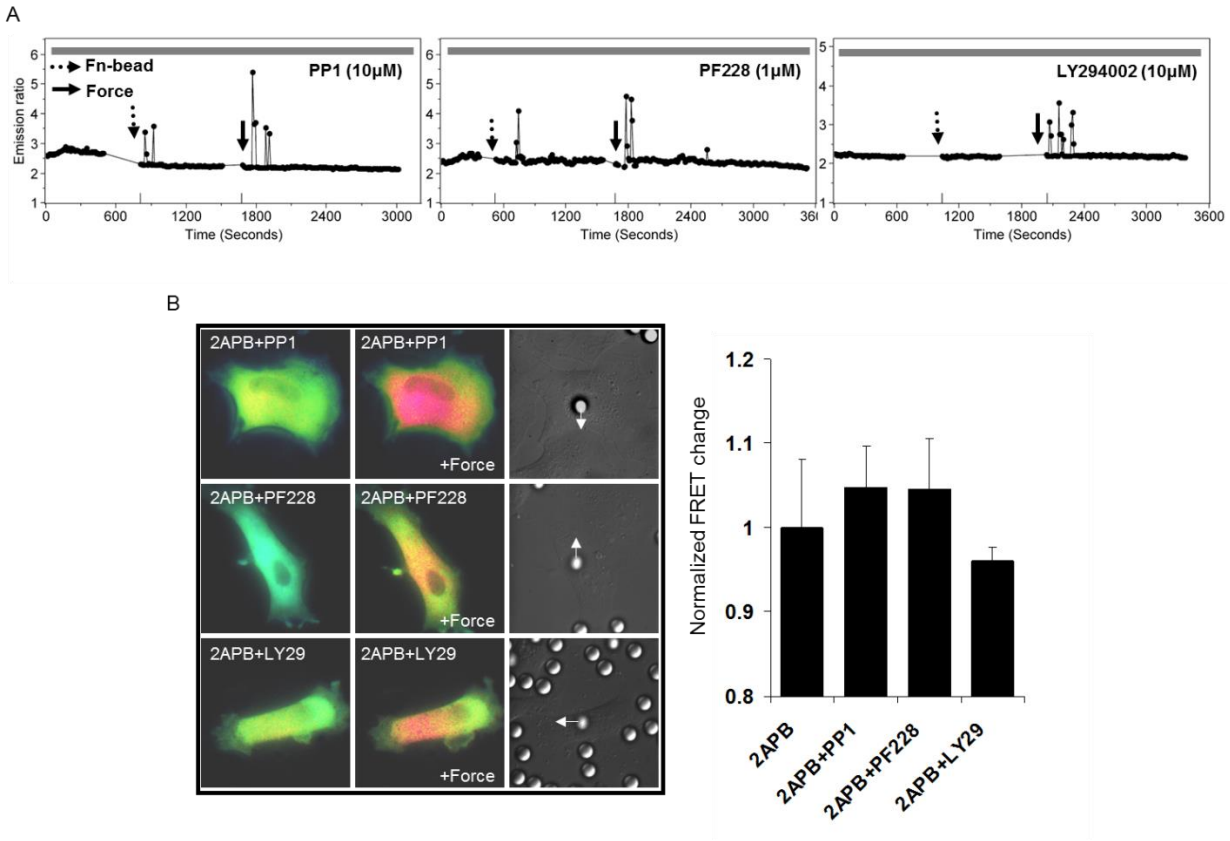

Supplementary Figure S3-2. Src, FAK or PI3K has no effect on the mechanical force induced Ca^{2+} signals. (**A**) The inhibition of neither Src by PP1 (n=4), FAK by PF228 (n=4), nor PI3K by LY294002 (n=3) abolished the force-induced cytosolic Ca^{2+} oscillations in HMSCs without extracellular Ca^{2+}. (**B**) The Ca^{2+} release from ER in all the HMSCs was blocked by pre-treatment with 2APB. Color images represent the YPet/ECFP emission ratio of the cytoplasmic Ca^{2+} biosensor in cells pretreated by 2APB together with PP1 (n=5), PF228 (n=4), or LY294002 (n=6). Arrows in DIC images point to the direction of applied force. Bar graphs represent the normalized change of YPet/ECFP emission ratio of the cytoplasmic Ca^{2+} biosensor under different conditions as indicated in (**A**). Error bars indicate standard errors of mean.

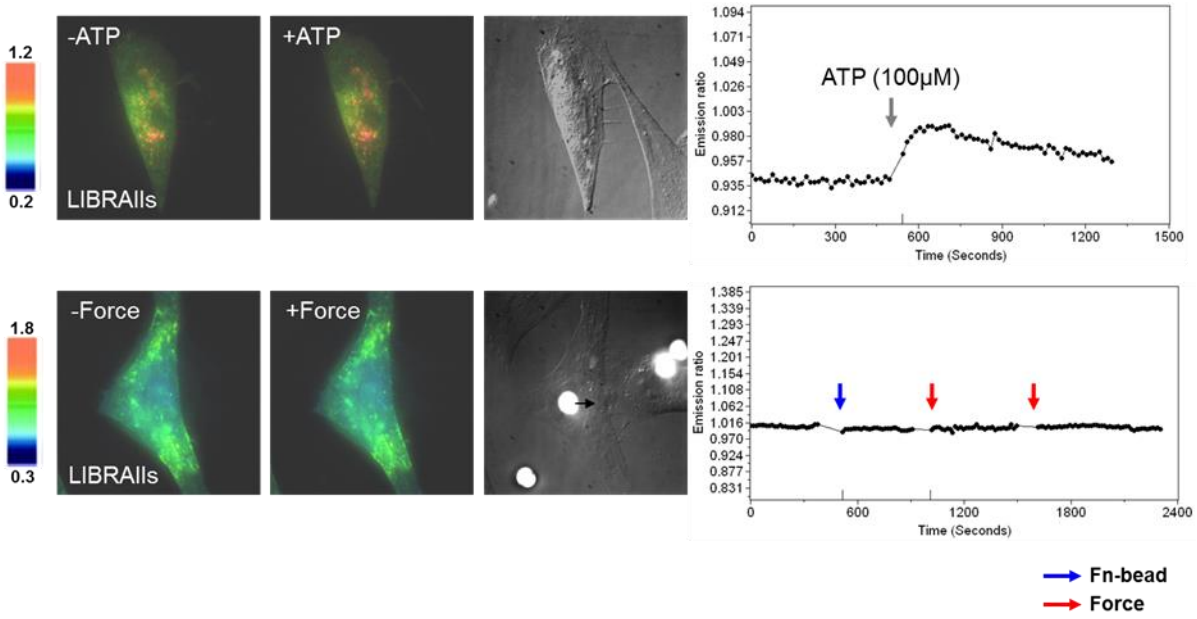

Supplementary Figure S3-3. IP_3 production is monitored by a FRET-based IP_3 biosensor, LIBRAIIs. ATP treatment induces IP_3 increase which can be clearly detected by an IP_3 biosensor LIBRAIIs (upper panels). However, laser-tweezer pulling of a Fn-bead to produce the mechanical force did not cause any increase in IP_3 (lower panels).

CHAPTER 4

cAMP-DEPENDENT PROTEIN KINASE A AND ENDOCYTOSIS OF β2-ADRENERGIC RECEPTOR IN RESPONSE TO SUBSTRATE RIGIDITY

The mechanical microenvironment, such as substrate stiffness, that surrounds cells has a great impact on cell structure and function. I first report that human mesenchymal stem cells (HMSCs) exposed to different magnitudes of substrate stiffness alter the signal activity of cAMP-dependent kinase (PKA) induced by a beta-adrenergic receptor (β-AR) agonist, Isoproterenol (Iso). Utilizing fluorescence resonance energy transfer (FRET) A-kinase activity reporter (AKAR), has revealed that HMSCs have shown a lower activity of Iso-induced PKA on soft substrates (0.1-1kPa), whereas they have shown much higher activity in response to stiffer or hard substrates (10-40kPa). Surprisingly, the application of forskolin (Fsk), non β-AR agonist has displayed a similar pattern of responses of PKA activity, regardless of the extent of stiffness. In further experiments, I have monitored that Iso-induced PKA activity was inhibited by the disruption of microtubules through Nocodazole (Noc, 5 μM), but not by cytochalasin D (Cyto D, 1 μM), an inhibitor of actin filaments. In contrast, the response pattern of Fsk-induced PKA activity was not affected by Noc, suggesting that substrate stiffness capable of affecting β-AR agonist induced PKA signaling is dependent on microtubules. In addition, the alteration of Iso-induced PKA signaling by substrate stiffness resulted in the occurrence of an abnormal endocytosis in β2-AR. The functional role of microtubules appeared to be correlated to the signaling cascade between β-AR agonist-induced PKA and its endocytosis, forming a feedback loop that modulates reciprocally. Taken together, these results indicate that the substrate stiffness consisting of mechanical microenvironment that is coordinated by microtubules may be an

important factor in regulating β-AR signaling cascade and PKA activation. Therefore, our study will provide critical cues to understand how alteration in tissue stiffness resulting from injury or disease can be involved in abnormal activity of G-protein coupled receptor-derived disease processes.

4.1 Introduction

Stem cells grown on the soft or stiffer substrate seem to alter their gene expression profile and behavior in response to their mechanical properties (Engler et al., 2006). In addition, recent reports have demonstrated that changes in tissue stiffness induce several pathological conditions such as cancer and fibrosis (Janmey et al., 2009; Liu et al.). In spite of a possible implication of the substrate stiffness giving rise to many types of diseases, how substrate stiffness may be correlated to cellular systems regarding a signal transduction is not yet well understood. G protein-coupled receptors (GPCRs) constitute the largest family of receptors. Over-expression or a functional impairment of GPCRs have appeared to be involved in not only tumor progression, but also in a variety of disease developments, including diabetes, heart disease and asthma (Deshpande and Penn, 2006; Hutchinson et al., 2008; Lee et al., 2008). Therefore, understanding the mechanisms that underlie the function and regulation of GPCRs, and knowledge of the mechanical microenvironment that have influence on their signaling cascades in stem cells may be required for the improvement of a therapeutic approach and for tissue engineering.

As one of the GPCRs, β-adrenergic receptors (β-ARs) have the three subtypes β1, β2 and β3. All these are linked to Gs proteins. In particular, β2 couples to Gi proteins, which in turn are linked to adenylyl cyclase (Chen-Izu et al., 2000; Ma and Huang, 2002). β-AR agonist binding results in increased levels of the intracellular second messenger cAMP that subsequently

mediates cAMP-dependent protein kinase (PKA) (Zhang et al., 2005). Protein kinase plays a role in regulating a wide variety of intracellular signaling cascades by enzymatically modifying other proteins through phosphorylation. Aberrant regulation of protein kinases in signal transduction can easily be exposed to a pathophysiological condition (Cohen et al., 2002). One of the major protein kinases, PKA, plays a crucial role in regulating many cellular processes including transcriptional control of cAMP response element (CRE), essential metabolisms, such as glycogen, sugar and lipids, and DNA replication (Rosenberg et al., 2006; Matyakhina et al., 2006; Costanzo et al., 1999). In spite of the emerging evidence that an appropriate PKA activity in vivo is very important for maintaining physiological conditions, how the stiffness of microenvironment can be correlated to the cAMP-dependent PKA signaling pathway is not well understood. To examine the effect of substrate stiffness on the cAMP-dependent PKA signaling, I have utilized fluorescent resonance energy transfer (FRET) technology. Genetically encoded FRET based A-kinase Activity Reporter (AKAR) has been regarded as a powerful tool to monitor dynamic PKA activity with high spatio-termporal resolutions in living cells (Depry et al.; Zhang et al., 2005).

In this chapter, I have observed the distinct signaling pathway in the receptor agonist-induced PKA, compared to the pharmacologically-induced PKA signals in response to different magnitudes of substrate stiffness, which led to an abnormal β2-AR endocytosis in a microtubules-dependent manner. These findings will not only shed new light on our understanding of how stem cells respond to the mechanical microenvironment to coordinate GPCR signal transduction, but they will also provide useful information for advancing stem cell therapy and tissue engineering.

4.2 Materials and Methods

4.2.1 Bis-acrylamide-PA gel fabrication

To make the polyacrylamide (PA) gel solution, acrylamide (5%) and bis-acrylamide (0.03-3%) solution (Bio-Rad, Hercules, CA) were mixed with distilled water. To polymerize the solutions, 10% w/v ammonium persulfate (Bio-Rad) and *N,N,N',N'*-Tetramethylethylenediamine (TEMED; Bio-Rad) were added following a method developed by Pelham and Wang (Pelham and Wang, 1997). After polymerization, sulfo-SANPAH [sulfosuccinimidyl6(4_-azide-2_-nitrophenyl-amino) hexanoate; Pierce Biotechnology, Rockford, IL] was used to crosslink the extracellular matrix molecules onto the gel surface. The surface of the gel was reacted with a 40 mg/ml solution of collagen type I.

4.2.2 Cell culture and transfection

Human mesenchymal stem cells (HMSCs; Lonza Walkersvile, Inc., Walkersvile, MD) were cultured with mesenchymal stem cell growth medium (MSCGM, PT-3001, Lonza) containing 10% fetal bovine serum, 2mM L-glutamine, 100 U/ml penicillin and 100 ug/ml streptomycin in a humidified incubator of 95% O_2 and 5% CO_2 at 37°C. The DNA plasmids were transfected into the cells using Lipofectamine 2000 (Invitrogen, Carlsbad, CA) reagent according to the product instructions.

4.2.3 Gene construction and DNA plasmids

The construct of FRET-based A-kinase activity reporter 2 (AKAR2) has been described in depth previously (Zhang et al., 2005). In order to enhance the FRET emission ratio, the FRET

pair was transformed into ECFP/YPet. Briefly, the fragment containing ECFP, forkhead associated domain 1 (FHA1) and PKA substrate sequence (SAGKPGSGEGSTKGLRRATLVDGGTGGS) was fused to YPet and subcloned into pcDNA3 for mammalian cell expression. A green fluorescent protein (GFP)-tagged version of β_2-adrenergic receptor (β_2AR) and of Gαs have been well-described in previous reports (Allen et al., 2005; Tao et al., 2003).

4.2.4 Imaging and microscopy

Cells were starved with 0.5% FBS for 36-48h before imaging experiments. During the imaging process, the cells were maintained in a CO_2-independent medium (Invitrogen, CA) without serum at 37℃. When indicated, cells were treated with Isoproterenol (Iso, 10 μM; Sigma) or forskolin (Fsk, 10 μM; Calbiochem). For inhibition studies of PKA activity, H89 (10 μM) was added before treatment of Iso. To disrupt the polymerization of actin filaments and microtubules, the experiments were performed by pretreating Cytochalasin D (CytoD, 1 μM) or Nocodazole (Noc, 5 μM) to the cells. To inhibit endocytosis of β-AR, methyl-beta-cyclodextrin (MβCD, 20 μM; Sigma) was pretreated with the cells for 1 h before imaging. Images were acquired on a Zeiss Axiovert 200M microscope (Carl Zeiss) equipped with a cooled charge-coupled device (CCD) camera (Cascade 512B, Photometrics) and a 440DF20 excitation filter, a 455DRLP dichroic mirror, and two emission filters controlled by a filter changer (480DF30 for CFP and 535DF25 for YFP). Time-lapse images were acquired every 1 min and the emission ratio images were computed and analyzed in Metafluor 6.2 software (Universal Imaging, West Chester, PA).

4.2.5 Statistical analysis

All statistical data were expressed as the mean ± standard error of the mean (SEM). Statistical evaluation was completed by using Excel software to perform a Student's t-test to determine the statistical differences between groups. A significant difference was determined by the P-value (< 0.05).

4.3 Results

4.3.1 Distinct signaling pattern of cAMP-dependent PKA upon β-AR agonist stimulation in response to substrate stiffness

Since mechanical factors play a crucial role in the production of intracellular second messengers (Hughes-Fulford, 2004; Sadoshima and Izumo, 1993), I have investigated whether substrate stiffness can regulate cAMP-dependent protein kinase A (PKA) activity in HMSCs. To perform this study, FRET technology was applied. The HMSCs expressing AKAR2 reporter were cultured on PA gel substrates with different magnitudes of stiffness, and then stimulated with a β-AR agonist, Isoproterenol (Iso), following PKA activity was assessed by real-time live cell imaging. As shown in Figure 4-1, I have observed Iso-induced PKA activity which occurred in a different way in response to each substrate stiffness. As cultured on hard gel substrate (40 kPa), the cells showed the largest increase in FRET ratio upon Iso treatment (0.182±0.018, n=10, P<0.01), whereas there were relatively small changes in FRET ratio in response to soft or stiffer substrates (0.1-10 kPa, 0.1 kPa; 0.031±0.01, n=6, 1 kPa; 0.093±0.012, n=7, and 10 kPa; 0.10±0.015, n=7). This suggests that β-AR agonist-induced PKA signaling can be activated in a stiffness-dependent manner in HMSCs. On the other hand, the pattern of Forskolin (Fsk)-induced

PKA activity appeared to be different from Iso-induced PKA signaling (Supplementary Fig. S4-1). It has shown a similar level of pattern in PKA activity upon Fsk stimulation, regardless of how much softer or stiffer the substrate is within the range from 0.1 to 40 kPa (0.1 kPa; 0.063±0.004, n=3, 1 kPa; 0.077±0.009, n=5 , 10 kPa; 0.07±0.004, n=3 and 40 kPa; 0.08±0.02, n=5) (Supplementary Fig. 1C). Therefore, these results indicate that substrate stiffness can regulate PKA activation induced by the β-AR agonist, but not Fsk-induced PKA activation.

4.3.2 Microtubule mediates β-AR agonist-induced PKA activity in response to substrate stiffness, but not Fsk-induced PKA signaling

Since there is some evidence showing the structure of cellular cytoskeleton is strongly dependent on the substrate stiffness to which the cell is bound (Bhadriraju and Hansen, 2002; Yeung et al., 2005), I have examined whether the cytoskeleton can mediate the distinct pattern of Iso-induced PKA signals in response to substrate stiffness in HMSCs. When cells were pretreated with Cyto D (1 μM for 1h), they still maintained the distinct level of pattern in Iso-induced PKA activity between soft substrates (0.1 kPa; 0.04±0.007, n=5 and 1 kPa; 0.02±0.008, n=5,) and hard substrate (40 kPa; 0.116±0.02, n=5, $P<0.05$), suggesting that actin cytoskeleton had no significant effect on the signals (Fig. 4-2A). However, when pretreated with Noc (5 μM for 1h), the pattern of Iso-induced PKA signal activity of the cells cultured on both stiffer (10 kPa, 0.015±0.005, n=6) and hard (40 kPa, 0.03±0.004, n=6) substrates was significantly inhibited and sustained a lower level of PKA activity than on soft substrates (0.1 kPa, 0.008±0.02, n=6 and 1 kPa, 0.018±0.008, n=6) (Fig. 4-2B). These results indicate that the structural support of microtubules mediates Iso-induced PKA signal transduction in response to substrate stiffness, but that actin filaments may not be involved in this process. Notably,

microtubules had no effect on Fsk-induced PKA signaling regardless of the extent of substrate stiffness (Supplementary Fig. S4-2). Thus, these results suggest that the functional role of microtubules is pivotal in maintaining β-AR agonist induced PKA signal pathway in HMSCs exposed to different substrate stiffness.

4.3.3 Substrate stiffness regulates the β_2-AR endocytosis via PKA signal that dependent on microtubules

After an agonist binds to β-ARs, they can be phosphorylated by PKA. Increased phosphorylation of the β-ARs is believed to be involved in the process of the desensitization that subsequently leads to sequestration and internalization of the receptors (Ma and Huang, 2002). Therefore, we hypothesized that an increase or decrease in the production of PKA regulated by substrate stiffness could affect the β-AR endocytosis. To carry out this study, I took advantage of β_2-AR-GFP construct and transfected it into the cells. As a result, I have observed that the endocytosis of β_2-AR took place strongly on hard substrate (40 kPa) in accordance with the strongest PKA activity. In contrast, β_2-AR endocytosis decreased significantly when it comes to soft substrate, (Fig. 4-3). A potent selective inhibitor of cAMP-dependent PKA, H89 treatment inhibited both Iso- and Fsk-induced PKA activity (Supplementary Fig. S4-3) and blocked the event of β_2-AR endocytosis upon Iso treatment in response to substrate stiffness (Supplementary Fig. S4-4A), suggesting that β-AR agonist-induced PKA activation, but not PKA itself, contributes to the endocytosis of β_2-AR (Supplementary Fig. S4-4B). In further experiments, I found that β_2-AR endocytosis was dependent on the support of microtubules. The result of co-transfection with mCherry-tubulin and β_2-AR-GFP in HMSCs cultured on hard gel substrate concurrently showed well-organized networks in microtubule structure and a high rate of event

in β_2-AR endocytosis, whereas they were inhibited on soft gel substrate (Fig. 4-4A). Unlike CytoD, which inhibited the actin filaments, Noc treatment for depolymerization of microtubules inhibited Iso-induced β_2-AR endocytosis on the hard substrate (Fig. 4-4B). Therefore, these results support the conclusion that substrate stiffness regulates agonist-induced β_2-AR endocytosis via PKA signaling depending on microtubules.

4.3.4 Feedback effect on β-AR agonist induced- PKA signaling and β_2-AR endocytosis

To examine whether β_2-AR endocytosis reciprocally affects β-AR agonist induced PKA signaling in response to substrate stiffness, we pretreated MβCD to inhibit β_2-AR endocytosis and monitored Iso-induced PKA activity in HMSCs. As shown in Figure 4-5A, MβCD treatment inhibited Iso-induced β_2-AR endocytosis on both soft (0.1 kPa) and hard substrates (40 kPa). Further experiments showed that pretreatment of MβCD significantly inhibited Iso-induced PKA activity on hard gel substrate (n=6) compared to that of MβCD-untreated cells (Fig. 4-5B, n=7). These results suggest that both β-AR agonist-induced endocytosis and PKA activity form a feedback effect to mediate reciprocally in a microtubule-dependent manner.

4.4 Discussion

The binding of the beta-adrenergic receptors (β-AR) agonist to its receptor initiates inside signal transduction, activating adenylyl cyclase and its downstream effector, cyclic AMP (cAMP). Consequentially, the regulation of the amount of intracellular cAMP could be very important in functionally controlling a target protein such as protein kinase (PKA), which ultimately regulates a wide variety of cellular processes. Recently, it has been reported that substrate stiffness could be a significant factor that contributes to the differentiation and

proliferation of stem cells. In fact, HMSCs have shown to be differentiated into various cell phenotypes, depending on the magnitude of substrate stiffness (Engler et al., 2006). For instance, on soft substrate that mimics soft tissue, such as brain tissue, they tend to alter their phenotypes into neuronal cell lineage that prefers to reside on soft tissue, whereas they show characteristics of osteoblast lineage in response to hard substrate that mimics hard tissue, like bone. Such a drastic alteration of cellular phenotypes might be accompanied by numerous changes in the cellular system, including GPCR signal transduction for their specialized tasks *in vivo*.

In this chapter, I have investigated not only whether or how substrate stiffness could be involved in PKA activation, but also how those factors could be correlated with endocytosis of β-AR in HMSCs. As a result, I first found the differential activity of β-AR agonist-induced PKA in response to substrate stiffness, although it had no effect on Fsk-induced PKA activity. This might be because Fsk binds to a different target to stimulate PKA signaling. In fact, Fsk directly activates the plasma membrane enzyme, adenylyl cyclase without any direct stimulation of β-adrenergic receptors (ARs) (Pinto et al., 2009; Seamon and Daly, 1986). Therefore, activated adenylyl cyclase catalyzes conversion of ATP to cAMP acts as a second messenger and stimulates a downstream molecule, PKA. However, the primary target for Iso appears to differ from that of Fsk. Iso binds to β-AR, one of the GPCRs at the plasma membrane, and may require more steps of signaling cascade to activate PKA (Schramm et al., 1986; Zhang et al., 2005). Thus, the findings of this study suggest that mechanical factors may have the potential to affect GPCR signal transduction. In fact, a few previous reports have demonstrated that mechanical stress affects a G-protein subunit Gαs recruitment to focal adhesions, and Gαs appears to mediate mechanical force-induced cAMP signaling through integrins (Alenghat et al., 2009; Meyer et al., 2000). However, in this study, neither soft substrate (0.1 kPa) nor hard substrate (40 kPa) had

any effect on Gαs recruitment and Gαs endocytosis in response to Iso (Supplementary Fig. S4-5). In addition, unlike Gαs increase within focal adhesions that are associated with β1 integrin, and a possible involvement of actin filaments in response to local mechanical stress (Alenghat et al., 2009; Geiger et al., 2009), this data has shown that actin filaments have no influence on substrate stiffness-dependent and Iso-induced PKA activation, as well as endocytosis of β_2-AR, suggesting that a global stimulation through substrate stiffness operates in a different manner. Importantly, I have elucidated that both PKA activity and the endocytosis of β_2-AR, stimulated by Iso in response to substrate stiffness, appear to be dependent on the microtubule. The disruption of microtubules inhibited the internalized β_2-AR-GFP particles (Fig. 4-4), which is consistent with the previous report that a microtubule inhibitor, Nocodazole, blocks the agonist-induced β_2-AR internalization in epidermoid carcinoma A431 cells, although an inhibitor of actin filaments Latrunculin-A, did not (Shumay et al., 2004). Although it is not yet clear how microtubules can mediate both β-AR agonist-induced PKA activation and β-AR endocytosis within HMSCs as exposed to substrate stiffness, our evidence demonstrates that two signals appear to be correlated by means of a feedback effect (Fig. 4-6). That is to say, the level of β-AR agonist-induced PKA activation of the cells in response to substrate stiffness may be able to regulate the event of β_2-AR endocytosis. Treatment of Fsk and H89 has revealed that PKA seems not only sufficient, but essential to the event of β_2-AR endocytosis. It requires the uncoupling of the receptor which is possible by two types of kinases, G-protein coupled receptor kinase 2 (GRK2) and PKA (Daaka et al., 1997; Whalen et al., 2007). Conversely, inhibition of β_2-AR endocytosis by MβCD can regulate the level of β-AR agonist-induced PKA activation, forming a feedback loop to each other while being modulated by microtubules. These findings are probably the first evidence of how substrate stiffness controls kinase activity and its associated signal.

In conclusion, this study is the first to show how HMSCs respond to mechanical stiffness and how this affects their signal transduction. This study reports that not only substrate stiffness affects β-AR agonist induced PKA activation and β_2-AR endocytosis, but also that two biological phenomena can be correlated by forming a feedback circuit in response to a mechanical factor. These findings will shed new light on our understanding of how mesenchymal stem cells respond to mechanical microenvironments to coordinate GPCR signal transduction, and they will also provide a useful strategy for advancing stem cell therapy and tissue engineering.

4.5 References

Alenghat, F.J., Tytell, J.D., Thodeti, C.K., Derrien, A., and Ingber, D.E. (2009). Mechanical control of cAMP signaling through integrins is mediated by the heterotrimeric Galphas protein. J Cell Biochem *106*, 529-538.

Allen, J.A., Yu, J.Z., Donati, R.J., and Rasenick, M.M. (2005). Beta-adrenergic receptor stimulation promotes G alpha s internalization through lipid rafts: a study in living cells. Mol Pharmacol *67*, 1493-1504.

Amano, M., Ito, M., Kimura, K., Fukata, Y., Chihara, K., Nakano, T., Matsuura, Y., and Kaibuchi, K. (1996). Phosphorylation and activation of myosin by Rho-associated kinase (Rho-kinase). J Biol Chem *271*, 20246-20249.

Berridge, M.J. (1993). Inositol trisphosphate and calcium signalling. Nature *361*, 315-325.

Berridge, M.J., Bootman, M.D., and Roderick, H.L. (2003). Calcium signalling: dynamics, homeostasis and remodelling. Nat Rev Mol Cell Biol *4*, 517-529.

Berridge, M.J., Lipp, P., and Bootman, M.D. (2000). The versatility and universality of calcium signalling. Nat Rev Mol Cell Biol *1*, 11-21.

Bhadriraju, K., and Hansen, L.K. (2002). Extracellular matrix- and cytoskeleton-dependent changes in cell shape and stiffness. Exp Cell Res *278*, 92-100.

Bhadriraju, K., Yang, M., Alom Ruiz, S., Pirone, D., Tan, J., and Chen, C.S. (2007). Activation of ROCK by RhoA is regulated by cell adhesion, shape, and cytoskeletal tension. Exp Cell Res *313*, 3616-3623.

Bootman, M.D., Collins, T.J., Mackenzie, L., Roderick, H.L., Berridge, M.J., and Peppiatt, C.M. (2002). 2-aminoethoxydiphenyl borate (2-APB) is a reliable blocker of store-operated Ca2+ entry but an inconsistent inhibitor of InsP3-induced Ca2+ release. Faseb J *16*, 1145-1150.

Chen-Izu, Y., Xiao, R.P., Izu, L.T., Cheng, H., Kuschel, M., Spurgeon, H., and Lakatta, E.G. (2000). G(i)-dependent localization of beta(2)-adrenergic receptor signaling to L-type Ca(2+) channels. Biophys J *79*, 2547-2556.

Cohen, C., Zavala-Pompa, A., Sequeira, J.H., Shoji, M., Sexton, D.G., Cotsonis, G., Cerimele, F., Govindarajan, B., Macaron, N., and Arbiser, J.L. (2002). Mitogen-actived protein kinase activation is an early event in melanoma progression. Clin Cancer Res *8*, 3728-3733.

D'Souza, S.J., Pajak, A., Balazsi, K., and Dagnino, L. (2001). Ca2+ and BMP-6 signaling regulate E2F during epidermal keratinocyte differentiation. J Biol Chem *276*, 23531-23538.

Daaka, Y., Luttrell, L.M., and Lefkowitz, R.J. (1997). Switching of the coupling of the beta2-adrenergic receptor to different G proteins by protein kinase A. Nature *390*, 88-91.

Dang, J.M., Sun, D.D., Shin-Ya, Y., Sieber, A.N., Kostuik, J.P., and Leong, K.W. (2006). Temperature-responsive hydroxybutyl chitosan for the culture of mesenchymal stem cells and intervertebral disk cells. Biomaterials *27*, 406-418.

den Dekker, E., Molin, D.G., Breikers, G., van Oerle, R., Akkerman, J.W., van Eys, G.J., and Heemskerk, J.W. (2001). Expression of transient receptor potential mRNA isoforms and Ca(2+) influx in differentiating human stem cells and platelets. Biochim Biophys Acta *1539*, 243-255.

Depry, C., Allen, M.D., and Zhang, J. Visualization of PKA activity in plasma membrane microdomains. Mol Biosyst *7*, 52-58.

Deshpande, D.A., and Penn, R.B. (2006). Targeting G protein-coupled receptor signaling in asthma. Cell Signal *18*, 2105-2120.

Ducibella, T., and Fissore, R. (2008). The roles of Ca2+, downstream protein kinases, and oscillatory signaling in regulating fertilization and the activation of development. Dev Biol *315*, 257-279.

Emmert, D.A., Fee, J.A., Goeckeler, Z.M., Grojean, J.M., Wakatsuki, T., Elson, E.L., Herring, B.P., Gallagher, P.J., and Wysolmerski, R.B. (2004). Rho-kinase-mediated Ca2+-independent contraction in rat embryo fibroblasts. Am J Physiol Cell Physiol *286*, C8-21.

Engler, A.J., Griffin, M.A., Sen, S., Bonnemann, C.G., Sweeney, H.L., and Discher, D.E. (2004). Myotubes differentiate optimally on substrates with tissue-like stiffness: pathological implications for soft or stiff microenvironments. J Cell Biol *166*, 877-887.

Engler, A.J., Sen, S., Sweeney, H.L., and Discher, D.E. (2006). Matrix elasticity directs stem cell lineage specification. Cell *126*, 677-689.

Engler, A.J., Sweeney, H.L., Discher, D.E., and Schwarzbauer, J.E. (2007). Extracellular matrix elasticity directs stem cell differentiation. J Musculoskelet Neuronal Interact *7*, 335.

Fewtrell, C. (1993). Ca2+ oscillations in non-excitable cells. Annu Rev Physiol *55*, 427-454.

Geiger, B., Spatz, J.P., and Bershadsky, A.D. (2009). Environmental sensing through focal adhesions. Nat Rev Mol Cell Biol *10*, 21-33.

Gollasch, M., Haase, H., Ried, C., Lindschau, C., Morano, I., Luft, F.C., and Haller, H. (1998). L-type calcium channel expression depends on the differentiated state of vascular smooth muscle cells. Faseb J *12*, 593-601.

Gronthos, S., Zannettino, A.C., Graves, S.E., Ohta, S., Hay, S.J., and Simmons, P.J. (1999). Differential cell surface expression of the STRO-1 and alkaline phosphatase antigens on discrete developmental stages in primary cultures of human bone cells. J Bone Miner Res *14*, 47-56.

Hayakawa, K., Tatsumi, H., and Sokabe, M. (2008). Actin stress fibers transmit and focus force to activate mechanosensitive channels. J Cell Sci *121*, 496-503.

Hughes-Fulford, M. (2004). Signal transduction and mechanical stress. Sci STKE *2004*, RE12.

Hutchinson, D.S., Summers, R.J., and Bengtsson, T. (2008). Regulation of AMP-activated protein kinase activity by G-protein coupled receptors: potential utility in treatment of diabetes and heart disease. Pharmacol Ther *119*, 291-310.

Jacob, R. (1990). Calcium oscillations in electrically non-excitable cells. Biochim Biophys Acta *1052*, 427-438.

Janmey, P.A., Winer, J.P., Murray, M.E., and Wen, Q. (2009). The hard life of soft cells. Cell Motil Cytoskeleton *66*, 597-605.

Kassem, M., and Abdallah, B.M. (2008). Human bone-marrow-derived mesenchymal stem cells: biological characteristics and potential role in therapy of degenerative diseases. Cell Tissue Res *331*, 157-163.

Kawano, S., Shoji, S., Ichinose, S., Yamagata, K., Tagami, M., and Hiraoka, M. (2002). Characterization of Ca(2+) signaling pathways in human mesenchymal stem cells. Cell Calcium *32*, 165-174.

Kimura, K., Ito, M., Amano, M., Chihara, K., Fukata, Y., Nakafuku, M., Yamamori, B., Feng, J., Nakano, T., Okawa, K., *et al.* (1996). Regulation of myosin phosphatase by Rho and Rho-associated kinase (Rho-kinase). Science *273*, 245-248.

Kiselyov, K.I., Semyonova, S.B., Mamin, A.G., and Mozhayeva, G.N. (1999). Miniature Ca2+ channels in excised plasma-membrane patches: activation by IP3. Pflugers Arch *437*, 305-314.

Kolossov, E., Fleischmann, B.K., Liu, Q., Bloch, W., Viatchenko-Karpinski, S., Manzke, O., Ji, G.J., Bohlen, H., Addicks, K., and Hescheler, J. (1998). Functional characteristics of ES cell-derived cardiac precursor cells identified by tissue-specific expression of the green fluorescent protein. J Cell Biol *143*, 2045-2056.

Kureishi, Y., Kobayashi, S., Amano, M., Kimura, K., Kanaide, H., Nakano, T., Kaibuchi, K., and Ito, M. (1997). Rho-associated kinase directly induces smooth muscle contraction through myosin light chain phosphorylation. J Biol Chem *272*, 12257-12260.

Lee, H.J., Wall, B., and Chen, S. (2008). G-protein-coupled receptors and melanoma. Pigment Cell Melanoma Res *21*, 415-428.

Li, Q., Wang, J., Shahani, S., Sun, D.D., Sharma, B., Elisseeff, J.H., and Leong, K.W. (2006). Biodegradable and photocrosslinkable polyphosphoester hydrogel. Biomaterials *27*, 1027-1034.

Li, S., Chen, B.P., Azuma, N., Hu, Y.L., Wu, S.Z., Sumpio, B.E., Shyy, J.Y., and Chien, S. (1999). Distinct roles for the small GTPases Cdc42 and Rho in endothelial responses to shear stress. J Clin Invest *103*, 1141-1150.

Liu, F., Mih, J.D., Shea, B.S., Kho, A.T., Sharif, A.S., Tager, A.M., and Tschumperlin, D.J. Feedback amplification of fibrosis through matrix stiffening and COX-2 suppression. J Cell Biol *190*, 693-706.

Ma, Y.C., and Huang, X.Y. (2002). Novel signaling pathway through the beta-adrenergic receptor. Trends Cardiovasc Med *12*, 46-49.

McBeath, R., Pirone, D.M., Nelson, C.M., Bhadriraju, K., and Chen, C.S. (2004). Cell shape, cytoskeletal tension, and RhoA regulate stem cell lineage commitment. Dev Cell *6*, 483-495.

Meyer, C.J., Alenghat, F.J., Rim, P., Fong, J.H., Fabry, B., and Ingber, D.E. (2000). Mechanical control of cyclic AMP signalling and gene transcription through integrins. Nat Cell Biol *2*, 666-668.

Miyawaki, A., Llopis, J., Heim, R., McCaffery, J.M., Adams, J.A., Ikura, M., and Tsien, R.Y. (1997). Fluorescent indicators for Ca2+ based on green fluorescent proteins and calmodulin. Nature *388*, 882-887.

Osipchuk, Y.V., Wakui, M., Yule, D.I., Gallacher, D.V., and Petersen, O.H. (1990). Cytoplasmic Ca2+ oscillations evoked by receptor stimulation, G-protein activation, internal application of inositol trisphosphate or Ca2+: simultaneous microfluorimetry and Ca2+ dependent Cl- current recording in single pancreatic acinar cells. Embo J *9*, 697-704.

Palmer, A.E., Jin, C., Reed, J.C., and Tsien, R.Y. (2004). Bcl-2-mediated alterations in endoplasmic reticulum Ca2+ analyzed with an improved genetically encoded fluorescent sensor. Proc Natl Acad Sci U S A *101*, 17404-17409.

Pelham, R.J., Jr., and Wang, Y. (1997). Cell locomotion and focal adhesions are regulated by substrate flexibility. Proc Natl Acad Sci U S A *94*, 13661-13665.

Pinto, C., Hubner, M., Gille, A., Richter, M., Mou, T.C., Sprang, S.R., and Seifert, R. (2009). Differential interactions of the catalytic subunits of adenylyl cyclase with forskolin analogs. Biochem Pharmacol *78*, 62-69.

Rodriguez, J.P., Gonzalez, M., Rios, S., and Cambiazo, V. (2004). Cytoskeletal organization of human mesenchymal stem cells (MSC) changes during their osteogenic differentiation. J Cell Biochem *93*, 721-731.

Rosada, C., Justesen, J., Melsvik, D., Ebbesen, P., and Kassem, M. (2003). The human umbilical cord blood: a potential source for osteoblast progenitor cells. Calcif Tissue Int *72*, 135-142.

Sadoshima, J., and Izumo, S. (1993). Mechanical stretch rapidly activates multiple signal transduction pathways in cardiac myocytes: potential involvement of an autocrine/paracrine mechanism. Embo J *12*, 1681-1692.

Schramm, M., Eimerl, S., Goodman, M., Verlander, M.S., Khan, M.M., and Melmon, K. (1986). High potency congeners of isoproterenol. Binding to beta-adrenergic receptors, activation of adenylate cyclase and stimulation of intracellular cyclic AMP synthesis. Biochem Pharmacol *35*, 2805-2809.

Seamon, K.B., and Daly, J.W. (1986). Forskolin: its biological and chemical properties. Adv Cyclic Nucleotide Protein Phosphorylation Res *20*, 1-150.

Shumay, E., Gavi, S., Wang, H.Y., and Malbon, C.C. (2004). Trafficking of beta2-adrenergic receptors: insulin and beta-agonists regulate internalization by distinct cytoskeletal pathways. J Cell Sci *117*, 593-600.

Soderling, T.R., and Stull, J.T. (2001). Structure and regulation of calcium/calmodulin-dependent protein kinases. Chem Rev *101*, 2341-2352.

Sun, S., Liu, Y., Lipsky, S., and Cho, M. (2007). Physical manipulation of calcium oscillations facilitates osteodifferentiation of human mesenchymal stem cells. Faseb J *21*, 1472-1480.

Takahashi, R., Nishimura, J., Seki, N., Yunoki, T., Tomoda, T., Kanaide, H., and Naito, S. (2007). RhoA/Rho kinase-mediated Ca2+ sensitization in the contraction of human prostate. Neurourol Urodyn *26*, 547-551.

Tao, J., Wang, H.Y., and Malbon, C.C. (2003). Protein kinase A regulates AKAP250 (gravin) scaffold binding to the beta2-adrenergic receptor. Embo J *22*, 6419-6429.

Totsukawa, G., Yamakita, Y., Yamashiro, S., Hartshorne, D.J., Sasaki, Y., and Matsumura, F. (2000). Distinct roles of ROCK (Rho-kinase) and MLCK in spatial regulation of MLC phosphorylation for assembly of stress fibers and focal adhesions in 3T3 fibroblasts. J Cell Biol *150*, 797-806.

Tsien, R.W., and Tsien, R.Y. (1990). Calcium channels, stores, and oscillations. Annu Rev Cell Biol *6*, 715-760.

Whalen, E.J., Foster, M.W., Matsumoto, A., Ozawa, K., Violin, J.D., Que, L.G., Nelson, C.D., Benhar, M., Keys, J.R., Rockman, H.A., *et al.* (2007). Regulation of beta-adrenergic receptor signaling by S-nitrosylation of G-protein-coupled receptor kinase 2. Cell *129*, 511-522.

Wozniak, M.A., Desai, R., Solski, P.A., Der, C.J., and Keely, P.J. (2003). ROCK-generated contractility regulates breast epithelial cell differentiation in response to the physical properties of a three-dimensional collagen matrix. J Cell Biol *163*, 583-595.

Yeung, T., Georges, P.C., Flanagan, L.A., Marg, B., Ortiz, M., Funaki, M., Zahir, N., Ming, W., Weaver, V., and Janmey, P.A. (2005). Effects of substrate stiffness on cell morphology, cytoskeletal structure, and adhesion. Cell Motil Cytoskeleton *60*, 24-34.

Yoshizaki, H., Ohba, Y., Kurokawa, K., Itoh, R.E., Nakamura, T., Mochizuki, N., Nagashima, K., and Matsuda, M. (2003). Activity of Rho-family GTPases during cell division as visualized with FRET-based probes. J Cell Biol *162*, 223-232.

Zhang, J., Hupfeld, C.J., Taylor, S.S., Olefsky, J.M., and Tsien, R.Y. (2005). Insulin disrupts beta-adrenergic signalling to protein kinase A in adipocytes. Nature *437*, 569-573.

4.6 Figures

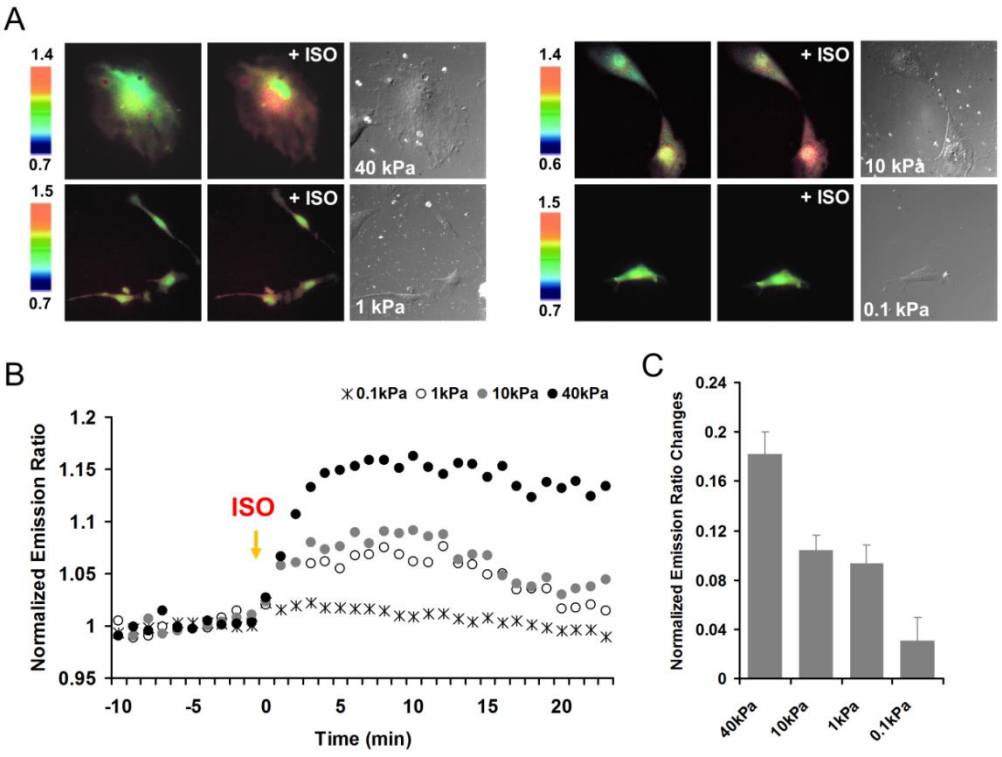

Figure 4-1. Distinct response of cAMP-dependent PKA activation upon Iso treatment in HMSCs cultured on different substrate stiffness. (A) Emission ratio images and (B) time courses in the cells expressing FRET-AKAR2 before and after being treated with a beta-AR agonist, Iso in response to substrate stiffness. (C) Bar graphs represent the emission ratio changes of the biosensor from multiple cells (mean ± SEM) where "n" indicates the sample number in each group and "#" represent the significant difference between indicated groups.

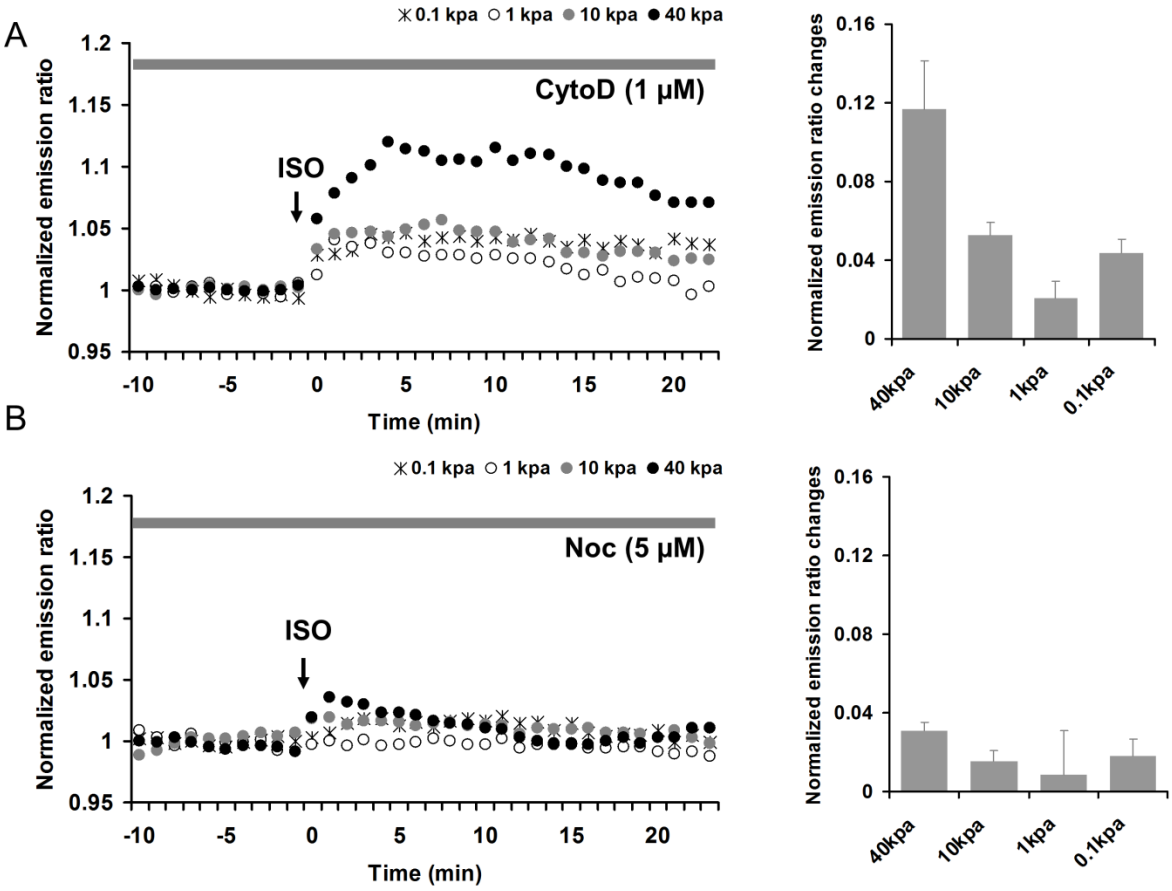

Figure 4-2. Effect of the cytoskeleton on β-AR agonist induced PKA activity in response to substrate stiffness. Time courses of the emission ratio of FRET-AKAR2 in the cells cultured on different substrate stiffness in response to Iso pretreated with (A) Cytochalasin D (Cyto D, 1μM), an inhibitor of actin filaments and (B) Nocodazole (Noc, 5μM), an inhibitor of microtubules. Contrary to CytoD-treated cells, in Noc-treated cells, β-AR agonist-induced PKA activity has been significantly inhibited. The bar graphs represent the emission ratio changes (mean ± SEM) of the biosensors where "n" denotes the sample number in each group, and "#" represents the significant difference between the groups.

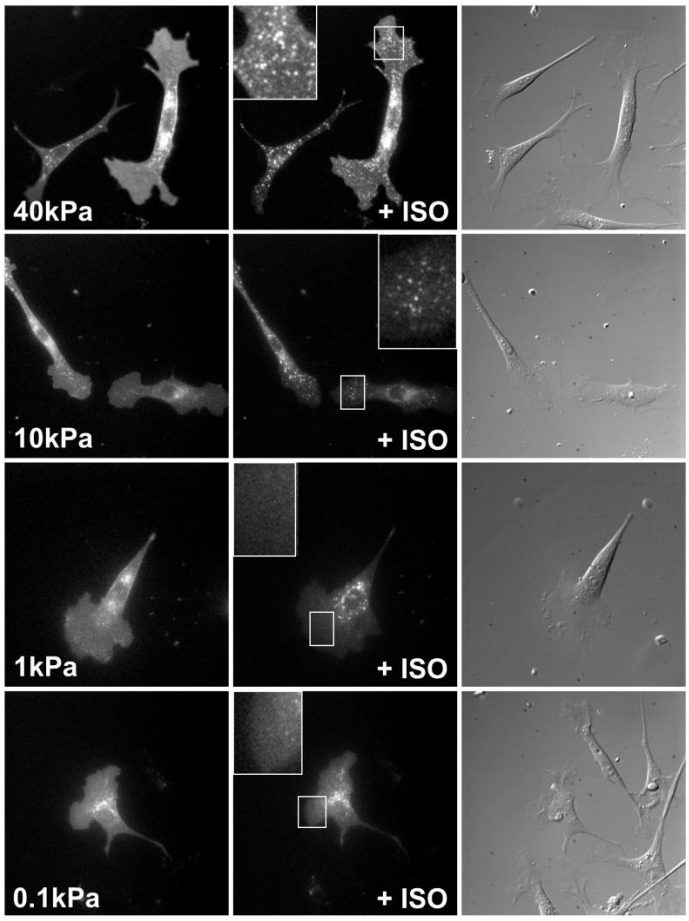

Figure 4-3. Effect of the substrate stiffness on β_2-AR endocytosis. As HMSCs expressing β_2-AR-GFP are cultured on different substrate stiffness, β_2-AR endocytosis takes place in a stiffness-dependent manner in response to the β-AR agonist, Iso.

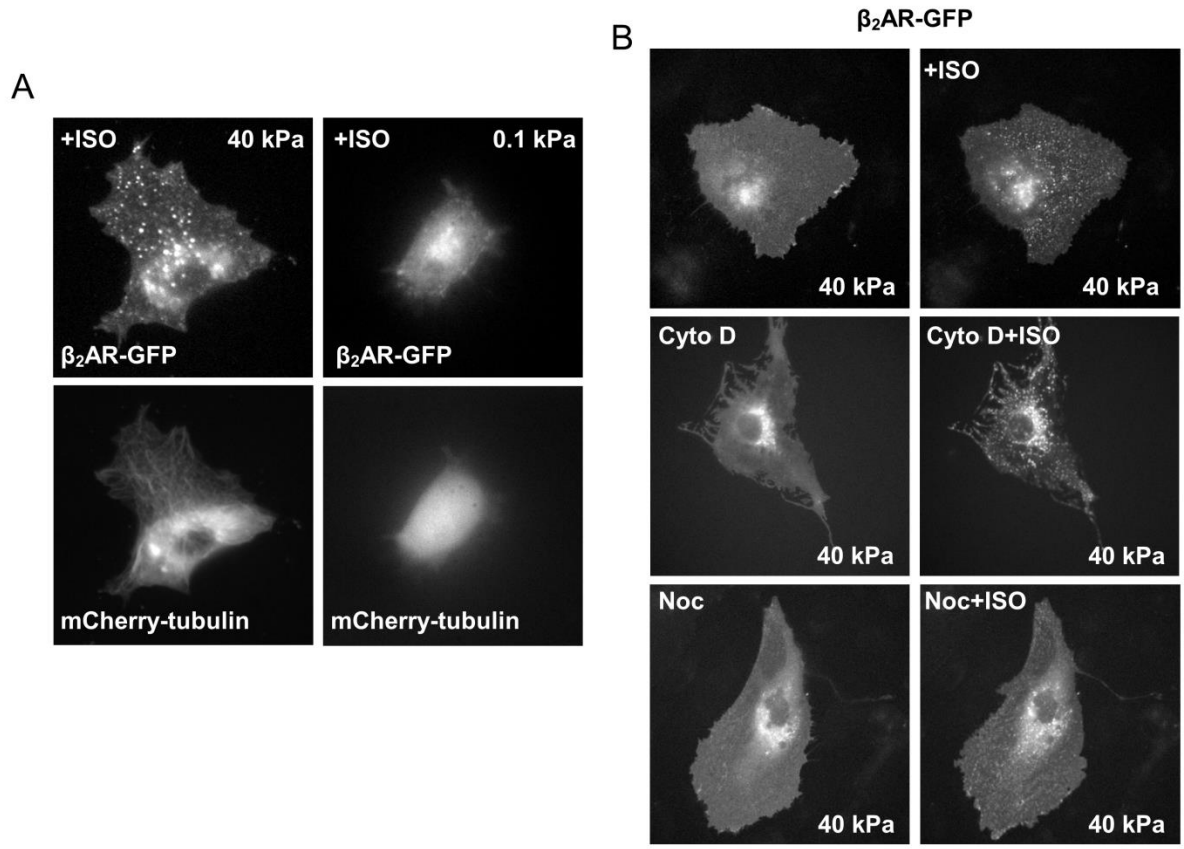

Figure 4-4. Agonist induced β_2-AR endocytosis in response to substrate stiffness is dependent on microtubules, but not on actin filaments. (A) HMSCs cultured on 40 kPa gel substrate exhibit many endocytic vesicles of β_2-AR showing well organized microtubule structure (mCherry-tubulin) compared to the cells on 0.1 kPa. (B) Neither control nor Cyto D treatment affects agonist induced β_2-AR endocytosis in response to substrate stiffness, whereas Noc does apparently inhibit this event.

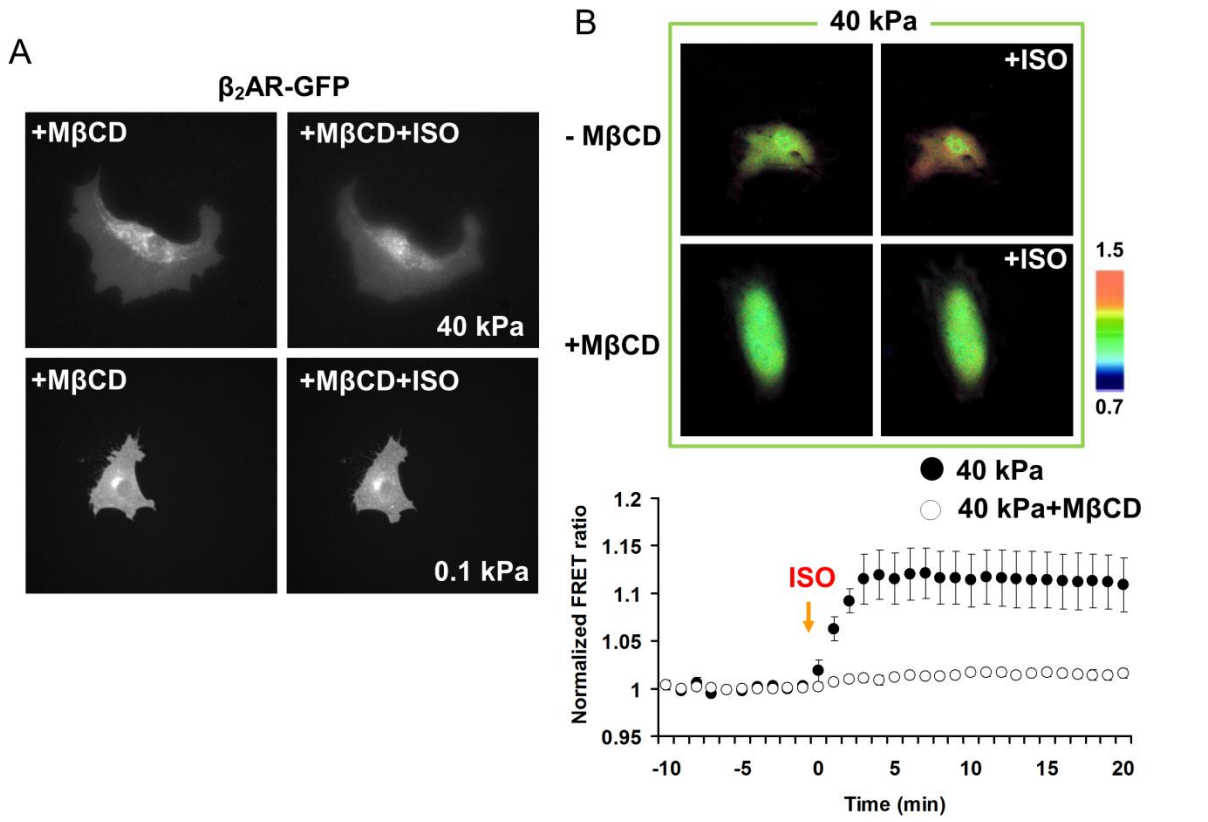

Figure 4-5. Inhibition of endocytosis suppresses β-AR agonist-induced PKA activation in response to substrate stiffness. (A) MβCD treatment inhibits β_2-AR endocytosis in HMSCs cultured on both soft and hard substrates. (B) Emission ratio images and time courses represent the disruption by MβCD in β_2-AR endocytosis (mean ± SEM, n=6). MβCD blocks agonist-induced PKA activation upon hard substrate compared to that of MβCD-untreated cells (mean ± SEM, n=7).

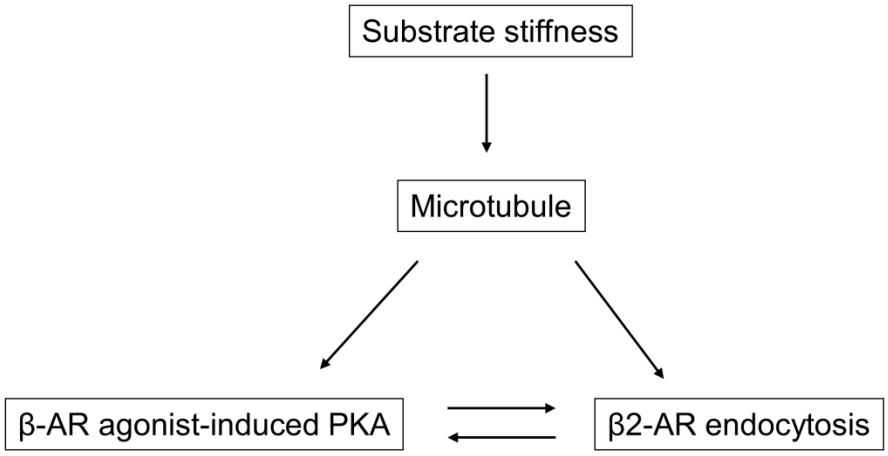

Figure 4-6. A proposed model showing a feedback effect between β-AR agonist induced PKA and β_2-AR endocytosis in response to substrate stiffness. These signals are mediated by the functional support of microtubules.

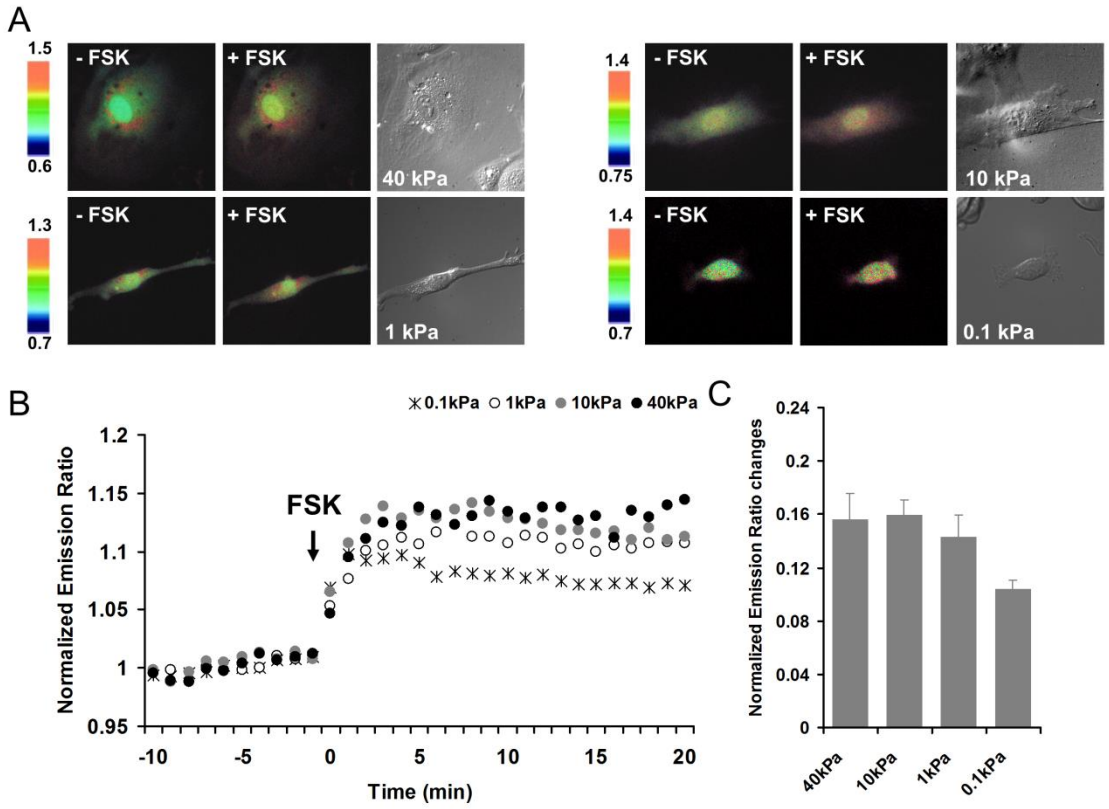

Supplementary Figure S4-1. Response pattern of cAMP-dependent PKA activation upon Fsk treatment in HMSCs cultured on different substrate stiffness. (A) Emission ratio images and (B) time courses in the cells expressing FRET-AKAR2 before and after being treated with Fsk in response to substrate stiffness. (C) Bar graphs represent the emission ratio changes of the biosensor from multiple cells (mean ± SEM) where "n" indicates the sample number in each group.

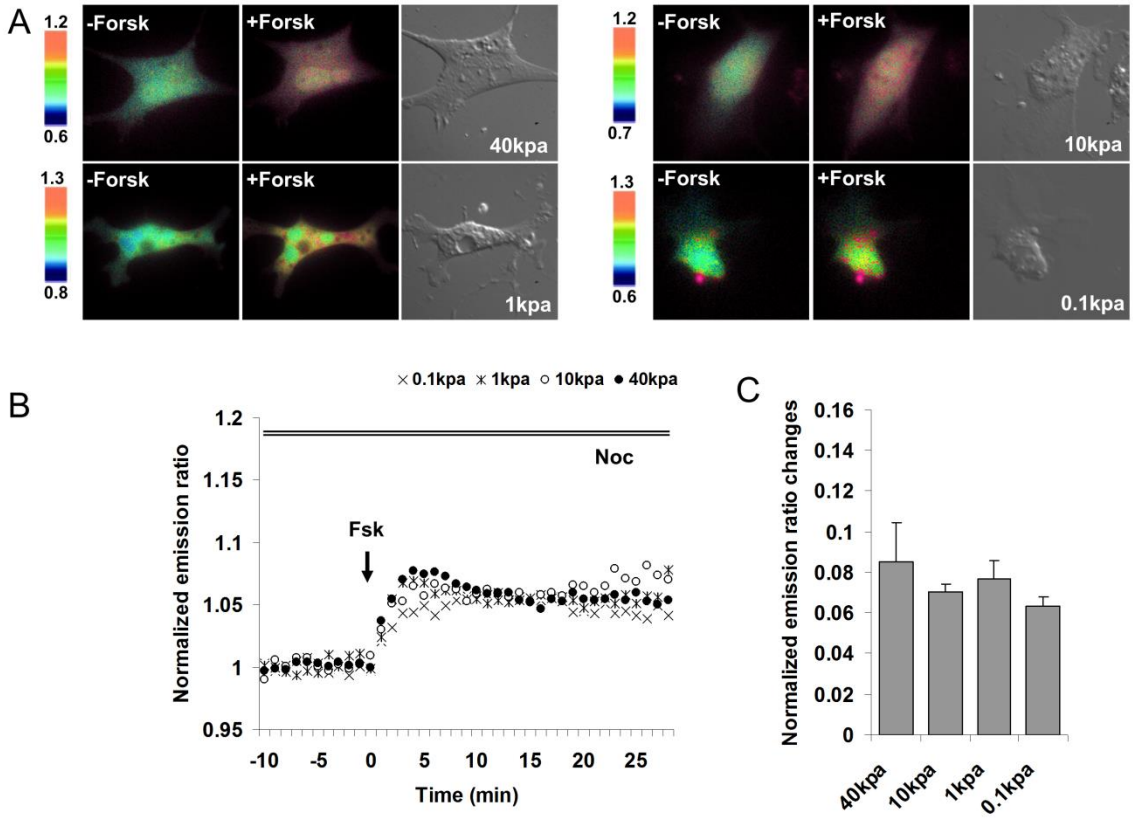

Supplementary Figure S4-2. Effect of Nocodazole on Fsk-induced PKA activity in response to substrate stiffness. (A) Emission ratio images and (B) time course ratio of FRET-AKAR2 in the cells cultured on different substrate stiffness in response to Fsk pretreated with Nocodazole (Noc, 5 μM), an inhibitor of microtubules. (C) The bar graphs represent the emission ratio changes (mean ± SEM) of the biosensors where "n" indicates the sample number in each group.

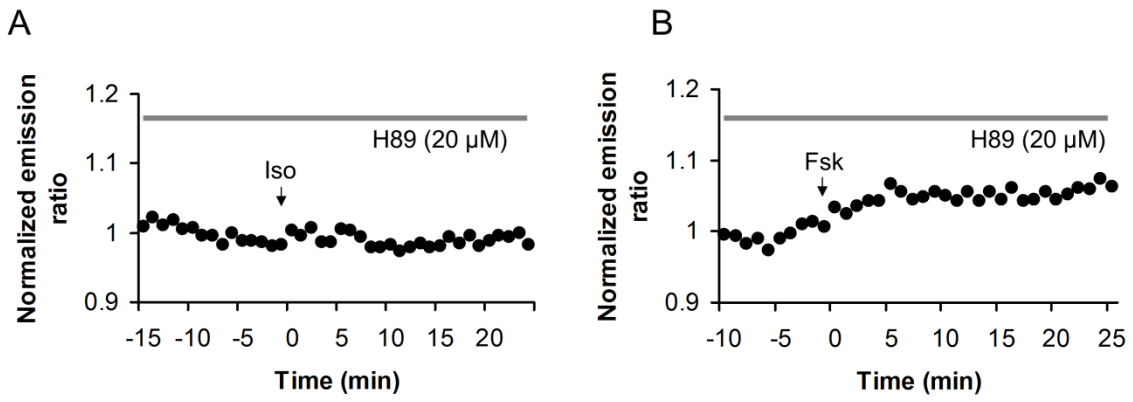

Supplementary Figure S4-3. H89 inhibits both Iso- and Fsk- induced PKA activation. Time courses of emission ratio in the cells pretreated with H89 (20μM), a PKA inhibitor in response to (A) Iso and (B) Fsk. H89 inhibits FRET emission ratio in AKAR2-transfect cells.

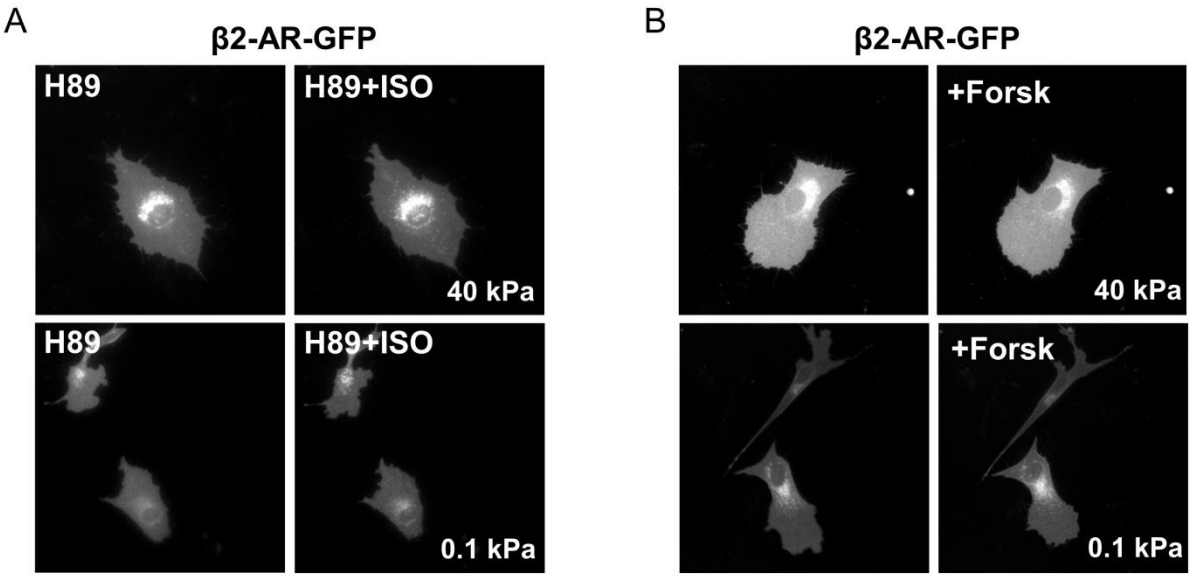

Supplementary Figure S4-4. The role of two types of PKA activation on β_2-AR endocytosis in response to substrate stiffness. (A) H89 inhibits Iso-induced β_2-AR endocytosis, suggesting that Iso-induced PKA activation is necessary for β_2-AR endocytosis. However, Fsk does not stimulate β_2-AR endocytosis, indicating Fsk-induced PKA activation is not required for that.

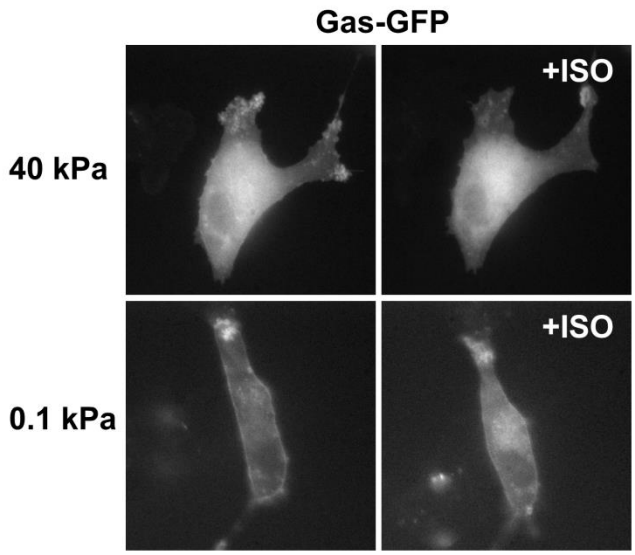

Supplementary Figure S4-5. Effect of substrate stiffness on Gas internalization upon Iso treatment in HMSCs. Substrate stiffness has no effect on Gas recruitment or internalization after Iso treatment.

CHAPTER 5

CALCIUM SIGNALING AT PLASMA MEMBRANE MICRODOMAINS IN RESPONSE TO SUBSTRATE RIGIDTY IN THE ADHESION PROCESS

The calcium ion (Ca^{2+}) plays an essential role in cell adhesion and migration. However, how Ca^{2+} signaling can be regulated at (the) subplasma membrane remains elusive in the early stages of cell-matrix adhesion. In this thesis, I demonstrate how the mechanical microenvironment affects Ca^{2+} mobilization at plasma membrane microdomains in the adhesion process. Taking advantage of fluorescence resonance energy transfer (FRET) sensors, it reveals that Ca^{2+} mobilization at detergent-resistant membrane (DRM) region of the plasma membrane is properly activated in human mesenchymal stem cells (HMSCs) seeded on hard gel (40 kPa) in the adhesion process. In contrast, the cells seeded on soft gel (0.6 kPa) show less activation of Ca^{2+} mobilization at this region. Importantly, Ca^{2+} mobilization at the DRM region is regulated by focal adhesion kinase (FAK). A negative mutant FAK (FAK NT) and kinase-dead FAK (FAK KD) as well as PF228, an inhibitor of FAK strongly inhibit Ca^{2+} mobilization at this region. The depletion of cholesterol by MβCD at the DRM region inhibits Ca^{2+} mobilization, but the disruption of caveolin-1 by a mutant Cav1S80E did not, suggesting that Ca^{2+} mobilization at the DRM region is independent of caveolin-1. Furthermore, this study also reveals that a mechanosensitive Ca^{2+} permeable channel, TRPM7 contributes to Ca^{2+} mobilization at the DRM region in the adhesion process. Taken together, our findings suggest that adhesion-dependent Ca^{2+} mobilization occurs selectively at DRM regions in which it is mediated by FAK and TRPM7 channels.

5.1 Introduction

It is not an exaggeration to emphasize that Ca^{2+} is the most fundamental intracellular messenger in eukaryotic cells that regulates many cellular processes including neurotransmitter release, metabolism, proliferation as well as apoptosis (Berridge, 2003; Berridge et al., 2003; Clapham, 2007). In spite of of the remarkable versatility of Ca^{2+}, it remains elusive as to how Ca^{2+} is mobilized into the intracellular space at the initial stages of cell-matrix adhesion. Hence, understanding how its relevant players and the mechanical environment regulate Ca^{2+} signaling in adhesion process should pose a great challenge.

The regulation of cell-matrix adhesion seems to be simultaneously mediated by many adhesion molecules including integrins (Clark and Brugge, 1995). In fact, integrins can lead to rapid mobilization of intracellular Ca^{2+} which is further revealed to regulate cell adhesion to the extracellular matrix (ECM) and migration (Sjaastad et al., 1996). It is well known that integrin ligation results in activation of various cellular signalings, in particular the focal adhesion kinase (FAK), which is also critically involved in cell adhesion and migration (Lawson et al., 2012; Schlaepfer et al., 1994). FAK is phosphorylated in response to integrin engagement and growth factors stimulation. Even though FAK is significantly connected to integrins, it remains unclear as to how FAK is directly or indirectly associated with Ca^{2+} mobilization in the process of cell adhesion.

Genetically-engineered FRET biosensors have been utilized for the better understanding of protein-protein interaction and enzymatic activities in live cells (Wang et al., 2008; Wang and Wang, 2009). For example, when a Src biosensor was first developed, it enabled the visualization of Src activity upon epidermal growth factor (EGF) stimulation in real-time. It further revealed the propagation of Src activity in response to local force that is dependent on the

cytoskeleton (Botvinick and Wang, 2007; Wang et al., 2005). One of the greatest advantages of using FRET biosensors is that they can detect and visualize the dynamic molecular hierarchy at subcellular levels. In fact, this Src biosensor has been modified to directly tether at different compartments of the plasma membrane in order to monitor and quantify the local Src activity (Seong et al., 2009; Seong et al., 2011a). Recently, two kinds of FAK biosensors have been developed, which are specifically capable of tethering at the plasma membrane microdomains, detergent-resistant membrane (DRM) and non-DRM regions and monitoring the local FAK activity in living cells (Seong et al., 2011b). Following this strategy, Ca^{2+} biosensors were also designed to tether at two types of membrane microdomains such as DRM and non-DRM regions.

In this chapter, I have attempted to answer three unsolved questions using these biosensors, Ca^{2+} and FAK: (1) Can different magnitude of substrate rigidity regulate Ca^{2+} mobilization and FAK? (2) Is FAK involved in Ca^{2+} mobilization? (3) Do mechanosensitive Ca^{2+} channels play a role in cell adhesion? I believe this study will provide new insights into understanding the relationship between Ca^{2+} signaling and FAK in cell-matrix based adhesion.

5.2 Materials and Methods

5.2.1 DNA plasmids

Lyn-FAK and KRas-FAK biosensors have been well-described in a previous study (Seong et al., 2011b). Briefly, Lyn-FAK biosensor was generated by insertion of a raft-targeting motif (M**GC**IKSKRKDNLNDDE) originated from Lyn kinase to the N-terminus of the cytosolic-FAK biosensor (Zacharias et al., 2002). KRas-FAK biosensor was also constructed by the insertion of a non-raft-targeting motif (KKKKKKSKTKCVIM) derived from KRas to the C-terminus of the cytosolic-FAK biosensor (Zacharias et al., 2002). The DNA encoding the FAK biosensors were

subcloned with the BamHI/EcoRI sites in pRSetB for the protein purification from Escherichia coli, and in pcDNA3 plasmid for the expression in mammalian cells. For FAK mutants, the kinase-dead FAK with its kinase domain mutated (FAK KD) and the N-terminal tail (containing the 1-400 amino acids) of FAK (FAK NT) were used in this study (Seong et al., 2011b). Based on this, Ca^{2+} biosensors were designed, as well with the same strategy. Lyn-D3cpv and KRas-D3cpv were constructed by adding of a raft-targeting motif (M**GC**IKSKRKDNLNDDE) to the N-terminus of the D3cpv and a non-raft-targeting motif (KKKKKKSKTKCVIM) to the C-terminus of the D3cpv (Palmer and Tsien, 2006). A dominant negative Caveolin-1 mutant (Cav1 S80E) was used to disrupt caveolar organization (Kubale et al., 2007; Shigematsu et al., 2003). Cav1 S80E was amplified by PCR and inserted into pcDNA3.1 by BamH I and EcoR I sites. The primers are forward (5' GCGCGGATCCGCCACCATGTCTGGGGGCAAATACGTAG3' and reverse (5'TCCGGAATTCTTATATTTCTTTCTGCAAGTTGATG3'). The S80E mutant was generated by quick change mutagenesis.

5.2.2 Cell culture and chemicals

Human mesenchymal stem cells (HMSCs; Lonza Walkersvile, Inc., Walkersvile, MD) were maintained in a mesenchymal stem cell growth medium (MSCGM, PT-3001, Lonza) containing 10% fetal bovine serum (FBS), 2mM L-glutamine, 100 U/ml penicillin and 100 μg/ml streptomycin in a humidified incubator of 95% O_2 and 5% CO_2 at 37℃. The DNA plasmids were transfected into the cells by using Lipofectamine 2000 (Invitrogen, Carlsbad, CA) reagent according to the product instructions. PF228, ML-7 and methyl-beta-cyclodextrin (MβCD) were purchased from Sigma.

5.2.3 Bis-acrylamide-PA gel fabrication

Polyacrylamide (PA) gels were prepared on aminosilanized glass coverslips according to previously established methods (Pelham and Wang, 1997). Briefly, 40% w/v acrylamide and 2% w/v bis-acrylamide stock solutions (Bio-Rad) were mixed to prepare a PA solution and then the gel's stiffness was achieved by varying the final concentrations of the PA solution (3% and 7.5%) and bis-acrylamide crosslinker (0.06% and 0.4%) for the corresponding stiffness of 0.6 and 40 kPa. To polymerize the solutions, 2.5 µl of 10% w/v ammonium persulfate (APS; Bio-Rad) and 0.25 µl of N,N,N9,N9-Tetramethylethylenediamine (TEMED; Bio-Rad) were added to yield a final volume of 500 µl PA solution. To crosslink extracellular matrix molecules onto the gel surface, a photoactivating cross-linker, sulfo-SANPAH (sulfosuccinimidyl6(4'-azide-2'-nitrophenyl-amino) hexanoate, Pierce) was used, and 200 µl of 0.1 mg/ml fibronectin solution (from bovine plasma, Sigma) was incubated on top of the PA gel at 37 ℃ overnight.

5.2.4 Imaging and microscopy

Cells were incubated for 1 hr in agarose dishes to maintain them in a state of suspension after detachment with 4mM EDTA in PBS. A Nikon fluorescence microscope was used for imaging under a perfect focus system (PFS) to minimize any possible change in focus during cell adhesion. During the imaging process, the cells were maintained with MSCGM in a chamber designed to provide constant humidified air containing 5% CO_2, 10% O_2 and 85% N_2. The 37℃ degree of temperature throughout the samples in the chamber was maintained by a controlled heater (Nevtek ASI 400). The software to control the imaging and analyze the imaging data was MetaFluor 7.6. The filter for ECFP was 420/20 nm for excitation and 480/40 nm for emission. The filter for YFP was 495/10 nm and 535/25 nm.

5.2.5 Statistical analysis

All statistical data were expressed as the mean ± standard error of the mean (SEM). Statistical evaluation was performed by using a Student's t-test function of the Excel software to determine the statistical differences between groups. A significant difference was determined by the P-value (< 0.05).

5.3 Results

5.3.1 Substrate-rigidity dependent Ca^{2+} mobilization during adhesion process

It is reported that substrate rigidity has a great impact on cell adhesion and it also regulates Ca^{2+} signaling in HMSCs (Discher et al., 2005; Kim et al., 2009). However, the question is how this mechanical factor is associated with cell adhesion and adhesion-triggered Ca^{2+} necessity in the early stage of cell-matrix adhesion. Therefore, we have monitored Ca^{2+} mobilization at different magnitudes of gel substrates at the level of the plasma membrane microdomains, DRM regions during adhesion process. Since Ca^{2+} signaling plays an important role in cell adhesion and migration, it is expected that Ca^{2+} mobilization is activated during cell adhesion and the membrane-targeting Ca^{2+} biosensor, Lyn-D3cpv ought to detect FRET changes caused by intracellular Ca^{2+} increase near the DRM region. As shown in Figure 5-1, on hard gel (40 kPa, n=8), the FRET ratio of Lyn-D3cpv has been increased up to ~20% during adhesion process. In contrast, on soft gel (0.6 kPa, n=5), the cells have shown less activation of FRET (~6%), indicating lower Ca^{2+} mobilization during adhesion. These results suggest Ca^{2+} mobilization at DRM regions is dependent on substrate rigidity during the cell-matrix adhesion process.

5.3.2 Inactivation of Ca^{2+} mobilization at non-DRM regions during adhesion process

The main source of Ca^{2+} mobilization near the plasma membrane is mostly due to Ca^{2+} influx through membrane channels (Rizzuto and Pozzan, 2006), and the composition of these channels between DRM and non-DRM regions must be different from each other (Dart, 2010; Pani and Singh, 2009). Hence, it is necessary to examine whether Ca^{2+} mobilization is differently activated at DRM and non-DRM regions. As shown in Figure 5-2, I compared Ca^{2+} mobilization in these areas to show how they respond to hard gel during the adhesion process using two types of Ca^{2+} sensors that are targeting the plasma membrane microdomains. Cells expressing Lyn-D3cpv have nicely shown FRET increase during the adhesion process on hard gel, but there was no significant FRET change in KRas-D3cpv. These results suggest that Ca^{2+} mobilization at DRM regions seems to be selectively activated in response to substrate rigidity during the adhesion process, but it is not activated at non-DRM regions.

5.3.3 Substrate rigidity-dependent FAK activation at the DRM region during the adhesion process

I then examined whether FAK activation is dependent of substrate rigidity in the adhesion process. As a result, I found that FAK activation is dependent on substrate rigidity, which is likely to be parallel to the FRET activation of Lyn-D3cpv. On hard gel (40 kPa), cell adhesion and spreading was clearly observed and the FRET ratio of the Lyn-FAK biosensor gradually increased upon (not the right word?) as a result of? this process in which the pattern of the signal looked similar to Lyn-D3cpv data. On the other hand, on soft gel (0.6 kPa), it seemed that cell adhesion and spreading were not robust, but rather inhibited. In accordance with this

observation, the FRET ratio of the Lyn-FAK biosensor also was not increased much. Therefore, these results suggest that FAK activation at DRM regions is substrate rigidity-dependent, implying there might be some connection between FAK and Ca^{2+} on the basis of their parallel activation in the adhesion process.

5.3.4 Distinct FAK activation in response to substrate rigidity and regulation of FAK at the DRM region

According to the previous study, FAK at DRM regions appears to be differently activated compared to that of non-DRM regions in response to biochemical stimulation, platelet-derived growth factor (PDGF) (Seong et al., 2011b). In this study, I monitored how FAK can respond to different substrate rigidities at two membrane microdomains in the adhesion process. As shown in Figure 5-4, the FRET increase of the Lyn-FAK biosensor on hard gel was inhibited by the addition of PF228, an FAK inhibitor, indicating that this FAK activation visualized as the FRET ratio was truly being accumulated at the DRM regions. Pretreatment of ML-7, an inhibitor of MLCK, blocked the FRET increase on hard gel in the adhesion process, suggesting that Lyn-FAK activation at DRM regions is dependent on actomyosin contractility (Fig 5-2B), which is also known to reduce FAK activity at the DRM regions. Surprisingly, I found that KRas-FAK at non-DRM regions was not activated regardless of the magnitude of substrate rigidity (Fig 5-2C). Therefore, these results suggest that FAK is selectively activated at DRM regions in the adhesion process, which is dependent on substrate rigidity, but not at non-DRM regions.

5.3.5 FAK regulates Ca^{2+} mobilization at the DRM region

Because the pattern of FRET increase between Lyn-FAK and Lyn-D3cpv seems to coincide, it is expected that both signals are correlated to each other. To examine this, I employed two FAK mutants, FAK NT and KD into the cells with Lyn-D3cpv. As shown in Figure 5-5, the FRET ratio of Lyn-D3cpv increased in the adhesion process in the control (without inhibition of FAK). However, cells inserted with both a negative mutant, FAK NT, and a kinase dead mutant, FAK KD, did not show any significant increase in the FRET ratio, which indicates FAK-mediated inactivation of Ca^{2+} mobilization at DRM regions in the adhesion process. Pharmacological assay revealed this result was consistent. PF228, an inhibitor of FAK and ML7 treatment to inhibit MLCK eventually inhibiting FAK also significantly inhibited Ca^{2+} mobilization at DRM regions (Supplementary Fig. S5-2 and 3). Therefore, these results suggest that FAK regulates Ca^{2+} mobilization at DRM regions in the adhesion process.

5.3.6 Depletion of cholesterol by MβCD inhibits Ca^{2+} mobilization at the DRM region

It is known that the depletion of cholesterol and its related disruption of membrane microdomains by MβCD downregulates FAK functions, and the removal of the lipid raft-related protein, Caveolin, at DRM regions blocks the FAK phosphorylation on integrin activation (Park et al., 2009; Wei et al., 1999). In fact, in the previous study, it was shown that PDGF-induced FAK activation is inhibited by MβCD treatment (Seong et al., 2011b). In this study, I examine whether MβCD can affect Ca^{2+} mobilization in response to substrate rigidity at DRM regions in the adhesion process. As shown in Figure 5-6, MβCD treatment inhibited FRET increase in Lyn-D3cpv, but a mutant of Caveolin-1 (Cav1 S80E) did not. These results suggest that proper localization of cholesterol at the DRM region may contribute to Ca^{2+} mobilization at these regions, but caveolin-1 itself is not sufficient to block in this process.

5.3.7 TRPM7 contributes to Ca^{2+} mobilization at the DRM region

TRPM7 belonging to mechanosensitive Ca^{2+} permeable channels is dominantly accumulated at DRM regions, but not at non-DRM regions. As a consequence, I examined whether TRPM7 affects Ca^{2+} mobilization at DRM regions during the adhesion process. As shown in Figure 5-7, I found that TRPM7 knockdown cells by siRNA significantly inhibited the substrate rigidity-dependent Ca^{2+} mobilization at DRM regions, but non-targeting (NT) siRNA used as a control did not. Therefore, I suggest that TRPM7 plays a crucial role in Ca^{2+} mobilization at DRM regions, contributing to Ca^{2+} influx in response to substrate rigidity during the adhesion process.

5.4 Discussion

It is surprising that the Ca^{2+} signal is mobilized differently near plasma membrane microdomains during the process of cell-matrix adhesion. The plasma membrane of cells consists of a combination of glycosphingolipids and protein receptors organized in glycolipoprotein microdomains called lipid rafts (Korade and Kenworthy, 2008; Thomas et al., 2004). Lipid rafts are cholesterol and sphingolipid-enriched microdomains at the plasma membrane that play a crucial role as unique signal transduction platforms (Anderson and Jacobson, 2002; Pike, 2005). For numerous years, the functional roles of these unique domains have been widely studied. Notably, due to the different composition of membrane proteins, including Ca^{2+} channels and FAK between lipid rafts and non-lipid raft membranes, it is more expected that their signal events might be unique and different.

In this study, I found that at lipid rafts microdomains called DRM regions, adhesive HMSCs showed greater Ca^{2+} mobilization and FAK activation in the adhesion process, both of which are substrate rigidity-dependent. In contrast, these two signals were not activated or were less activated at non-DRM regions. Further investigation revealed the Ca^{2+} mobilization at DRM regions was regulated by FAK. In the presence of mutants (FAK NT and FAK KD) and PF228 treatment, the FRET ratio of Lyn-D3cpv was significantly inhibited. The physiological interpretation of these phenomena seems to require further investigation to understand the detailed mechanism as to how FAK affects Ca^{2+} mobilization. One possibility is that FAK directly affects Ca^{2+} channels at DRM regions. Even though FAK is mainly interacting with integrin at the plasma membrane, it is possible that FAK can physically interact with mechanosensitive membrane channels (Rezzonico et al., 2003). Another possibility is that FAK indirectly affects Ca^{2+} channels in an integrin dependent manner. In fact, FAK modulates many types of voltage-gated Ca^{2+} channels at the plasma membrane via integrin (Chao et al., 2011; Wu et al., 2001). Additionally, Ca^{2+} influx through plasma membrane is closely related to the activation of a high affinity of β2 integrin and subsequent adhesive signals due to their synchronized events (Schaff et al., 2008). Similarly, I also observed Ca^{2+} mobilization at DRM regions is synchronizing with FAK activation during the adhesion process. FAK is dominantly recruited to DRM regions in response to growth factor stimulation like PDGF (Seong et al., 2011). It is also involved in mechanosensing and is obviously activated by mechanical stimulation (Hanks et al., 1992; Torsoni et al., 2003; Wang et al., 2001). However, it is unknown whether FAK is dominantly accumulated or recruited to adhesive partners at DRM regions by mechanical factors such as substrate rigidity, in particular in the process of cell-matrix adhesion, so our finding may be the first evidence to show that FAK does likewise.

Most importantly, I found that TRPM7 is critically involved in Ca^{2+} mobilization at DRM regions in the adhesion process. The distribution of TRP Ca^{2+} channels at DRM regions is different from that of non-DRM regions. For example, TRPC3 and TRPC6 are dominantly expressed at non-DRM regions, but other TRPC channels are expressed throughout the plasma membrane (Pani and Singh, 2009). Interestingly, TRPM7 channels appear to be distributed exclusively at DRM regions upon bradykinin stimulation (Yogi et al., 2009) and they are also Ca^{2+} permeable channels accumulated at the plasma membrane by mechanical stimulation (Oancea et al., 2006). In addition, it is reported that TRPM7 seems to be an adhesion-associated channel that regulates actomyosin contractility (Clark et al., 2007). Our finding suggests that TRPM7 is one of the important regulators for substrate rigidity-dependent Ca^{2+} mobilization at DRM regions in the adhesion process, which is consistent with previous data.

As expected, the depletion of cholesterol by MβCD at DRM regions abolished Ca^{2+} mobilization at DRM regions. In contrast, disruption of caveolae by the mutant of caveolin-1 (Cav1 80SE) at DRM regions did not cease the FRET increase in Lyn3-D3cpv in the adhesion process. Even though it is known that caveolae disruption prevents Ca^{2+} influx, it might not have a significant impact on the adhesion process or target different TRP channels like TRPC,1 which also localizes to cholesterol-enriched lipid rafts (Lockwich et al., 2000; Venkatachalam and Montell, 2007). Therefore, the detailed mechanisms of Ca^{2+} and FAK signals at DRM regions have to be investigated further to understand how these biochemical signals are correlated to each other along with the mechanical microenvironment.

In conclusion, this chapter clearly shows how Ca^{2+} and FAK signaling are activated at DRM regions in the adhesion process, which is dependent on substrate rigidity. The results in this chapter also show that FAK regulates Ca^{2+} mobilization, which can be modulated by the

proper localization of cholesterol and the function role of TRPM7. This data will provide new insights into understanding the underlying mechanism between Ca^{2+} and FAK signals and the relationship between biochemical/mechanical factors and cellular processes.

5.5 References

Anderson, R.G., and Jacobson, K. (2002). A role for lipid shells in targeting proteins to caveolae, rafts, and other lipid domains. Science *296*, 1821-1825.

Berridge, M.J. (2003). Cardiac calcium signalling. Biochem Soc Trans *31*, 930-933.

Berridge, M.J., Bootman, M.D., and Roderick, H.L. (2003). Calcium signalling: dynamics, homeostasis and remodelling. Nat Rev Mol Cell Biol *4*, 517-529.

Botvinick, E.L., and Wang, Y. (2007). Laser tweezers in the study of mechanobiology in live cells. Methods Cell Biol *82*, 497-523.

Chao, J.T., Gui, P., Zamponi, G.W., Davis, G.E., and Davis, M.J. (2011). Spatial association of the Cav1.2 calcium channel with alpha5beta1-integrin. Am J Physiol Cell Physiol *300*, C477-489.

Clapham, D.E. (2007). Calcium signaling. Cell *131*, 1047-1058.

Clark, E.A., and Brugge, J.S. (1995). Integrins and signal transduction pathways: the road taken. Science *268*, 233-239.

Dart, C. (2010). Lipid microdomains and the regulation of ion channel function. J Physiol *588*, 3169-3178.

Discher, D.E., Janmey, P., and Wang, Y.L. (2005). Tissue cells feel and respond to the stiffness of their substrate. Science *310*, 1139-1143.

Hanks, S.K., Calalb, M.B., Harper, M.C., and Patel, S.K. (1992). Focal adhesion protein-tyrosine kinase phosphorylated in response to cell attachment to fibronectin. Proc Natl Acad Sci U S A *89*, 8487-8491.

Kim, T.J., Seong, J., Ouyang, M., Sun, J., Lu, S., Hong, J.P., Wang, N., and Wang, Y. (2009). Substrate rigidity regulates Ca2+ oscillation via RhoA pathway in stem cells. J Cell Physiol *218*, 285-293.

Korade, Z., and Kenworthy, A.K. (2008). Lipid rafts, cholesterol, and the brain. Neuropharmacology *55*, 1265-1273.

Kubale, V., Abramovic, Z., Pogacnik, A., Heding, A., Sentjurc, M., and Vrecl, M. (2007). Evidence for a role of caveolin-1 in neurokinin-1 receptor plasma-membrane localization, efficient signaling, and interaction with beta-arrestin 2. Cell Tissue Res *330*, 231-245.

Lawson, C., Lim, S.T., Uryu, S., Chen, X.L., Calderwood, D.A., and Schlaepfer, D.D. (2012). FAK promotes recruitment of talin to nascent adhesions to control cell motility. J Cell Biol *196*, 223-232.

Lockwich, T.P., Liu, X., Singh, B.B., Jadlowiec, J., Weiland, S., and Ambudkar, I.S. (2000). Assembly of Trp1 in a signaling complex associated with caveolin-scaffolding lipid raft domains. J Biol Chem *275*, 11934-11942.

Oancea, E., Wolfe, J.T., and Clapham, D.E. (2006). Functional TRPM7 channels accumulate at the plasma membrane in response to fluid flow. Circ Res *98*, 245-253.

Pani, B., and Singh, B.B. (2009). Lipid rafts/caveolae as microdomains of calcium signaling. Cell Calcium *45*, 625-633.

Park, E.K., Park, M.J., Lee, S.H., Li, Y.C., Kim, J., Lee, J.S., Lee, J.W., Ye, S.K., Park, J.W., Kim, C.W., *et al.* (2009). Cholesterol depletion induces anoikis-like apoptosis via FAK down-regulation and caveolae internalization. J Pathol *218*, 337-349.

Pelham, R.J., Jr., and Wang, Y. (1997). Cell locomotion and focal adhesions are regulated by substrate flexibility. Proc Natl Acad Sci U S A *94*, 13661-13665.

Pike, L.J. (2005). Growth factor receptors, lipid rafts and caveolae: an evolving story. Biochim Biophys Acta *1746*, 260-273.

Rezzonico, R., Cayatte, C., Bourget-Ponzio, I., Romey, G., Belhacene, N., Loubat, A., Rocchi, S., Van Obberghen, E., Girault, J.A., Rossi, B., *et al.* (2003). Focal adhesion kinase pp125FAK interacts with the large conductance calcium-activated hSlo potassium channel in human osteoblasts: potential role in mechanotransduction. J Bone Miner Res *18*, 1863-1871.

Rizzuto, R., and Pozzan, T. (2006). Microdomains of intracellular Ca2+: molecular determinants and functional consequences. Physiol Rev *86*, 369-408.

Schaff, U.Y., Yamayoshi, I., Tse, T., Griffin, D., Kibathi, L., and Simon, S.I. (2008). Calcium flux in neutrophils synchronizes beta2 integrin adhesive and signaling events that guide inflammatory recruitment. Ann Biomed Eng *36*, 632-646.

Schlaepfer, D.D., Hanks, S.K., Hunter, T., and van der Geer, P. (1994). Integrin-mediated signal transduction linked to Ras pathway by GRB2 binding to focal adhesion kinase. Nature *372*, 786-791.

Seong, J., Lu, S., Ouyang, M., Huang, H., Zhang, J., Frame, M.C., and Wang, Y. (2009). Visualization of Src activity at different compartments of the plasma membrane by FRET imaging. Chem Biol *16*, 48-57.

Seong, J., Lu, S., and Wang, Y. (2011a). Live Cell Imaging of Src/FAK Signaling by FRET. Cell Mol Bioeng *2*, 138-147.

Seong, J., Ouyang, M., Kim, T., Sun, J., Wen, P.C., Lu, S., Zhuo, Y., Llewellyn, N.M., Schlaepfer, D.D., Guan, J.L., *et al.* (2011b). Detection of focal adhesion kinase activation at membrane microdomains by fluorescence resonance energy transfer. Nat Commun *2*, 406.

Shigematsu, S., Watson, R.T., Khan, A.H., and Pessin, J.E. (2003). The adipocyte plasma membrane caveolin functional/structural organization is necessary for the efficient endocytosis of GLUT4. J Biol Chem *278*, 10683-10690.

Sjaastad, M.D., Lewis, R.S., and Nelson, W.J. (1996). Mechanisms of integrin-mediated calcium signaling in MDCK cells: regulation of adhesion by IP3- and store-independent calcium influx. Mol Biol Cell *7*, 1025-1041.

Thomas, S., Kumar, R.S., and Brumeanu, T.D. (2004). Role of lipid rafts in T cells. Arch Immunol Ther Exp (Warsz) *52*, 215-224.

Torsoni, A.S., Constancio, S.S., Nadruz, W., Jr., Hanks, S.K., and Franchini, K.G. (2003). Focal adhesion kinase is activated and mediates the early hypertrophic response to stretch in cardiac myocytes. Circ Res *93*, 140-147.

Venkatachalam, K., and Montell, C. (2007). TRP channels. Annu Rev Biochem *76*, 387-417.

Wang, H.B., Dembo, M., Hanks, S.K., and Wang, Y. (2001). Focal adhesion kinase is involved in mechanosensing during fibroblast migration. Proc Natl Acad Sci U S A *98*, 11295-11300.

Wang, Y., Botvinick, E.L., Zhao, Y., Berns, M.W., Usami, S., Tsien, R.Y., and Chien, S. (2005). Visualizing the mechanical activation of Src. Nature *434*, 1040-1045.

Wang, Y., Shyy, J.Y., and Chien, S. (2008). Fluorescence proteins, live-cell imaging, and mechanobiology: seeing is believing. Annu Rev Biomed Eng *10*, 1-38.

Wang, Y., and Wang, N. (2009). FRET and mechanobiology. Integr Biol (Camb) *1*, 565-573.

Wei, Y., Yang, X., Liu, Q., Wilkins, J.A., and Chapman, H.A. (1999). A role for caveolin and the urokinase receptor in integrin-mediated adhesion and signaling. J Cell Biol *144*, 1285-1294.

Wu, X., Davis, G.E., Meininger, G.A., Wilson, E., and Davis, M.J. (2001). Regulation of the L-type calcium channel by alpha 5beta 1 integrin requires signaling between focal adhesion proteins. J Biol Chem *276*, 30285-30292.

Yogi, A., Callera, G.E., Tostes, R., and Touyz, R.M. (2009). Bradykinin regulates calpain and proinflammatory signaling through TRPM7-sensitive pathways in vascular smooth muscle cells. Am J Physiol Regul Integr Comp Physiol *296*, R201-207.

5.6 Figures

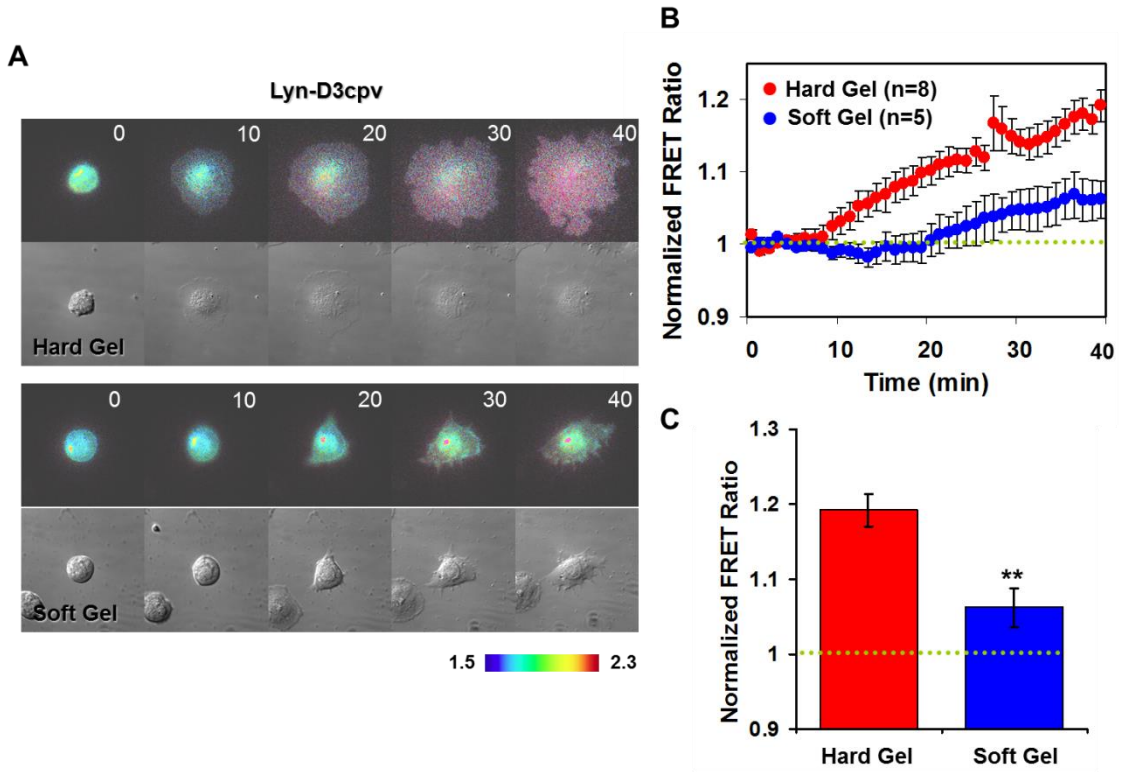

Figure 5-1. Substrate rigidity-dependent Ca^{2+} mobilization in the adhesion process. (A) The FRET ratio of Lyn-D3cpv that presents Ca^{2+} signals near detergent-resistant membrane (DRM) region. On hard gels (40 kPa, n=8), the cells show better adhesion and spreading with higher FRET increase than that of soft gels (0.6 kPa, n=5). (B, C) Time course image and bar graph show that the increased ratio of FRET is different from each other and a significant difference between them.

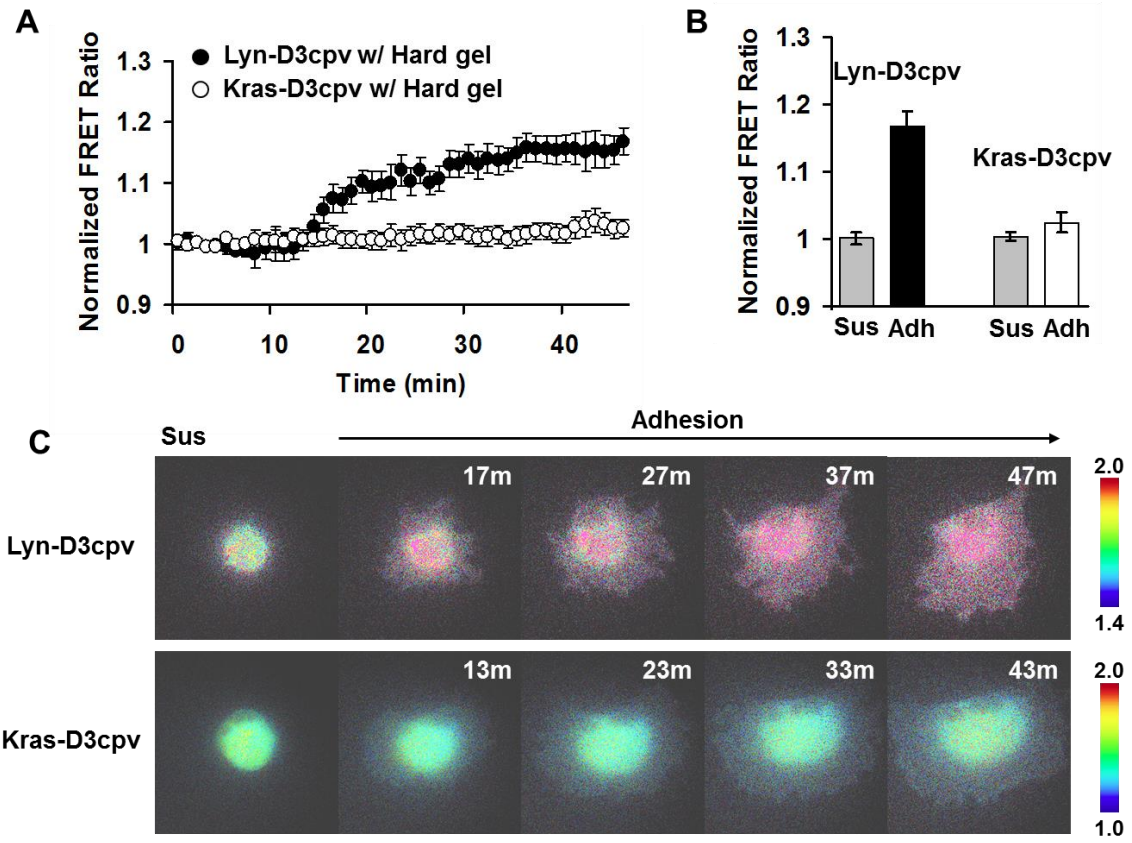

Figure 5-2. Differential Ca^{2+} activation at between DRM and non-DRM regions. (A) Lyn-D3cpv is activated upon hard gel in the adhesion process, but Kras-D3cpv that targets non-DRM region is not. (B) The comparison in FRET ratio on between suspension cells and adhesive cells in which Lyn-D3cpv and Kras-D3cpv sensors were inserted. (C) FRET images that represent the changes in ratio between Lyn-D3cpv and Kras-D3cpv. Contrary to Lyn-D3cpv, the FRET ratio of Kras-D3cpv does not chang during adhesion.

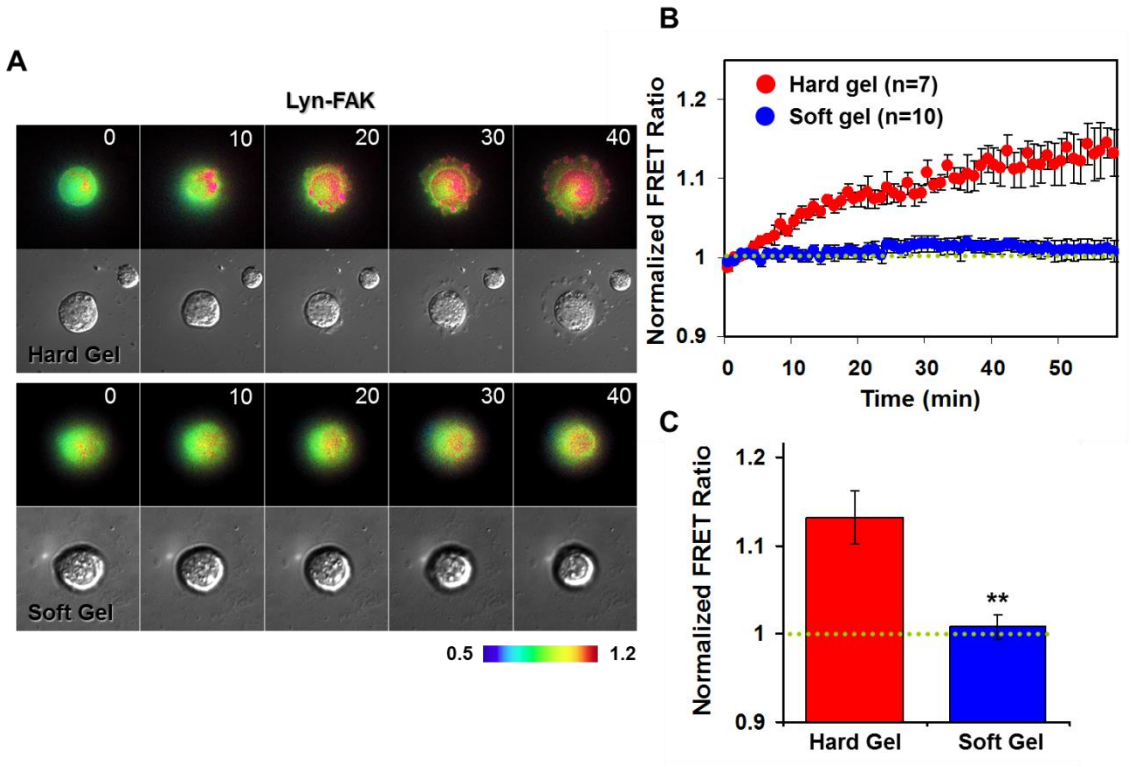

Figure 5-3. Substrate rigidity-dependent focal adhesion kinase (FAK) activation at the DRM region in the adhesion process. (A) Lyn-FAK biosensor allows us to monitor FRET changes in FAK activation at DRM regions. Two images showing the FRET ratio are comparable. The red color represents a high FRET ratio, indicating high FAK activation, and the green/blue color represent a low ratio, representing low FAK activation. (B) The normalized FRET ratio of the Lyn-FAK biosensor in the cells cultured on hard gels and soft gels. The cells on hard gels show the FRET increase up to ~15% in the adhesion process. However, the FRET ratio of the cells on soft gels is seldom activated. (C) Two groups are significantly different (n=7-10, $P<0.01$).

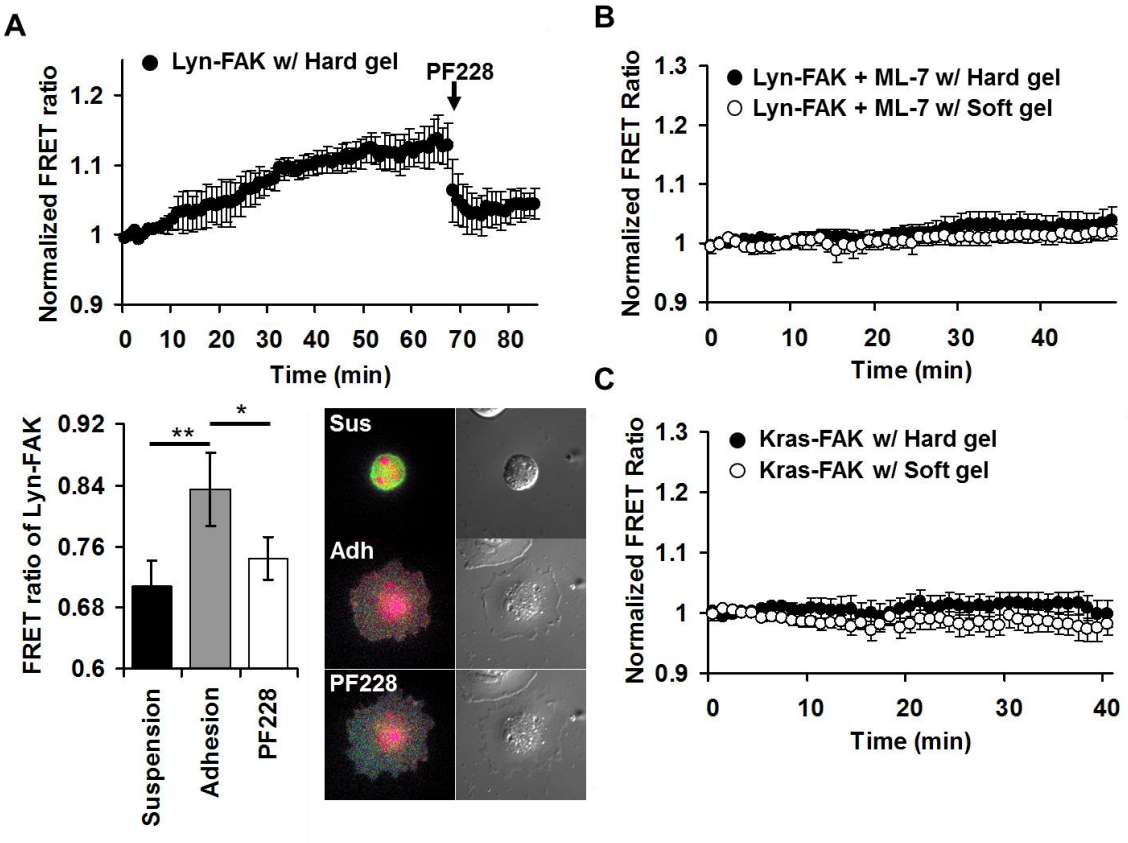

Figure 5-4. Distinct FAK activation in at the DRM region in response to substrate rigidity. (A) The FRET signal of Lyn-FAK is inhibited by PF228, a FAK inhibitor, indicating that the FRET increase is a true signal that reflects FAK activation at the DRM region. The bar graphs show that the adhesive process increases the FRET ratio and that it significantly decreases after PF228 treatment. (B) The FRET ratio of Lyn-FAK is not activated in the presence of ML-7, an inhibitor of MLCK, suggesting that FAK activation in response to substrate rigidity is dependent on actomyosin contractility. (C) The FRET ratio of Kras-FAK indicating FAK signal at non-DRM regions is not activated in the cells on both hard gels and soft gels in the adhesion process.

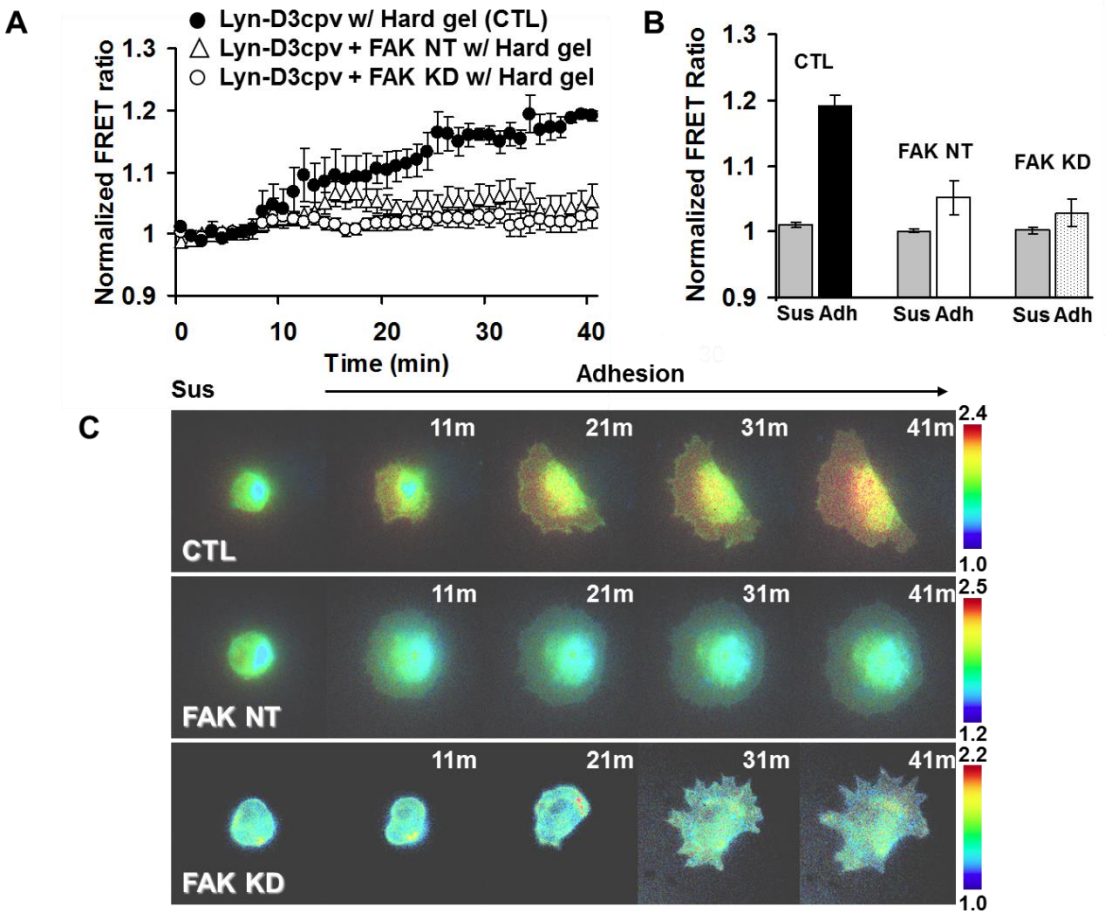

Figure 5-5. FAK mutants inhibit substrate rigidity dependent Ca^{2+} mobilization at the DRM region. (A) Normally, the FRET ratio of Lyn-D3cpv is increased in the adhesion process on hard gel. However, two mutant-inserted cells expressing Lyn-D3cpv do not show any significant FRET increase in response to hard gel. (B) The FRET ratio comparison in each group of cells (A) between suspension and adhesion states, suggesting that both mutants, FAK NT and FAK KD, inhibit Ca^{2+} mobilization. (C) FRET images in each group. The blue/green colors represent a low FRET ratio and the yellow/red colors represent a high FRET ratio. (N=6, ***P<0.001)

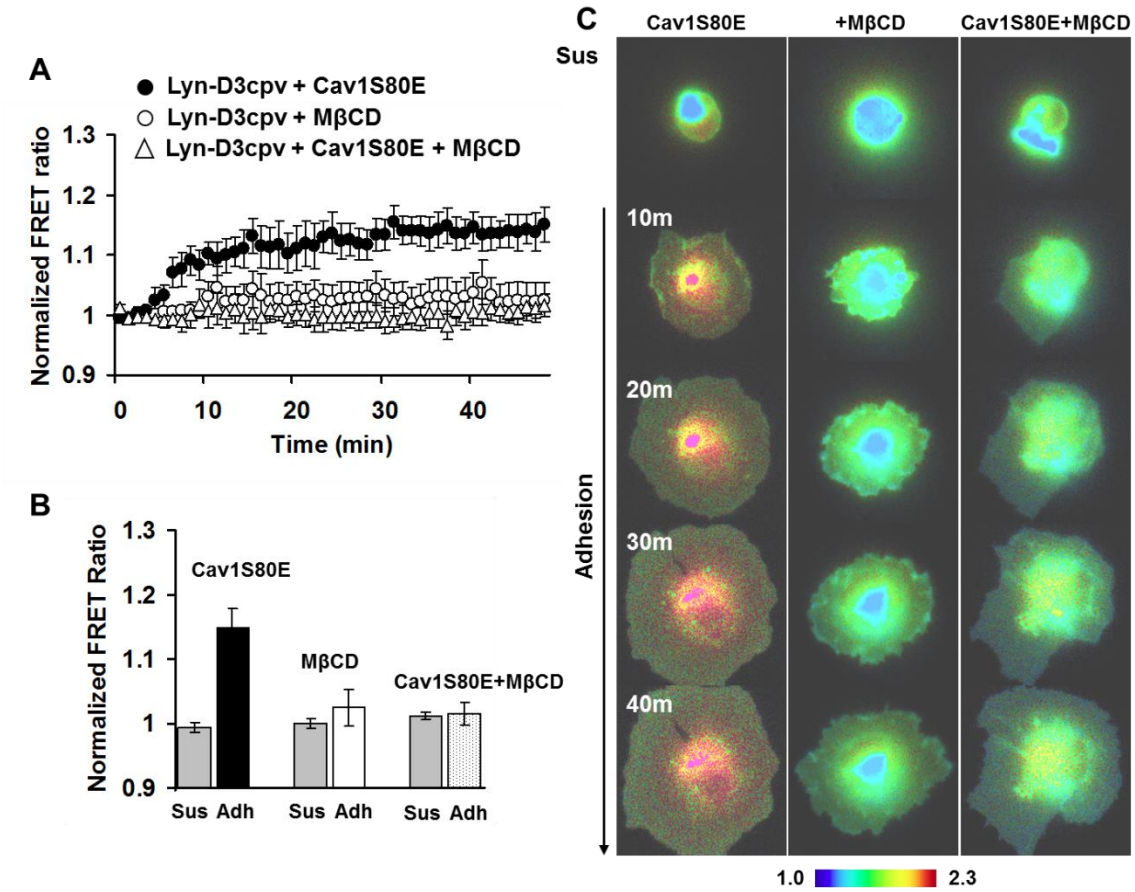

Figure 5-6. Effects of disruption of lipid rafts on Ca^{2+} mobilization in the adhesion process. (A) Depletion of cholesterol by MβCD inhibits the FRET ratio of Lyn-D3cpv, suggesting inhibition of Ca^{2+} mobilization at the DRM region. The mutant caveolin-1 used for disruption of caveolar structure at lipid rafts does not significantly affect Ca^{2+} mobilization at the DRM region. (B) The FRET ratio comparison in each group of cells (A) between suspension and adhesion states, suggesting that MβCD inhibits Ca^{2+} mobilization. (C) FRET images in each group. The blue/green colors represent a low FRET ratio and the yellow/red colors represent a high FRET ratio. (N=6, ***P<0.001)

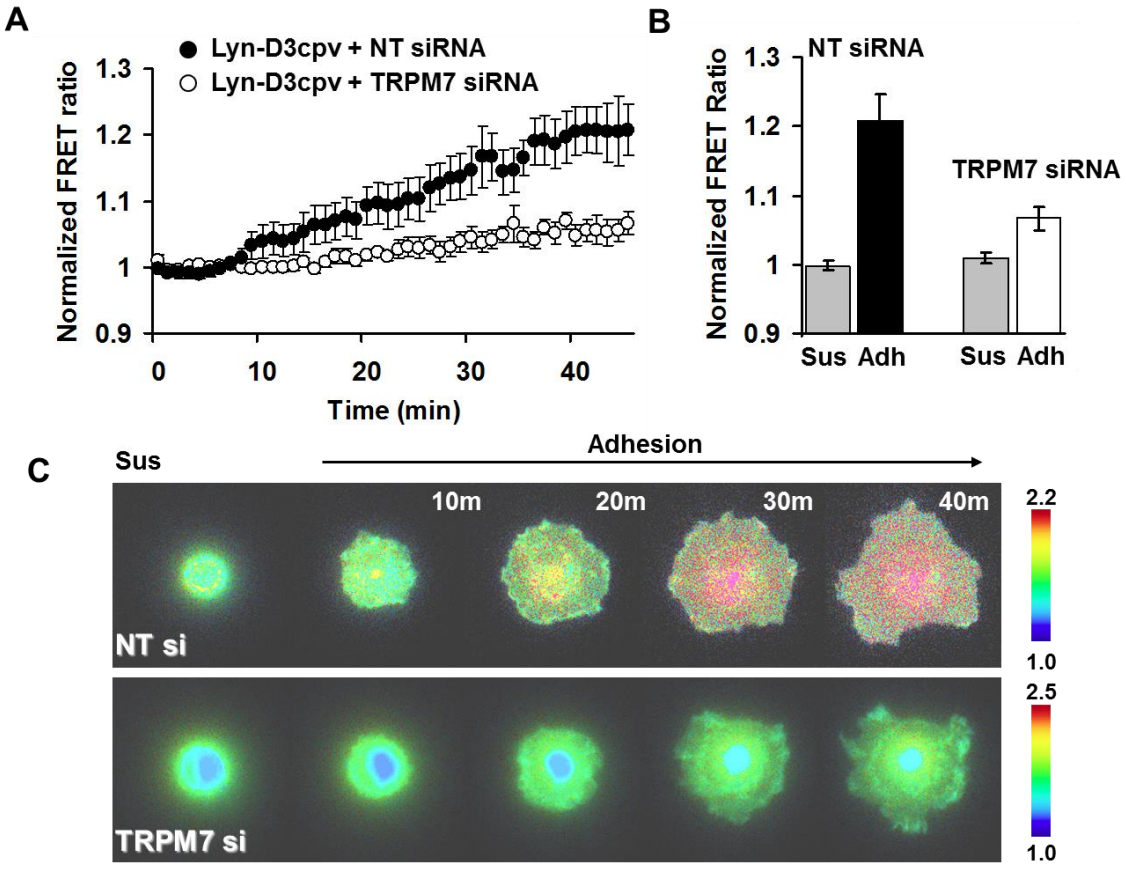

Figure 5-7. TRPM7 siRNA is important for Ca^{2+} mobilization at the DRM region. (A) The cells co-transfected with Lyn-D3cpv and TRPM7 siRNA show no significant Ca^{2+} mobilization at the DRM region in the adhesion process, but the control group of cells does, suggesting the involvement of TRPM7 in Ca^{2+} mobilization at the DRM region. (B) The FRET ratio comparison in each group of cells (A) between suspension and adhesion states, suggesting that TRPM7 siRNA inhibits Ca^{2+} mobilization. There is a significant difference between NT siRNA (adhesion) and TRPM7 siRNA (adhesion) (N=6, ***P<0.001) (C) FRET images in each group. The blue/green colors represent a low FRET ratio and the yellow/red colors represent a high FRET ratio.

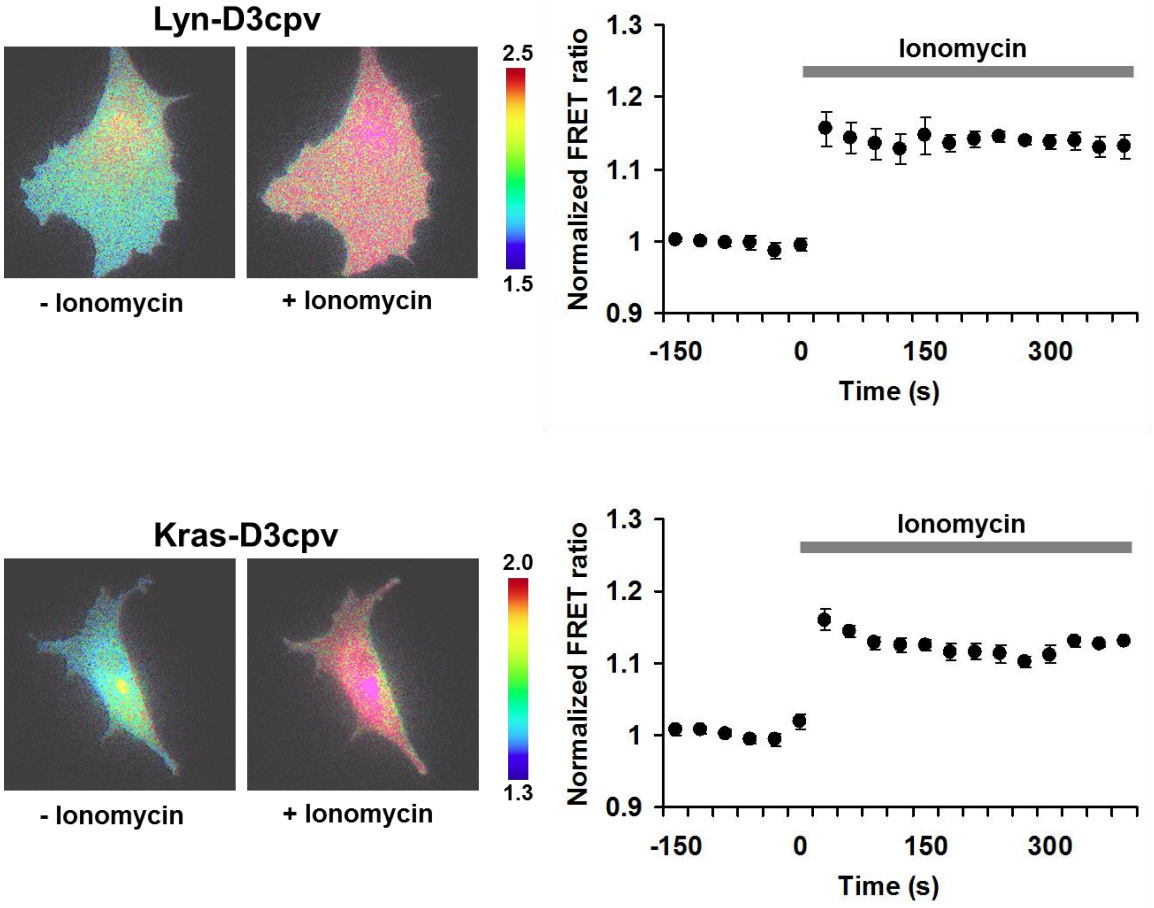

Supplementary Figure S5-1. The comparison of the FRET signal for Lyn-D3cpv and Kras-D3cpv in response to Ionomycin. Both sensors are equally sensitive to Ca^{2+} increase upon Ionomycin treatment, supporting that the capability of the two sensors to detect Ca^{2+} at the plasma membrane is minimally different (Lyn-D3cpv; n=3, Kras-D3cpv; n=3).

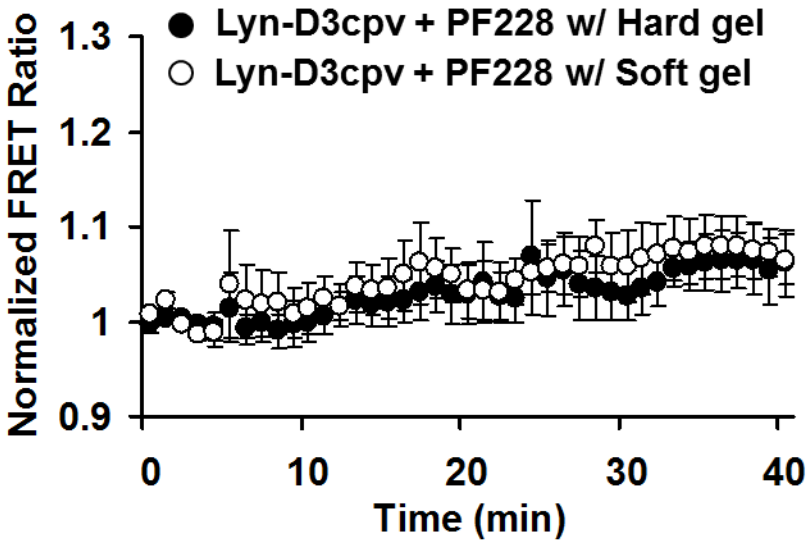

Supplementary Figure S5-2. FRET measurement in the Lyn-D3cpv sensor in cells on both hard and soft gels in the presence of FAK inhibitor. Substrate rigidity dependent Ca^{2+} mobilization at the DRM region is inhibited by PF228 treatment, an inhibitor of FAK (n=6).

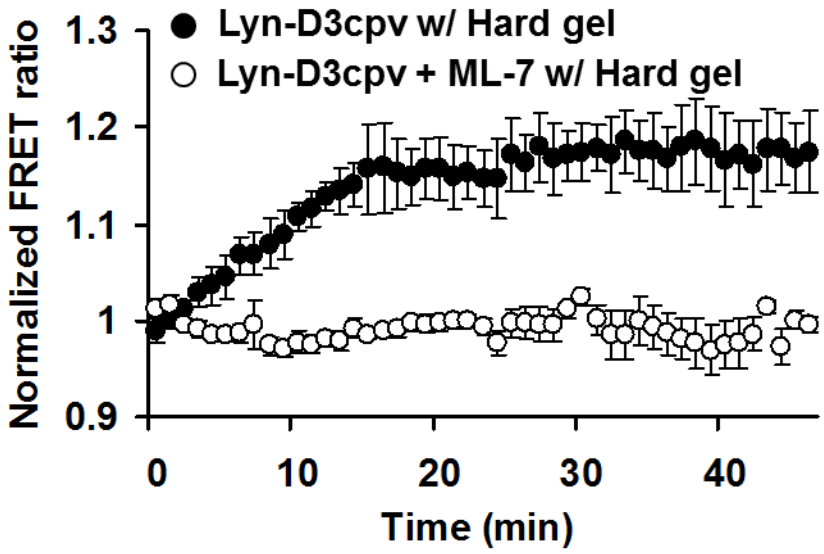

Supplementary Figure S5-3. FRET response of Lyn-D3cpv in cells on hard gel in the presence of ML-7. ML-7 is known to inhibit myosin dependent FAK activation. ML-7 inhibited Ca^{2+} mobilization at the DRM region.

CHAPTER 6

SUMMARY AND POTENTIAL OUTCOME OF THE RESEARCH

Emerging evidence demonstrates that mechanical forces play vital roles in regulating cell and tissue functions (Kassab, 2006; Solon et al., 2007). Recently, mechanical factors have also been shown to play important roles in determining the differentiation lineage and commitment of HMSCs. For example, the stiffness of mechanical microenvironments can affect the HMSCs lineage specification (Engler et al., 2006). Intracellular cytoskeletal tension and RhoA have also been reported to regulate HMSCs lineage commitment (McBeath et al., 2004). While substantial progress has been made toward understanding how differentiated cells sense mechanical stiffness (Laurent et al., 2002; Discher et al., 2005; Chiu et al., 2008), the molecular mechanism by which stem cells perceive these mechanical cues to coordinate signaling networks to determine their lineage destinations remains elusive.

Calcium ions play a versatile role in the regulation of many aspects of cellular activity. They control most cellular functions, such as muscle contraction, embryogenesis, cell differentiation, proliferation, gene expression, secretion, learning and memory, and apoptosis (Mckinsey et al., 2002; Soderling, 1993; Berridge et al., 2000; Landsberg and Yuan, 2004; Maeda et al., 2007; Clapham, 2007). Recent evidence indicates that mechanical stimulation plays an important role in regulating various cellular functions, including Ca^{2+} signaling (Kassab, 2006; Solon et al., 2007, Hayakawa et al., 2008, Kim et al., 2008). Capacity Ca^{2+} entry channels and mechanosensitive channels can be activated through mechanical stimulation, which results in an increase in intracellular calcium concentration and consequently the alteration of a variety of

cellular activities (Hayakwa et al., 2008). In chapter two, spontaneous Ca^{2+} oscillations were observed inside the cytoplasm and the endoplasmic reticulum (ER) using FRET biosensors targeted at subcellular locations. Lowering the substrate stiffness to 1 kPa significantly inhibited both the magnitude and frequency of the cytoplasmic Ca^{2+} oscillation in comparison to those on stiffer or rigid substrate. This Ca^{2+} oscillation was shown to be dependent on ROCK, a downstream effector molecule of RhoA, but independent of actin filaments, microtubules, myosin light chain kinase, or myosin activity. Lysophosphatidic acid, which activates RhoA, inhibited the magnitude and frequency of Ca^{2+} oscillation. Either a constitutive active mutant of RhoA (RhoA-V14) or a dominant negative mutant of RhoA (RhoA-N19) inhibited Ca^{2+} oscillation. Further investigation revealed that HMSCs cultured on gels with low elastic moduli displayed low RhoA activity, suggesting that RhoA and its downstream molecule ROCK may mediate the substrate rigidity-regulated Ca^{2+} oscillation.

Over the past two decades, the application of fluorescent dyes for the imaging of intracellular calcium dynamics and the improvement in fluorescence microscopy systems have led to a revolution in our understanding of the ubiquitous roles of Ca^{2+} in the physiological functions of cells. The introduction of fluorescent proteins (FPs) with a variety of spectra, and the advancement of genetically encoded calcium indicators have made it possible to visualize calcium signaling in a living single cell at subcellular levels with high spatiotemporal resolutions. These calcium imaging techniques, in combination with modern technologies that are able to create diverse mechanical environments, have allowed us to explore the calcium signaling of a single cell in response to mechanical stimulation. In chapter three, I provided the integration of genetically encoded calcium FRET biosensors with an optical laser-tweezer. In this chapter, I determined distinct calcium signaling at the plasma membrane and endoplasmic reticulum

membrane in response to mechanical stimulation. In fact, laser-tweezer traction of the cell membrane induced intracellular Ca^{2+} oscillations caused by Ca^{2+} release from endoplasmic reticulum (ER) in the absence of extracellular Ca^{2+}. These force-induced Ca^{2+} oscillations produced by ER Ca^{2+} release are mediated not only by the mechanical support of cytoskeleton and actomyosin contractility, but also by mechanosensitive Ca^{2+} channels on the plasma membrane, specifically TRPM7. When the ER Ca^{2+} release is inhibited and the extracellular Ca^{2+} level is restored, laser-tweezer traction of the cell can induce intracellular Ca^{2+} increase, which is mediated by the cytoskeletal structure, but not actomyosin contractility, suggesting that active actomyosin contractility regulated by MLCK and myosin II is essential for force transmission into the deep intracellular organelles, but dispensable for the mechanical regulation of plasma membrane channels.

As one of the GPCRs, β-adrenergic receptors (β-ARs) have the three subtypes β_1, β_2 and β_3. All these are linked to Gs proteins, in particular β_2 couples to Gi proteins, which in turn are linked to adenylyl cyclase (Chen-Izu et al., 2000; Ma and Huang, 2002). β-AR agonist-binding results in increased level of the intracellular second messenger cAMP that subsequently mediates cAMP-dependent protein kinase (PKA) (Zhang et al., 2005). Protein kinase plays a crucial role in regulating a wide variety of intracellular signaling cascades by enzymatically modifying other proteins through phosphorylation. Aberrant regulation of protein kinases in signal transduction can easily be exposed to pathophysiological conditions (Cohen et al., 2002). As one of the major protein kinases, PKA plays essential roles in regulating many cellular processes including transcriptional control of cAMP response element (CRE), essential metabolisms such as glycogen, sugar and lipids, and DNA replication (Matyakhina et al., 2006; Costanzo et al., 1999). Recently, PKA is regarded as a regulator of cell adhesion, cytoskeletal dynamics and cell

migration, since it is enriched within the leading edge of migrating cells. In addition, PKA activation in the leading edge of migrating cells is inhibited by the depletion of extracellular Ca2+ and by the inhibition of stretch-activated Ca2+ channels (SACCs). In spite of the emerging evidence that an appropriate PKA activity *in vivo* is very important for maintaining physiological conditions and sensing mechanical microenvironments, how the stiffness of microenvironments can be correlated to the cAMP-dependent PKA signaling pathway is not well understood. In chapter four, I investigated the effect of substrate stiffness on the cAMP-dependent PKA signaling, utilizing a fluorescent resonance energy transfer (FRET) biosensor. Genetically encoded FRET based A-kinase Activity Reporter (AKAR) has been regarding as a powerful tool for monitoring dynamic PKA activity with high spatiotermporal resolutions in living cells (Depry et al.; Zhang et al., 2005). As a result, I first report that HMSCs exposed to different magnitudes of substrate stiffness alter the signal activity of cAMP-dependent kinase (PKA) induced by a beta-adrenergic receptor (β-AR) agonist, Isoproterenol (Iso). This chapter reveals that HMSCs show a lower activity of Iso-induced PKA on soft substrates (0.1-1kPa), while they show much higher activity in response to stiffer or hard substrates (10-40kPa). Surprisingly, the application of forskolin (Fsk), non β-AR agonist displays a similar pattern of PKA response activity regardless of the extent of stiffness. In a further study, I visualized how Iso-induced PKA activity is inhibited by the disruption of microtubule through Nocodazole (Noc, 5 μM), but not by cytochalasin D (Cyto D, 1 μM), an inhibitor of actin filaments. In contrast, the response pattern of Fsk-induced PKA activity is not affected by Noc, suggesting that substrate stiffness capable of affecting β-AR agonist-induced PKA signaling is dependent on microtubules. In addition, the alteration of Iso-induced PKA signaling by substrate stiffness resulted in the event of an abnormal endocytosis in β_2-AR. The functional role of microtubules appears to be

correlated to the signaling cascade between β-AR agonist-induced PKA and its endocytosis, forming a feedback loop that modulates reciprocally. Taken together, these results indicate that the substrate stiffness consisting of mechanical microenvironments, coordinated by microtubules, may be an important factor in regulating β-AR signaling cascade and PKA activation. Therefore, the study performed in chapter four provides critical cues to understand how alteration in tissue stiffness resulting from injury or disease can be involved in abnormal activity of G-protein coupled receptor-derived disease processes.

The regulation of cell-matrix adhesion seems to be simultaneously mediated by many adhesion molecules including integrins. Recently, two kinds of FAK biosensors have been developed, which are specifically capable of tethering at the plasma membrane microdomains, detergent-resistant membrane (DRM) and non-DRM regions and monitoring the local FAK activity in living cells. Ca^{2+} biosensors also can be designed to tether at two types of membrane microdomains, such as DRM and non-DRM regions. In chapter five, I found that Ca^{2+} mobilization at DRM regions is dependent on substrate rigidity during the cell-matrix adhesion process. This Ca^{2+} mobilization at DRM regions seems to be selectively activated in response to substrate rigidity during the adhesion process, but it is not activated at non-DRM regions. Surprisingly, I found that FAK activation at DRM regions is also substrate rigidity-dependent, and this observation implies that there might be some connection between FAK and Ca^{2+} based on their parallel activation in the adhesion process. Further investigation reveals that FAK regulates Ca^{2+} mobilization at DRM regions in the adhesion process, and that TRPM7 plays a crucial role in Ca^{2+} mobilization at DRM regions by contributing to Ca^{2+} influx in response to substrate rigidity during the adhesion process. In conclusion, this chapter clearly shows how Ca^{2+} and FAK signaling are activated at DRM regions in the adhesion process, which is dependent on

substrate rigidity. The results in this chapter also show that FAK regulates Ca^{2+} mobilization that can be modulated by the proper localization of cholesterol and the functional role of TRPM7. This data will provide new insights into understanding the underlying mechanism between Ca^{2+} and FAK signals and the relationship between biochemical/mechanical factors and cellular processes.

References

Kassab GS. 2006. Biomechanics of the cardiovascular system: the aorta as an illustratory example. J R Soc Interface 3(11):719-740.

Solon J, Levental I, Sengupta K, Georges PC, Janmey PA. 2007. Fibroblast adaptation and stiffness matching to soft elastic substrates. Biophys J 93(12):4453-4461.

Engler AJ, Sen S, Sweeney HL, Discher DE. 2006. Matrix elasticity directs stem cell lineage specification. Cell 126(4):677-689.

McBeath R, Pirone DM, Nelson CM, Bhadriraju K, Chen CS. 2004. Cell shape, cytoskeletal tension, and RhoA regulate stem cell lineage commitment. Dev Cell 6(4):483-495.

Laurent VM, Canadas P, Fodil R, Planus E, Asnacios A, Wendling S, Isabey D. 2002. Tensegrity behaviour of cortical and cytosolic cytoskeletal components in twisted living adherent cells. Acta Biotheor 50(4):331-356.

Discher DE, Janmey P, Wang YL. 2005. Tissue cells feel and respond to the stiffness of their substrate. Science 310(5751):1139-1143.

Chiu WT, Tang MJ, Jao HC, Shen MR. 2008. Soft Substrate Up-regulates the Interaction of STIM1 with Store-operated Ca2+ Channels That Lead to Normal Epithelial Cell Apoptosis. Mol Biol Cell 19(5):2220-2230.

McKinsey TA, Zhang CL, Olson EN. MEF2: a calcium-dependent regulator of cell division,

differentiation and death. Trends Biochem Sci. Jan 2002;27(1):40-47.

Soderling TR, Stull JT. 2001. Structure and regulation of calcium/calmodulin-dependent protein kinases. Chem Rev 101(8):2341-2352.

Berridge MJ, Lipp P, Bootman MD. 2000. The versatility and universality of calcium signalling. Nat Rev Mol Cell Biol 1(1):11-21.

Landsberg JW, Yuan JX. Calcium and TRP channels in pulmonary vascular smooth muscle cell proliferation. News Physiol Sci. Apr 2004;19:44-50.

Maeda Y, Nitanai Y, Oda T. From the crystal structure of troponin to the mechanism of calcium regulation of muscle contraction. Adv Exp Med Biol. 2007;592:37-46.

Clapham DE. 2007. Calcium signaling. Cell 131(6):1047-1058.

Hayakawa K, Tatsumi H, Sokabe M. 2008. Actin stress fibers transmit and focus force to activate mechanosensitive channels. J Cell Sci 121(Pt 4):496-503.

Chen-Izu, Y., R.P. Xiao, L.T. Izu, H. Cheng, M. Kuschel, H. Spurgeon, and E.G. Lakatta. 2000. G(i)-dependent localization of beta(2)-adrenergic receptor signaling to L-type Ca(2+) channels. *Biophys J*. 79:2547-56

Ma, Y.C., and X.Y. Huang. 2002. Novel signaling pathway through the beta-adrenergic receptor. *Trends Cardiovasc Med*. 12:46-9.

Zhang J, Hupfeld CJ, Taylor SS, Olefsky JM, Tsien RY. 2005. Insulin disrupts beta-adrenergic signalling to protein kinase A in adipocytes. *Nature*. 437(7058):569-73.

Cohen, C., A. Zavala-Pompa, J.H. Sequeira, M. Shoji, D.G. Sexton, G. Cotsonis, F. Cerimele, B. Govindarajan, N. Macaron, and J.L. Arbiser. 2002. Mitogen-actived protein kinase activation is an early event in melanoma progression. *Clin Cancer Res*. 8:3728-33.

Depry C and Zhang J. 2011. Using FRET-based reporters to visualize subcellular dynamics of protein kinase A activity. *Methods Mol Biol*. 756:285-94.

Depry C, Allen MD, and Zhang J. 2011. Visualization of PKA activity in plasma membrane microdomains. *Mol Biosyst*. 1:52-8.